DOE/[illegible] N7829409
NASA
UCID-3983

# MATHEMATICAL AND COMPUTATIONAL STUDIES OF THE STABILITY OF AXISYMMETRIC ANNULAR CAPILLARY FREE SURFACES

Norman Albright, Paul Concus,
and Ilkka Karasalo
Lawrence Berkeley Laboratory
University of California
Berkeley, California 94720

November 1977

Prepared for
National Aeronautics and Space Administration
Lewis Research Center
Cleveland, Ohio 44135
Under Contract 67705-C

and

U.S. Department of Energy
Washington, D.C. 20545
Under Contract W-7405-ENG-48

# MATHEMATICAL AND COMPUTATIONAL STUDIES OF THE STABILITY OF AXISYMMETRIC ANNULAR CAPILLARY FREE SURFACES

by Norman Albright, Paul Concus, and Ilkka Karasalo

We present here the results of our mathematical and computational studies of the stability of a liquid in a rotationally symmetric container subject to gravitational and surface forces. Of specific interest is the case for which the contact angle is zero, or nearly zero. The application of primary concern is that of stability in a vertical right circular cyclindrical container with a concave spheroidal bottom, for the case in which the volume of liquid is sufficiently small so that liquid lies only in an annular region of the container. Numerical computations are presented for a container used for the storage of liquid fuels in National Aeronautics and Space Administration Centaur space vehicles, for which the axial ratio of the container bottom is 0.724.

Our studies consist of several self-contained parts, which are discussed independently in the appendices that follow. In Appendices I and II are derived the mathematical results on which our static-analysis computations are based. These results are concerned with the conditions for the contained liquid to be in stable equilibrium. Of particular interest is the case of zero contact angle, which has previously not received adequate mathematical treatment in the literature.

A configuration is in stable equilibrium if and only if it strictly minimizes the sum of the surface and gravitational potential energies, among all nearby configurations with the same liquid volume. With a suitable choice of variables, the problem of stability may be approached as a variable-endpoint problem in the calculus of variations.

Using this approach conditions are obtained that distinguish between stable and unstable cases in a satisfactory way, if the contact angle is not zero. If the contact angle is zero, the formal limits of the endpoint conditions depend crucially on whether or not the curvatures of the equilibrium interface and the container wall coincide at the three phase contact lines. If they do not, the limiting endpoint conditions will be of the fixed type.

It is shown that for zero contact angle the stability criteria based on the fixed end-point conditions apply if only the analytic continuation of the equilibrium liquid-vapor interface does not penetrate the container walls at the three-phase contact lines. If it does penetrate, then the configuration will be unstable regardless of the conditions on the second variation of the total potential energy.

A computational study based on the mathematical results in Appendices I and II is carried out in Appendix III. The critical Bond number for stability is calculated for the Centaur space vehicle tank as a function of the liquid volume for contact angles of 0°, 1°, 2°, and 4°. For the zero-contact-angle case, the specially derived end-point conditions are used, while for the latter three cases the usual variable end-point conditions are used. The zero-contact angle results are found to be consistent with the limiting ones for the nonzero angles.

Of particular interest for the case of zero contact angle is the appearance, for this problem, of a critical liquid volume marking a qualitative change in the nature of the solution. For liquid volumes less than the critical one the stability limit is determined by the fixed end-point conditions, whereas for liquid volumes larger than the critical one the stability limit is determined by the non-penetration criteria discussed above. This feature corresponds to the existence of (unstable) equilibrium configurations for Bond numbers larger in magnitude than the critical one only for the small volume case. The critical liquid volume for the Centaur tank corresponds to a fill height of 0.5031 a, where a is the radius of the tank.

The numerical results presented in Appendix III have been found to be consistent with preliminary experimental results obtained by E. P. Symons at the NASA Lewis Research Center.

In Appendix IV small-amplitude, periodic sloshing modes are calculated for the container configuration studied in Appendix III, for zero contact angle. As must be the case for a conservative mechanical system, the critical Bond numbers for stability obtained from the dynamic analysis are found to agree with those calculated from the static analysis. Agreement is also found on the value of the critical liquid volume for which equilibrium configurations can exist nearby the critically stable one.

Oscillation frequencies or growth rates are calculated for several Bond numbers and liquid volumes, for normal modes having up to six angular nodes. The computations indicate that for liquid

volumes smaller than the critical one, the sloshing modes without radial nodes generally become unstable before those with one or more radial nodes, as the magnitude of the Bond number is increased. The calculations for larger liquid volumes indicate that all modes become unstable together, in agreement with the cessation of existence of a nearby equilibrium for this case.

The above results are depicted graphically, and growth rates for the dominant unstable mode for a liquid volume corresponding to a dimensionless mean fill height of 0.30 are given for three different liquids.

APPENDIX I

# SUFFICIENT CONDITIONS FOR STABILITY OF AXISYMMETRIC ANNULAR LIQUID INTERFACES

by

Ilkka Karasalo

Issued as Lawrence Berkeley Laboratory Report LBL-4898, June 1976

# SUFFICIENT CONDITIONS FOR STABILITY OF AXISYMMETRIC ANNULAR LIQUID INTERFACES

by

Ilkka Karasalo

Lawrence Berkeley Laboratory
University of California
Berkeley, California 94720
June 1976

ABSTRACT

The stability, in terms of minimum static energy, of axisymmetric annular liquid interfaces in axisymmetric containers is studied mathematically. The sufficiency of stability conditions based on the Jacobi accessory minimization problem with respect to volume conserving, "weak" perturbations is proved in two cases: Firstly, sufficient conditions for stability in the general case of nonzero liquid-wall contact angle are considered. Secondly, the formal limit of these conditions, as the contact angle tends to zero is proved to be correct, provided that the curvatures of the unperturbed liquid-vapor interface and the container wall are not equal at their contact lines.

## 1. FORMULATION OF THE PROBLEM

In this paper we study mathematically the stability of certain configurations of liquid contained in an axially symmetric tank in a gravitational field directed along the axis of symmetry. We require that the tank shape and the liquid volume are such that the liquid-vapor interface is annular, i.e. it does not intersect the axis of symmetry, cf., fig. 1:

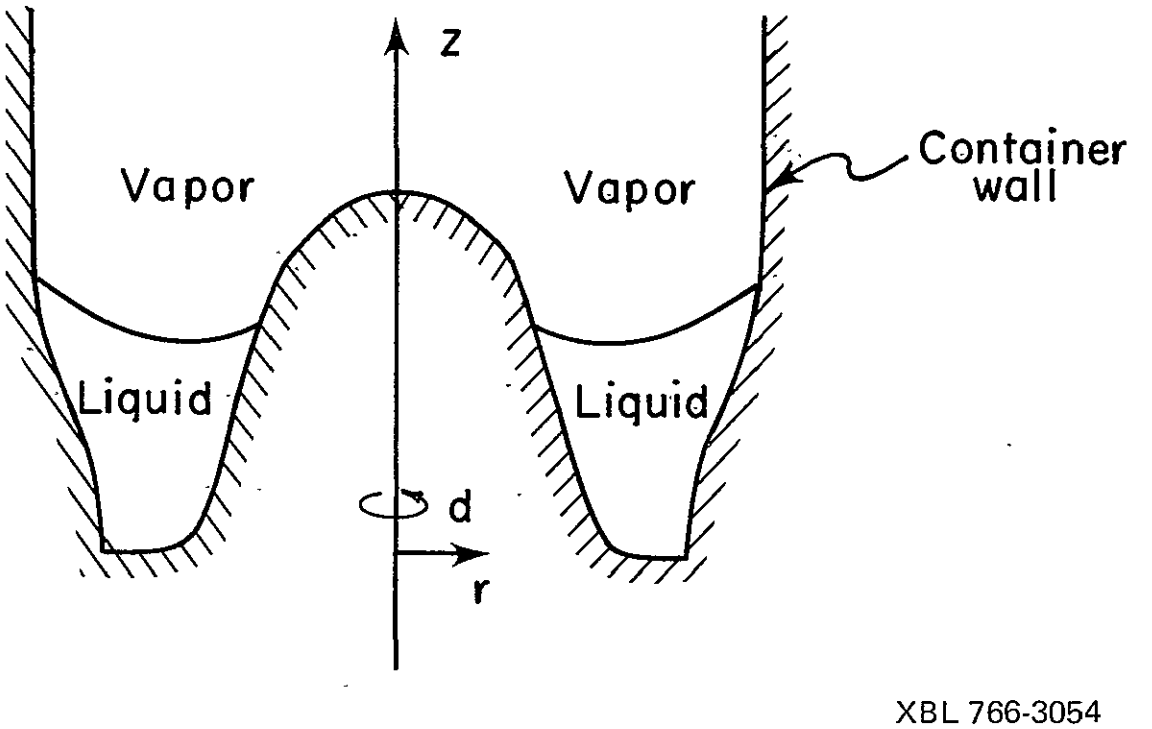


Figure 1: Example of permissible liquid-tank configuration and the associated cylindrical coordinate system.

A configuration is one of stable equilibrium if and only if it

strictly minimizes the total static potential energy of the system, given by

$$E = \sigma(A_f - \cos\gamma\, A_w) + E_g \ , \tag{1.1}$$

compared to all nearby configurations with the same liquid volume V. Here $\sigma \geq 0$ and $0 \leq \gamma \leq \pi$ are constants determined by the physical properties of the liquid and the wall, $A_f$ and $A_w$ are the areas of the liquid-vapor and liquid-container interfaces, respectively, and $E_g$ is the gravitational potential energy of the liquid.

We shall study below the behavior of the energy (1.1) when the liquid is perturbed slightly (but not necessarily rotational symmetrically) from a configuration of rotational symmetry. For our purposes, a parametric arc-length, normal displacement representation of the surfaces (cf., e.g. Reynolds, Saad, Satterlee [ 2 ]) offers some advantage. Hence we let the unperturbed surface be described by the equations

$$\begin{cases} r = R(s) \ ; \ 0 \leq \phi \leq 2\pi \\ \\ z = Z(s) \ ; \ s_o \leq s \leq s_1 \end{cases} \tag{1.2}$$

in the polar co-ordinate system of figure 1 where the parameter $s$ is the arc-length along the curve of intersection between the liquid-vapor surface and any plane $\phi$ = constant. Then the equations

$$\begin{cases} r = R(s) - \eta(s,\phi)Z'(s) \ ; \ 0 \leq \phi \leq 2\pi \\ \\ z = Z(s) + \eta(s,\phi)R'(s) \ ; \ s_o(\phi) \leq s \leq s_1(\phi) \end{cases} \tag{1.3}$$

describe a surface obtained by moving each point of the surface (1.2) the distance $\eta(s,\phi)$ in the direction of the principal normal. In general, since we want the perturbed surface (1.3) to intersect the container walls, the functions R and Z of (1.2) must be continued in the s-direction to some open interval containing $[s_o,s_1]$, cf. figure 2. A convenient way of doing this, which we will use in the sequel, is provided by the differential equations (1.11) below.

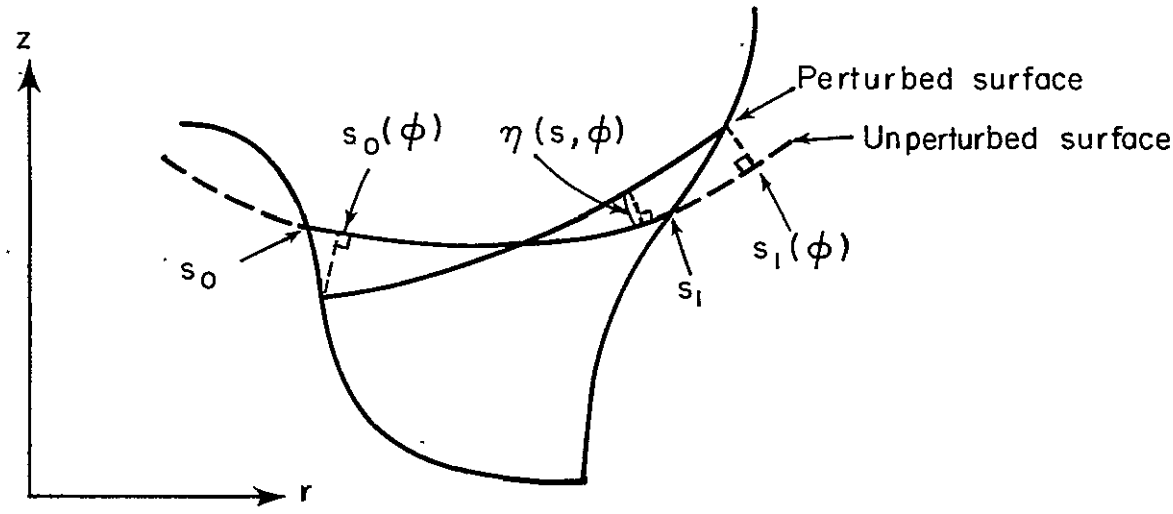


XBL 767-3072

Figure 2: The arc-length, normal displacement coordinates: Intersection between the surfaces and some plane $\phi$ = constant.

Similarly, we let the container wall in some neighborhoods of the unperturbed contact lines ($s = s_o$ and $s = s_1$ in (1.2)) be given by

$$\begin{cases} r = R(s) - w(s)Z'(s) \\ \\ z = Z(s) + w(s)R'(s) \end{cases} \qquad 0 \leq \phi \leq 2\pi . \tag{1.4}$$

((1.4) is not adequate if the contact angle, $\gamma$, between the unperturbed surface and the wall is $\pi/2$. To avoid unnecessary detail we therefore assume $\gamma \neq \pi/2$ in the following).

For any equilibrium configurations, the functions R and Z will be sufficiently smooth for the perturbed surface (1.3) not to intersect itself when $|\eta(s,\phi)|$, $|\eta_s(s,\phi)|$ and $|\eta_\phi(s,\phi)|$ are small. (For this, it is sufficient that R"(s) and Z"(s) are bounded in some open interval containing $[s_o,s_1]$, cf. Concus, Crane, Satterlee [5], p. 4-6, while in fact it follows from the

differential equations (1.11) below that R and Z may be continued analytically to some open region containing $[s_o,s_1]$ in the complex s-plane). Then the increments of the quantities appearing in (1.1) and of the volume may be calculated in a straightforward way. One obtains

$$\begin{aligned}\delta E(\eta) &= \sigma \cdot (\delta A_f - \cos\gamma \cdot \delta A_w) + \delta E_g \\ &= \int_0^{2\pi}\int_{s_o(\phi)}^{s_1(\phi)} \left\{ f_A(\underline{\eta},s) - f_A(\underline{0},s) + f_g(\underline{\eta},s)\right\} ds d\phi \\ &\quad - \int_0^{2\pi}\int_{\Delta\phi} \left\{\cos\gamma \cdot f_A(\underline{w},s) - f_A(\underline{0},s) + f_g(\underline{w},s)\right\} ds d\phi \end{aligned} \tag{1.5}$$

$$\delta V(\eta) = \int_0^{2\pi}\int_{s_o(\phi)}^{s_1(\phi)} f_V(\underline{\eta},s)\, ds d\phi - \int_0^{2\pi}\int_{\Delta\phi} f_V(\underline{w},s)\, ds d\phi \tag{1.6}$$

where we have put

$$\begin{aligned}\underline{\eta} &= \underline{\eta}(s,\phi) = (\eta(s,\phi),\ \eta_s(s,\phi),\ \eta_\phi(s,\phi))^T \\ \underline{w} &= \underline{w}(s) = (w(s),w'(s),0)^T \\ \Delta\phi &= \text{the interval } (s_o(\phi),s_o)\cup(s_1,s_1(\phi))\end{aligned} \tag{1.7}$$

and, denoting $R = R(s)$, $Z = Z(s)$,

$$\begin{aligned} f_A(\underline{\eta},s) &= \sigma \cdot \{(R - \eta Z')^2(\eta_s^2 + (1 + \eta(R''Z' - Z''R'))^2) \\ &\quad + \eta_\phi^2(1 + \eta(R''Z' - Z''R'))^2\}^{1/2} \\ f_V(\underline{\eta},s) &= \eta\{1 + \tfrac{\eta}{2}(R''Z' - Z''R')\}(R - \tfrac{\eta}{2}Z') \\ f_g(\underline{\eta},s) &= \rho g \cdot (Z + \tfrac{\eta}{2}R') \cdot f_V(\underline{\eta},s) \end{aligned} \tag{1.8}$$

where $\rho$, the liquid density, is assumed to be constant and g is the gravitation constant with $g > 0$ if the gravitation force is directed towards the negative z-axis. We note that when $R > 0$ all of the functions $f_A$, $f_V$ and $f_g$ are smooth (in fact analytic) in the arguments $\eta$, $\eta_s$ and $\eta_\phi$ in a neighborhood of $\underline{\eta} = \underline{0}$.

A first necessary condition for $\eta = 0$ to be a local minimizer of $\delta E$ (We shall need to make the meaning of "local" more precise below. For the moment we may consider all $\eta$ which are continuous and smooth in some open region containing $s_o(\phi) \leq s \leq s_1(\phi)$, $0 \leq \phi \leq 2\pi$.) when $\delta V = 0$ is that, for some constant $\lambda$ all first-order $\eta$-terms in $\delta E - \lambda \delta V$ vanish. Using the notation in (1.5) - (1.8) this necessary condition is expressed by the Euler-Lagrange equation

$$\left.\begin{aligned} &\frac{\partial f_A}{\partial \eta}(\underline{0},s) + \frac{\partial f_g}{\partial \eta}(\underline{0},s) - \lambda \frac{\partial f_V}{\partial \eta}(\underline{0},s) \equiv 0 \\ &\text{in } s_o \leq s \leq s_1, \text{ with the additional condition} \\ &\cos\gamma\, f_A(\underline{w}(s_i),s_i) - f_A(\underline{0},s_i) = 0 \quad ; \quad i=0,1. \end{aligned}\right\} \tag{1.9}$$

Putting $B_o = \rho g/\sigma$, $H_o = \lambda/\sigma$, using (1.8) and the identity

$$R'(s)^2 + Z'(s)^2 \equiv 1 \tag{1.10}$$

(1.9) becomes:

$$\left.\begin{aligned} Z'' &= R'(B_o Z - H_o - Z'/R) \\ R'' &= -Z'(B_o Z - H_o - Z'/R) \\ &\text{with the boundary condition, that the curve} \\ &(R(s),Z(s)) \text{ intersects the container walls} \\ &\text{at } s = s_o \text{ and } s = s_1, \text{ under the contact} \\ &\text{angle } \gamma. \end{aligned}\right\} \tag{1.11}$$

(without loss of generality we have excluded the contact angles $\pi - \gamma$ also allowed by (1.9)).

Assuming now that R and Z are such that (1.11) and, consequently, (1.9) are satisfied, a second necessary condition will be that the terms of second order in $\eta$, $\eta_s$ and $\eta_\phi$ will give a non-negative contribution to $\delta E$ for all $\eta$ satisfying the volume constraint. When $\gamma > 0$, we may formulate this condition as follows:

$$\left.\begin{aligned} &\int_0^{2\pi}\int_{s_o}^{s_1} \underline{\eta}^T\left\{f_{A\underline{\eta}\underline{\eta}}(\underline{0},s) + f_{g\underline{\eta}\underline{\eta}}(\underline{0},s) - \lambda f_{V\underline{\eta}\underline{\eta}}(\underline{0},s)\right\}\underline{\eta}\ ds d\phi \\ &+ \int_0^{2\pi}\left\{\alpha_o \eta(s_o,\phi)^2 + \alpha_1 \eta(s_1,\phi)^2\ d\phi\right\} \geq 0 \\ &\text{for all } \eta \text{ such that} \\ &\int_0^{2\pi}\int_{s_o}^{s_1} \frac{\partial f_V}{\partial \eta}(\underline{0},s)\cdot\eta(s,\phi)\ ds d\phi = 0 \end{aligned}\right\} \qquad (1.12)$$

Here we have put $\alpha_i$

$$= \frac{(-1)^i}{\tan^2\gamma}\cdot\frac{d}{ds}\left\{\cos\gamma\ f_A(\underline{w}(s),s) - f_A(\underline{0},s) + f_g(\underline{w}(s),s) - \lambda f_V(\underline{w}(s),s)\right\}_{s=s_i}$$

$$i=0,1. \qquad (1.13)$$

Using (1.7) - (1.8), the second derivatives appearing in the first integral in (1.12) are seen to be diagonal 3 X 3 matrices, and (1.12) reduces to

$$\left.\begin{aligned} &\int_0^{2\pi}\int_{s_o}^{s_1}\left\{A(s)\eta_s^2 + B(s)\eta_\phi^2 + C(s)\eta^2\right\}ds\,d\phi \\ &+ \int_0^{2\pi}\left\{\alpha_o\eta(s_o,\phi)^2 + \alpha_1\eta(s_1,\phi)^2\right\}d\phi \geq 0 \\ &\text{for all } \eta \text{ such that} \\ &\int_0^{2\pi}\int_{s_o}^{s_1} A(s)\eta(s,\phi)\,ds\,d\phi = 0 \quad , \end{aligned}\right\} \tag{1.14}$$

where $A(s) = \sigma R(s)$, $B(s) = \sigma/R(s)$ and $C(s)$ is smooth (analytic) in $[s_o, s_1]$, see (5.1) below.

By standard results for symmetric, semibounded quadratic forms in Hilbert space (see e.g. Kato [1] p. 322 and pp. 352-353), (1.14) may be analyzed in terms of the eigenvalues and eigenfunctions of an associated selfadjoint differential generator:

$$\left.\begin{aligned} &T\eta = -\frac{\partial}{\partial s}(A(s)\eta_s) - \frac{\partial}{\partial\phi}(B(s)\eta_\phi) + C(s)\eta \\ &\text{in } s_o \leq s \leq s_1,\ 0 \leq \phi \leq 2\pi, \text{ with the} \\ &\text{boundary conditions, that } \eta \text{ should be} \\ &\text{periodic in } \phi \text{ with period } 2\pi \text{ and} \\ &A(s_i)\eta_s(s_i,\phi) = (-1)^i\alpha_i\eta(s_i,\phi)\ ,\ 0 \leq \phi \leq 2\pi, \\ &\qquad\qquad\qquad\qquad\qquad\qquad i=0,1\ . \end{aligned}\right\} \tag{1.15}$$

T has a complete, orthogonal system of eigenfunctions of the form

$$\left\{\mu_{ik}(s)\cos k\phi\right\}_{i=1,k=0}^{\infty} \qquad \left\{\mu_{ik}(s)\sin k\phi\right\}_{i=1,k=1}^{\infty} \tag{1.16}$$

with associated eigenvalues (in increasing order in the index i)

$$\left\{\lambda_{ik}\right\}_{i=1,k=0}^{\infty}$$

determined from the boundary-value problems

$$\begin{cases} -\frac{d}{ds}(A(s)\mu'_{ik}(s)) + \{k^2B(s) + C(s)\}\mu_{ik}(s) = \lambda_{ik}\mu_{ik}(s) \\ A(s_j)\mu'_{ik}(s_j) = (-1)^j\alpha_j\mu_{ik}(s_j) \quad ; \quad j=0,1 \end{cases} \qquad \begin{matrix} k=0,1,2\ldots \\ i=1,2,3\ldots \end{matrix} \tag{1.17}$$

We notice that all eigenfunctions (1.16) but those with $k = 0$ satisfy the side condition in (1.14). Furthermore, since $B(s) > 0$ in $s_o \leq s \leq s_1$, we see from (1.17) that the eigenvalues $\lambda_{ik}$ are increasing functions of k. It then follows that (1.14) holds for all $\eta$ in the class of continuous functions in $s_o \leq s \leq s_1$, $0 \leq \phi \leq 2\pi$ which are periodic in $\phi$ with period $2\pi$ and have square integrable first derivatives (see e.g. Kato [1], p. 323, Cor. 2.3) if and only if

$$\lambda_o = \min\left\{\beta_1^2\lambda_{10} + \beta_2^2\lambda_{20},\ \lambda_{11}\right\} \geq 0 \tag{1.18}$$

where, denoting $(f,g)_o = \int_0^{2\pi}\int_{s_o}^{s_1} f(s,\phi)g(s,\phi)dsd\phi$, $\beta_1^2$ and $\beta_2^2$ are the solutions to

$$\begin{cases} \beta_1^2(\mu_{10},A)_o^2 - \beta_2^2(\mu_{20},A)_o^2 = 0 \\ \beta_1^2(\mu_{10},\mu_{10})_o + \beta_2^2(\mu_{20},\mu_{20})_o = 1 \end{cases} \tag{1.19}$$

(with $\beta_2 = 0$ if the solutions are non-unique).

The purpose of the present paper is to provide a theoretical complement to a computational study of this kind (Concus, Karasalo[7]). There the necessary condition (1.18) is used to distinguish between stable and unstable equilibrium surfaces in the limiting case $\gamma = 0$. We will therefore here first show, that when $\gamma > 0$, <u>(1.18) with strict inequality</u> is a <u>sufficient condition</u> for our constrained minimization problem, when $\eta$ is allowed to vary in a "weak" type of neighborhood (cf. e.g. Bolza [3], p. 68-70) of $\eta = 0$. Then, as the main result (which may be new cf. Gillette [4], p. 23), we will show that <u>(1.18) with strict inequality and the eigenvalues computed from (1.17) but the boundary condition</u>

$$\mu_{ik}(s_j) = 0 \; ; \; j = 0,1 \; ; \qquad \begin{matrix} k=0,1... \\ i=1,2... \end{matrix} \tag{1.20}$$

is a sufficient condition for the constrained minimization problem (again, in a "weak" sense [3]) when $\gamma = 0$ provided that the curvatures of the unperturbed surface and the container wall are not equal at the unperturbed contact lines. (This additional condition on the unperturbed surface in fact turns out to be necessary (see (5.3) below) in order for the boundary conditions of (1.17) to converge formally to (1.20) as $\gamma \to 0$.)

## 2. SOME NOTATION AND LEMMAS

We denote by $\Sigma$ the closed domain $s_o(\phi) \leq s \leq s_1(\phi)$, $0 \leq \phi \leq 2\pi$ in the $(s,\phi)$-plane. We require that a permissible perturbing function $\eta = \eta(s,\phi)$ in (1.3) should have the following regularity properties:

a) $\eta$ is continuous in $\Sigma$ and periodic in $\phi$ with period $2\pi$.

b) $\eta_s$ and $\eta_d$ are continuous in $\Sigma$ except possibly at finitely many points or finitely many piecewise smooth curves with finite length. In particular, $\eta_s$ is piecewise continuous as function of $s$ for all $\phi$.

c) $$d(\eta) = \sup|\eta(s,\phi)| + \sup|\eta_s(s,\phi)| + \sup|\eta_\phi(s,\phi)| < \infty \tag{2.1}$$
where the supremum is taken over all points of $\Sigma$ where $\eta_s$ and $\eta_\phi$ are continuous.

d) The functions $s_i(\phi)$; $i=0,1$ are continuous, and such that $s_i(\phi) - s_i$, $i=0,1$, change sign at most finitely many times in $0 \leq \phi \leq 2\pi$. $s_i'(\phi)$; $i=0,1$, are continuous except possibly at finitely many points in $0 \leq \phi \leq 2\pi$ and

$$d(\Sigma) = \sum_{i=0}^{1} (\sup|s_i(\phi) - s_i| + \sup|s_i'(\phi)|) < \infty \tag{2.2}$$

where the supremum is taken over all points of $0 \leq \phi \leq 2\pi$ where $s_o'(\phi)$ and $s_1'(\phi)$ are continuous.

We notice, in particular, that conditions a), b) and c) ensure that $\eta$, $\eta_s$ and $\eta_\phi$ are square integrable on $\Sigma$. We also require that the function $w$ for the container walls (1.4) is sufficiently smooth in some neighborhoods of $s = s_o$ and $s = s_1$. We will further denote the closed rectangle $s_o \leq s \leq s_1$, $0 \leq \phi \leq 2\pi$ with $\Sigma_o$ and use the notation

$$(f,g) = \int_0^{2\pi} \int_{s_o(\phi)}^{s_1(\phi)} f(s,\phi)g(s,\phi)\, ds d\phi \tag{2.3}$$

$$\|f\|^2 = (f,f) \tag{2.4}$$

$$(f,g)_o = \int_0^{2\pi} \int_{s_o}^{s_1} f(s,\phi)g(s,\phi)\, ds d\phi \tag{2.5}$$

$$\|f\|_o^2 = (f,f)_o \tag{2.6}$$

for real-valued functions f and g for which the integrals exist.

The following lemma will be useful in the $\gamma > 0$ case:

Lemma 2.1: Let $\mu(s,\phi)$ satisfy the requirements a) - c) above on the rectangle $\Sigma_o$. Then there exists a constant $\beta$, depending only on $s_o$ and $s_1$ but not on $\mu$, such that for all $r \geq 1$,

$$\int_0^{2\pi} \{\mu(s_o,\phi)^2 + \mu(s_1,\phi)^2\} d\phi \leq \beta(r^{-1}\|\mu_s\|_o^2 + r\|\mu\|_o^2) \tag{2.7}$$

Proof: For any continuous function $y(x)$ with a square integrable first derivative in $a \leq x \leq b$ and any $r \geq 1$ it holds

$$|y(x)|^2 \leq \frac{2(b-a)}{2r+1} \int_a^b y'(t)^2 dt + \frac{2r^2}{(b-a)(2r-1)} \int_a^b y(t)^2 dt$$

$$\text{in } a \leq x \leq b \,. \tag{2.8}$$

((2.8) is the Sobolew inequality (see e.g. Agmon [6], p. 32) in a special case. The constants appearing on the right may be derived by elementary methods (Kato [1], p. 192-193)). Hence, we obtain for any $\mu(s,\phi)$ with the assumed properties, any $r \geq 1$ and any $0 \leq \phi \leq 2\pi$,

$$\mu(s_o,\phi)^2 + \mu(s_1,\phi)^2 \leq \frac{2(s_1-s_o)}{r} \int_{s_o}^{s_1} \mu_s(s,\phi)^2 ds + \frac{4r}{s_1-s_o} \int_{s_o}^{s_1} \mu(s,\phi)^2 ds$$

The lemma follows by integrating this inequality over $0 \leq \phi \leq 2\pi$

Now denote the quadratic form appearing in the first inequality in (1.14) with $Q_o(\underline{\eta})$. We then have

Cor 2.1: Let $\mu(s,\phi)$ satisfy the requirements a) - c) in the rectangle $\Sigma_o$ and assume that, in (1.14), $A_{max} \geq A(s) \geq A_{min} > 0$, $B_{max} \geq B(s) \geq B_{min} > 0$, $C_{max} \geq |C(s)|$ holds in $s_o \leq s \leq s_1$. Let $Q_o(\underline{\mu})$ be the quadratic form defined above. Then there exist positive constants $K_o$, $K_1$, $L_o$, $L_1$, depending on $s_o$, $s_1$, $A_{min}$, $A_{max}$, $B_{min}$, $B_{max}$ and $C_{max}$ but not on $\mu$, such that

$$K_o Q_o(\underline{\mu}) - L_o \|\mu\|_o^2 \leq \|\mu_s\|_o^2 + \|\mu_\phi\|_o^2 \leq K_1 Q_o(\underline{\mu}) + L_1 \|\mu\|_o^2 \tag{2.9}$$

Proof: The statement follows by using the mean value theorem and (2.7)(with a sufficiently large r to obtain the right inequality in (2.9)).

We remark, that the A(s), B(s) and C(s) in (1.14) will satisfy the above assumptions in some closed interval containing $[s_o,s_1]$ in its interior, because of (1.11) and the assumption that the unperturbed surface does not intersect the z-axis.

Our sufficiency proofs will rely mainly on the following perturbation result for the quadratic form $Q_o(\underline{\mu})$:

Lemma 2.2: Let A(s), B(s) and C(s) satisfy the requirements in Cor. 2.1, and let $\delta A(s,\phi)$, $\delta B(s,\phi)$ and $\delta C(s,\phi)$ be bounded and integrable in $\Sigma_o$. Further, let $\delta\alpha_o(\phi)$ and $\delta\alpha_1(\phi)$ be bounded and integrable in $0 \leq \phi \leq 2\pi$, let $\varepsilon > 0$ and let $\Phi$ be the functional

$$\Phi = \Phi(\delta A,\ \delta B,\ \delta C,\ \delta\alpha_o,\ \delta\alpha_1,\ \varepsilon)$$

$$= \inf \left\{ \int_0^{2\pi} \int_{s_o}^{s_1} \{(A + \delta A)\mu_s^2 + (B + \delta B)\mu_\phi^2 + (C + \delta C)\mu^2\}\, ds d\phi \right.$$

$$\left. + \int_0^{2\pi} \{(\alpha_o + \delta\alpha_o)\mu(s_o,\phi)^2 + (\alpha_1 + \delta\alpha_1)\mu(s_1,\phi)^2\}\, d\phi \right\} \tag{2.10}$$

over all $\mu$ satisfying conditions a) - c) above and such that

$$\begin{cases} \|\mu\|_o = 1 & (2.11) \\ |(A,\mu)_o| \leq \varepsilon(\|\mu_s\|_o + \|\mu_\phi\|_o + \|\mu\|_o) \ . & (2.12) \end{cases}$$

Let $\|f\|_\infty$ denote, as usual, the supremum of $|f|$ over the domain of f and assume that $\Phi_o = \Phi(0,0,0,0,0,0,) > 0$. Then there exists positive constants K and $\delta_o$ independent of $\delta A$, $\delta B$, $\delta C$, $\delta\alpha_o, \delta\alpha_1$, and $\varepsilon$, such that

$$\Phi \geq \Phi_o - K \cdot \delta_A \qquad (2.13)$$

holds true, if only

$$\delta_A = \|\delta A\|_\infty + \|\delta B\|_\infty + \|\delta C\|_\infty + \|\delta\alpha_o\|_\infty + \|\delta\alpha_1\|_\infty + \varepsilon \leq \delta_o \ . \qquad (2.14)$$

Remark: K and $\delta_o$ may depend on A, B, C, $\alpha_o$, $\alpha_1$, $s_o$ and $s_1$. A similar upper bound also exists, and the results apply, with obvious modifications, also to the case $\Phi_o < 0$.

Proof of Lemma 2.2: Let $Q_o(\underline{\mu})$ be defined as in Cor. 2.1 and denote, similarly, the quadratic form in (2.10) with $(Q_o + \delta Q_o)(\underline{\mu})$. Then, by (2.7) and (2.9), it holds for any $\mu$ satisfying (2.11) and conditions a) - c) above,

$$(1 - M_o \cdot \delta_A)Q_o(\underline{\mu}) - N_o \cdot \delta_A \leq (Q_o + \delta Q_o)(\underline{\mu}) \leq (1 + M_1 \cdot \delta_A)Q_o(\underline{\mu}) + N_1 \cdot \delta_A \qquad (2.15)$$

where $M_o$, $M_1$, $N_o$ and $N_1$ are positive constants, independent of $\delta A$, $\delta B$, $\delta C$, $\delta\alpha_o$, $\delta\alpha_1$, and $\varepsilon$. Since by (2.12) $\Phi$ is non-increasing as function of $\varepsilon$, we obtain from (2.15)

$$\Phi \leq (1 + M_1 \cdot \delta_A)\Phi_o + N_1 \cdot \delta_A \ . \qquad (2.16)$$

Now let e.g. $\delta_A \leq \frac{1}{2M_o}$ and assume that $\mu$ is any function satisfying a) - c), (2.11) and (2.12) such that

$$(Q_o + \delta Q_o(\underline{\mu}) \leq (1 + \frac{M_1}{N_o})\Phi_o + \frac{N_1}{M_o} \tag{2.17}$$

Then by (2.15) and (2.9),

$$\|\mu_s\|_o^2 + \|\mu_\phi\|_o^2 \leq M_2\phi_o + N_2 \tag{2.18}$$

for some positive constants $M_2$ and $N_2$, independent of $\delta A$, $\delta B$, $\delta C$, $\delta\alpha_o$, $\delta\alpha_1$ and $\varepsilon$. Obviously, then, when forming the infimum in (2.10), only the subset of $\mu$ satisfying (2.18) need to be considered. Now put

$$f^*(s,\phi) = (s - s_o)(s_1 - s) \tag{2.19}$$

$$\tilde{\mu} = C_1(\mu - C_2 f^*) \tag{2.20}$$

where $C_1$ and $C_2$ are chosen so as to make $\tilde{\mu}$ satisfy (2.11) and (2.12) with $\varepsilon = 0$, i.e.:

$$C_2 = \frac{(A,\mu)_o}{(A,f^*)_o} \quad ; \quad C_1 = \frac{1}{\|\mu - C_2 f^*\|_o} \tag{2.21}$$

Notice that $(A,f^*)_o$ is a positive constant, dependent only on A, $s_o$ and $s_1$. By (2.11), (2.12), (2.14), (2.18) and (2.21),

$$|C_2| \leq C_3\delta_A \quad ; \quad \frac{1}{C_1} \geq 1 - C_4\delta_A \tag{2.22}$$

Here, and below, $C_k$, k = 3,4,5... will be some positive constants, independent of $\delta A$, $\delta B$, $\delta C$, $\delta\alpha_o$, $\delta\alpha_1$ and $\varepsilon$. Now form, noting that $f^*(s,\phi)$ vanishes on $s = s_o$ and $s = s_1$,

$$\begin{aligned} &Q_o(\underline{\mu} - C_2\underline{f^*}) - Q_o(\underline{\mu}) \\ &= C_2^2 Q_o(\underline{f^*}) - 2C_2\int_0^{2\pi}\int_{s_o}^{s_1}\{A(s)\mu_s f_s^* + C(s)\mu f^*\}dsd\phi \ . \end{aligned} \tag{2.23}$$

Using the mean value theorem and Schwartz inequality in the last term, we obtain by (2.22) and (2.18)

$$Q_o(\underline{\mu} - C_2\underline{f}^*) - Q_o(\underline{\mu}) \leq C_5\delta_A + C_6\delta_A^2 \tag{2.24}$$

We can now form

$$\begin{aligned}\Phi_o - (Q_o + \delta Q_o)(\underline{\mu}) &\leq Q_o(\tilde{\underline{\mu}}) - (Q_o + \delta Q_o)(\underline{\mu}) \\ &\leq C_1^2 Q_o(\underline{\mu} - C_2\underline{f}^*) - (1 + M_o\delta_A)Q_o(\underline{\mu}) + N_o\delta_A \\ &= C_1^2\{Q_o(\underline{\mu} - C_2\underline{f}^*) - Q_o(\underline{\mu})\} + (C_1^2 - 1 - M_o\delta_A)Q_o(\underline{\mu}) + N_o\delta_A ,\end{aligned} \tag{2.25}$$

where we have used, in turn, the definition of $\Phi_o$ and (2.15). Then we use (2.22), (2.24), (2.15) and (2.17) to obtain

$$\Phi_o \leq (Q_o + \delta Q_o)(\underline{\mu}) + K \cdot \delta_A \tag{2.26}$$

if only $\delta_A \leq \delta_o$, where e.g. $\delta_o = \min\left\{\frac{1}{2C_4}, \frac{1}{2M_o}\right\}$ and K is some positive constant, independent of $\delta A$, $\delta B$, $\delta C$, $\delta\alpha_o$, $\delta\alpha_1$, $\varepsilon$ and $\mu$. The statement of Lemma 2.2 follows immediately from (2.26).

For the case $\gamma = 0$ we will need a slightly modified version of the above result:

Lemma 2.3: Let the assumptions of Lemma 2.2 hold and let $\Phi = \Phi(\delta A, \delta B, \delta C)$ be defined as in (2.10), (2.11), (2.12) but under the additional condition:

$$\mu(s_o,\phi) = \mu(s_1,\phi) = 0 \quad , \quad 0 \leq \phi \leq 2\pi \tag{2.27}$$

Put $\Phi_o = \Phi(0,0,0)$. Then (2.13) holds true, where now

$$\delta_A = \|\delta A\|_\infty + \|\delta B\|_\infty + \|\delta C\|_\infty \leq \delta_o \ . \tag{2.28}$$

Remark: The constants K, $\delta_o$ may possibly be different from those applying to the case of Lemma 2.2.

The proof of Lemma 2.3 is similar to that of Lemma 2.2 and is omitted. We notice, though, that when the boundary terms are lacking in the quadratic form $Q_o$ and $Q_o + \delta Q_o$, (2.15) is a simple consequence of the mean value theorem and the strict positivity of A(s) and B(s), so that Lemma 2.7 is not needed for the proof.

## 3. SUFFICIENT CONDITIONS FOR THE CASE $\gamma > 0$

The following theorem specifies sufficient conditions for stability in the general case $\gamma > 0$:

Theorem 3.1: Let $\gamma > 0$ in (1.1) and assume that the perturbed surface satisfies the Euler equations (1.11) with the associated boundary conditions. Let further $\lambda_o > 0$ in (1.18) and let $d(\eta)$ be defined as in (2.1). Then there exists a constant $d_o > 0$, such that in (1.5)

$$\delta E(\eta) \geq 0 \text{ with equality iff } \eta = 0 \text{ in } \Sigma \tag{3.1}$$

holds for all $\eta$ satisfying the volume constraint $\delta V(\eta) = 0$ in (1.6), the conditions a) - d) of Section 2 and

$$d(\eta) \leq d_o \tag{3.2}$$

Proof: Denote again the quadratic form in (1.14) with $Q_o(\underline{\eta})$. Then by the definitions (1.15) - (1.19) and by the representation theorem for quadratic forms in Hilbert space (Kato [1], p. 322-323):

$$\inf Q_o(\underline{\mu}) = \lambda_o > 0 \tag{3.3}$$

where the infimum is taken over all $\mu$ satisfying a) - d) of Section 2 and

$$\|\mu\|_o = 1 \tag{3.4}$$

$$(A,\mu)_o = 0 \ . \tag{3.5}$$

Now consider the expressions (1.5) and (1.6) for $\delta E(\eta)$ and $\delta V(\eta)$. Firstly, since $R(s)$ is positive in some open interval containing $[s_o,s_1]$ there exists by (2.2) some $d_1 \geq 0$ such that if $d(\Sigma) \leq d_1$, then $R(s) \geq R_o > 0$ in $\Sigma$. By (1.8) then, when $d(\Sigma) \leq d_1$ there exists some constant $d_2 > 0$, such that the functions $f_A(\underline{\eta},s)$, $f_g(\underline{\eta},s)$ and $f_V(\underline{\eta},s)$ are analytic in the arguments $\eta$, $\eta_s$ and $\eta_\phi$ in the region $|\eta| + |\eta_s| + |\eta_\phi| \leq d_2$ at all points of $\Sigma$. By (2.1) then at all points of $\Sigma$ where $\eta_s$ and $\eta_\phi$ are continuous, we obtain by Taylor expanding at $\underline{\eta} = \underline{0}$:

$$f_A(\underline{\eta},s) - f_A(\underline{0},s) = \frac{\partial f_A}{\partial \eta}(\underline{0},s) \cdot \eta + \frac{1}{2}\underline{\eta}^T f_{A\underline{\eta}\underline{\eta}}(\underline{0},s)\underline{\eta} + h_A(\underline{\eta},s)$$

$$f_g(\underline{\eta},s) = \frac{\partial f_g}{\partial \eta}(\underline{0},s) \cdot \eta + \frac{1}{2}\underline{\eta}^T f_{g\underline{\eta}\underline{\eta}}(\underline{0},s)\underline{\eta} + h_g(\underline{\eta},s) \tag{3.6}$$

$$f_V(\underline{\eta},s) = \frac{\partial f_V}{\partial \eta}(\underline{0},s) \cdot \eta + \frac{1}{2}\underline{\eta}^T f_{V\underline{\eta}\underline{\eta}}(\underline{0},s)\underline{\eta} + h_V(\underline{\eta},s)$$

where, for some positive constants $C_A$, $C_g$ and $C_V$, independent of $\underline{\eta}$,

$$|h_A(\underline{\eta},s)| \le C_A \cdot d(\eta)(\eta_s^2 + \eta_\phi^2 + \eta^2)$$

$$|h_g(\underline{\eta},s)| \le C_g \cdot d(\eta)\eta^2 \tag{3.7}$$

$$|h_V(\underline{\eta},s)| \le C_V \cdot d(\eta)\eta^2$$

if only $d(\eta) \le d_2$. Secondly, since the perturbed surface and the container wall intersect at $s = s_i(\phi)$, we have $w(s_i(\phi)) = \eta(s_i(\phi),\phi)$, $0 \le \phi \le 2\pi$, $i=0,1$. Hence, since by (1.11) $w'(s_i) = (-1)^{i+1}\tan\gamma \neq 0$, we obtain by the inverse function theorem

$$s_i(\phi) - s_i = \frac{\eta(s_i(\phi),\phi)}{w'(s_i)} + h_s(\eta(s_i(\phi),\phi)) \tag{3.8}$$

where, for some positive constants $d_3$ and $C_s$, $|h_s(\eta)| \le C_s\eta^2$ when $|\eta| \le d_3$. Now inserting the expression (3.6) for $f_V$ into (1.6) and using the volume constraint $\delta V(\eta) = 0$ we get

$$\int_0^{2\pi}\int_{s_o(\phi)}^{s_1(\phi)} \frac{\partial f_V}{\partial \eta}(\underline{0},s)\eta\, ds d\phi$$

$$= \int_0^{2\pi}\int_{s_o(\phi)}^{s_1(\phi)} -\left\{\frac{1}{2}\underline{\eta}^T f_{V\underline{\eta}\underline{\eta}}(\underline{0},s)\underline{\eta} + h_V(\underline{\eta},s)\right\} ds d\phi - \int_0^{2\pi}\int_{\Delta\phi} f_V(\underline{w},s)\, ds d\phi. \tag{3.9}$$

Similarly inserting (3.6) for $f_A$ and $f_g$ into (1.5) and using (1.9) and (3.9) gives

$$\delta E(\eta) = \int_0^{2\pi} \int_{s_o(\phi)}^{s_1(\phi)} \left\{ \frac{1}{2} \underline{\eta}^T \left\{ f_{A\underline{\eta}\underline{\eta}}(\underline{0},s) + f_{g\underline{\eta}\underline{\eta}}(\underline{0},s) - \lambda f_{V\underline{\eta}\underline{\eta}}(\underline{0},s) \right\} \underline{\eta} + h(\underline{\eta},s) \right\} ds d\phi$$

$$+ \int_0^{2\pi} \int_{\Delta\phi} \left\{ \cos\gamma f_A(\underline{w},s) - f_A(\underline{0},s) + f_g(\underline{w},s) - \lambda f_V(\underline{w},s) \right\} ds d\phi \quad , \qquad (3.10)$$

where $h(\underline{\eta},s) = h_A(\underline{\eta},s) + h_g(\underline{\eta},s) - \lambda h_V(\underline{\eta},s)$ satisfies by (3.7),

$$|h(\underline{\eta},s)| \leq C \cdot d(\eta)(\eta_s^2 + \eta_\phi^2 + \eta^2) \qquad (3.11)$$

at all points of $\Sigma$ where $\eta_s$ and $\eta_\phi$ are continuous. Here again $C$ is some positive constant independent of $\eta$, and we have assumed $d(\eta) \leq d_2$ as in (3.7). Introduce for the second integrand in (3.10) for convenience

$$f_R(s) = \cos\gamma\, f_A(\underline{w},s) - f_A(\underline{0},s) + f_g(\underline{w},s) - \lambda f_V(\underline{w},s) \qquad (3.12)$$

Then, by (1.7) - (1.9), $f_R(s_o) = f_R(s_1) = 0$. Assuming $w(s)$ to be sufficiently smooth for $f_R$ to be twice continuously differentiable in some neighborhoods of $s = s_o$ and $s = s_1$ and using the definition (1.7) for $\Delta\phi$, Taylor's theorem gives

$$\int_{\Delta\phi} f_R(s)ds = \sum_{i=0}^{1} \frac{(-1)^{i+1}}{2} f_R'(s_i)(s_i(\phi) - s_i)^2 + h_i(\phi) \qquad (3.13)$$

where, for some positive constants $d_3$, $C_o$ and $C_1$, independent of $\phi$, $|h_i(\phi)| \leq C_i |s_i(\phi) - s_i|^3$, if only $d(\Sigma) \leq d_3$. Using (3.8), (3.13) and the notation in (1.13) and (1.14), (3.10) takes the form

$$\delta E(\eta) = \int_0^{2\pi} \int_{s_o(\phi)}^{s_1(\phi)} \left\{ \frac{1}{2}\{A(s)\eta_s^2 + B(s)\eta_\phi^2 + C(s)\eta^2\} + h(\eta,s)\right\} ds d\phi$$

$$+ \frac{1}{2}\int_0^{2\pi} \left\{ \{\alpha_o + \delta\alpha_o(\phi)\}\eta(s_o(\phi),\phi)^2 + \{\alpha_1 + \delta\alpha_1(\phi)\}\eta(s_1(\phi),\phi)^2 \right\} d\phi \qquad (3.14)$$

where (3.11) and

$$|\delta\alpha_i(\phi)| \leq C_R \cdot d(\eta) \quad , \quad i=0,1 \qquad (3.15)$$

hold, if only $d(\eta) + d(\Sigma) \leq d_4$, where again $C_R$ and $d_4$ are positive constants independent of $\eta$. Treating the last integral in (3.9) by Taylor expanding the integrand in the same way as in (3.12) - (3.13) and using (3.8) the volume constraint gives

$$\left| \int_0^{2\pi} \int_{s_o}^{s_1} A(s)\eta ds d\phi \right|$$

$$\leq K_{V1} \int_0^{2\pi} \int_{s_o}^{s_1} \eta(s,\phi)^2 ds d\phi + K_{V2} \int_0^{2\pi} \{\eta(s_o(\phi),\phi)^2 + \eta(s_1(\phi),\phi)^2\} d\phi \qquad (3.16)$$

if only $d(\eta) + d(\Sigma) \leq d_5$, for some positive $\eta$-independent constants $K_{V1}, K_{V2}$ and $d_5$.

In order to relate the above expressions for $\delta E(\eta)$ and $\delta V(\eta)$ to the conditions (3.3) - (3.5)(which involve integrals over the rectangle $\Sigma_o$) we now perform a transformation of variable in (3.14) and (3.16):

$$s = s(s',\phi) = s_o(\phi) + \frac{s' - s_o}{s_1 - s_o}(s_1(\phi) - s_o(\phi)) \qquad (3.17)$$

$$\mu(s',\phi) = \eta(s(s',\phi),\phi) \qquad (3.18)$$

We note, in particular, that $\mu$ will satisfy the requirements a) - c) of Section 2 if only $d(\Sigma)$ is sufficiently small to ensure $|s_1(\phi) - s_o(\phi)| \geq s_{min} > 0$ in $0 \leq \phi \leq 2\pi$. Furthermore

$$
\begin{aligned}
s &= s' + k_1(s',\phi) \\
\frac{\partial(s,\phi)}{\partial(s',\phi)} &= 1 + k_2(\phi) \\
\eta_s(s(s',\phi),\phi) &= (1 + k_2(\phi))\mu_{s'}(s',\phi) \\
\eta_\phi(s(s',\phi),\phi) &= \mu_\phi(s',\phi) + k_3(s',\phi) \cdot \mu_{s'}(s',\phi)
\end{aligned}
\tag{3.19}
$$

where, for some positive constants $d_6$ and $C_1$ independent of $\eta$,

$$
\sup \left\{ |k_1(s',\phi)|, |k_2(\phi)|, |k_3(s',\phi)| \right\} \leq C_1 \cdot d(\Sigma) \tag{3.20}
$$

at all $s_o \leq s' \leq s_1$ and all $0 \leq \phi \leq 2\pi$ where $s_o'(\phi)$ and $s_1'(\phi)$ are continuous, if only $d(\Sigma) \leq d_6$.

Inserting (3.17) - (3.19) into (3.14) and (3.16) we get:

$$
\begin{aligned}
\delta E(\eta) = &\int_0^{2\pi} \int_{s_o}^{s_1} \frac{1}{2} \left\{ (A + \delta A)\mu_{s'}^2 + (B + \delta B)\mu_\phi^2 + (C + \delta C)\mu^2 \right\} ds'd\phi \\
&+ \int_0^{2\pi} \frac{1}{2} \left\{ (\alpha_o + \delta\alpha_o(\phi))\mu(s_o,\phi)^2 + (\alpha_1 + \delta\alpha_1(\phi))\mu(s_1,\phi)^2 \right\} d\phi
\end{aligned}
\tag{3.21}
$$

and

$$
\begin{aligned}
&\left| \int_0^{2\pi} \int_{s_o}^{s_1} (A + \delta' A)\mu ds'd\phi \right| \\
&\leq K_{V3} \|\mu\|_o^2 + K_{V2} \int_0^{2\pi} \left\{ \mu(s_o,\phi)^2 + \mu(s_1,\phi)^2 \right\} d\phi \quad ,
\end{aligned}
\tag{3.22}
$$

where, by (3.11), (3.19) and (3.20), $\delta A$, $\delta B$, $\delta C$ and $\delta' A$ are functions of $s'$ and $\phi$, integrable in $\Sigma_o$ and such that

$$\sup\{|\delta A(s',\phi)| + |\delta B(s',\phi)| + |\delta C(s',\phi)| + |\delta' A(s',\phi)|\} \leq C_2\{d(\eta) + d(\Sigma)\} \quad (3.23)$$

when $d(\eta) + d(\Sigma) \leq d_7$ where $C_2$ and $d_7$ are some positive constants, independent of $\eta$. The supremum in (3.23) is formed over all points of $\Sigma_o$ where the functions are continuous. Note, in particular, that the argument in the functions A, B and C in (3.21) and (3.22) is $s'$, whence in obtaining (3.23) we have made use of the fact that A, B and C of (3.14) (as defined in (1.14)) have a bounded derivative in $\Sigma$ (they are in fact analytic functions of s), if only $d(\Sigma)$ is sufficiently small.

Using Lemma 2.1, (3.23) and the mean-value theorem in (3.22) gives in a straightforward way

$$|(A,\mu)_o| \leq C_3 \cdot \{d(\eta) + d(\Sigma)\}(\|\mu_s\|_o + \|\mu_\phi\|_o + \|\mu\|_o) \quad (3.24)$$

if only $d(\eta) + d(\Sigma) \leq d_8$, where $C_3$ and $d_8$ are some positive constants, independent of $\eta$.

Now using Lemma 2.2 on (3.21) and (3.24) (noting (3.15) and (3.23)) we conclude by (3.3) that, e.g.,

$$\delta E(\eta) \geq \frac{\lambda_o}{3}\|\mu\|_o^2 \quad (3.25)$$

if only

$$d(\eta) + d(\Sigma) \leq d_9 \quad (3.26)$$

for some $\eta$-independent constant $d_9$. Since, however $w(s_i(\phi)) = \eta(s_i(\phi),\phi)$, $0 \leq \phi \leq 2\pi$, $i=0,1$, it holds

$$s_i'(\phi) = \frac{\eta_\phi(s_i(\phi),\phi)}{w'(s_i(\phi)) - \eta_s(s_i(\phi),\phi)} \quad (3.27)$$

at all points of the boundary of $\Sigma$, where $\eta_\phi$ and $\eta_s$ are continuous. Since

further $w'(s_i) = (-1)^{i+1} \tan \gamma \neq 0$, it follows from (3.27) that

$$d(\Sigma) \leq C_4 d(\eta) \tag{3.28}$$

if only $d(\eta) \leq d_{10}$, where $d_{10}$ and $C_4$ are some positive, $\eta$-independent constants. Hence, by (3.26) and (3.28), (3.25) holds true, if only $d(\eta) \leq d_o$, where $d_o$ is some $\eta$-independent constant, and the first part of the statement (3.1) of Theorem 3.1 follows. Since, by (3.18), $\|\eta\| = 0$ if and only if $\|\mu\|_o = 0$, the second part of the statement also follows from (3.25).

## 4. SUFFICIENT CONDITIONS IN THE CASE $\gamma = 0$

In this section we will show that the statement of Theorem 3.1 also holds in the limit $\gamma = 0$ (defining the limit of the boundary conditions in (1.17) as $|\alpha_j| \to \infty$, j=0,1 to be (1.20)), if the curvatures of the unperturbed surface and the container wall are not equal at the unperturbed contact lines. The statement is, in more precise terms, the following:

Theorem 4.1: Let $\gamma = 0$ in (1.1) and assume that the unperturbed surface satisfies the Euler equations (1.11) and the associated boundary conditions at $s = s_o$ and $s = s_1$. Assume further that the function w(s) of (1.4) satisfies

$$w''(s_i) < 0 \quad , \quad i=0,1 \tag{4.1}$$

Let $\lambda_o$ be defined as in (1.17 - 1.19), but with the boundary conditions of (1.17) replaced by (1.20), and assume that $\lambda_o > 0$. Let $d(\eta)$ and $d(\Sigma)$ be defined as in (2.1) and (2.2). Then there exists a constant $d_o > 0$, such that in (1.5)

$$\delta E(\eta) \geq 0 \text{ with equality iff } \eta = 0 \text{ in } \Sigma \tag{4.2}$$

holds for all $\eta$ satisfying the volume constraint $\delta V(\eta) = 0$ in (1.6), the conditions a) - d) of Section 2 and the condition

$$d(\eta) + d(\Sigma) \leq d_o \, . \tag{4.3}$$

Remark: In the case $\gamma = 0$, both the energy (1.1) and the liquid volume of any configuration are unchanged if the liquid-vapor interface is continued by "wetting" the "dry" container walls (and we will make use of this property of the "wetting" perturbation in the proof below). With $\Sigma$ in (4.2) (see also the beginning of Section 2) for such "wetting" perturbations is meant a closed domain, containing no interior points where the liquid-vapor interface coincides with the container walls (i.e. possibly wetted portions of the container walls are not included in the $\Sigma$). Note, further, that since by (1.11) $w'(s_i) = 0$, i=0,1, and since $w(s) < 0$ for $s_o < s < s_1$, we must have $w''(s_i) \leq 0$, i=0,1. $w''(s_i) = 0$

means by (1.4) that the curvatures of the unperturbed surface and the wall coincide at the unperturbed contact line $s = s_i$ (and is a limiting case among all solutions to (1.11) that correspond to permissible liquid-tank configurations).

Proof of Theorem 4.1: Let again $Q_o(\underline{\eta})$ be the quadratic form in (1.14). Then, as in (3.3)

$$\inf Q_o(\underline{\mu}) = \lambda_o > 0 \tag{4.4}$$

where the infimum is taken over all $\mu$ satisfying a) - d) of Section 2 and the conditions:

$$\|\mu\|_o = 1 \tag{4.5}$$

$$(A,\mu)_o = 0 \tag{4.6}$$

$$\mu(s_o,\phi) = \mu(s_1,\phi) = 0 \quad , \quad 0 \leq \phi \leq 2\pi \ . \tag{4.7}$$

Here we denote, for brevity,

$$f_E(\underline{\eta},s) = f_A(\underline{\eta},s) - f_A(\underline{0},s) + f_g(\underline{\eta},s) - \lambda f_V(\underline{\eta},s) \tag{4.8}$$

where $f_A$, $f_g$ and $f_V$ are the functions in (1.8). Then, as in (3.10), we have since $\gamma = 0$,

$$\delta E(\eta) = \int_0^{2\pi} \int_{s_o(\phi)}^{s_1(\phi)} f_E(\underline{\eta},s)\,ds\,d\phi - \int_0^{2\pi} \int_{\Delta\phi} f_E(\underline{w},s)\,ds\,d\phi \tag{4.9}$$

Now denote, for convenience in the following,

$$\begin{aligned} \Sigma_+ &= \text{complement of } (\Sigma \cap \Sigma_o) \text{ w.r.t. } \Sigma \\ \Sigma_- &= \text{complement of } (\Sigma \cap \Sigma_o) \text{ w.r.t. } \Sigma_o \end{aligned} \tag{4.10}$$

Let $\tilde{\eta}(s,\phi)$ be the function obtained by extending $\eta(s,\phi)$ by "wetting" those parts of the container walls which were "dried" because of the perturbation $\eta$, i.e.:

$$\tilde{\eta}(s,\phi) = \begin{cases} \eta(s,\phi) \text{ in } \Sigma \\ \\ w(s) \text{ in } \Sigma_- \ . \end{cases} \tag{4.11}$$

Put, further, $\tilde{\Sigma} = \Sigma \cup \Sigma_o = \Sigma_- \cup \Sigma_+$ , with the boundaries

$$\begin{cases} \tilde{s}_o(\phi) = \min\{s_o(\phi), s_o\} \\ \\ \tilde{s}_1(\phi) = \max\{s_1(\phi), s_1\} \end{cases} \qquad 0 \leq \phi \leq 2\pi \ . \tag{4.12}$$

Then it follows from (4.9) (and, more generally, from the remark after the statement of Theorem 4.1), that

$$\delta E(\eta) = \int_0^{2\pi} \int_{\tilde{s}_o(\phi)}^{\tilde{s}_1(\phi)} f_E(\underline{\tilde{\eta}},s)\,ds\,d\phi - \int_0^{2\pi} \int_{\tilde{\Delta}\phi} f_E(\underline{w},s)\,ds\,d\phi \tag{4.13}$$

where $\tilde{\Delta}\phi$ is defined from $\tilde{s}_o(\phi)$ and $\tilde{s}_1(\phi)$ as in the last formula in (1.7) (in other words, the domains of integration in (4.13) are $\tilde{\Sigma}$ and $\Sigma_+$, respectively). Put further

$$\eta^*(s,\phi) = \begin{cases} 0 \text{ in } \Sigma_o \\ \\ w(s) \text{ in } \Sigma_+ \end{cases} \tag{4.14}$$

$$\nu(s,\phi) = \tilde{\eta}(s,\phi) - \eta^*(s,\phi) \text{ in } \tilde{\Sigma} \tag{4.15}$$

Then, noting that $f_E(\underline{0},s) = 0$, it follows from (4.13), that

$$\delta E(\eta) = \int_0^{2\pi} \int_{\tilde{s}_o(\phi)}^{\tilde{s}_1(\phi)} \{f_E(\underline{\eta}^* + \underline{\nu}, s) - f_E(\underline{\eta}^*, s)\} \, ds d\phi \tag{4.16}$$

Similarly, we obtain by (1.6)

$$\delta V(\eta) = \int_0^{2\pi} \int_{\tilde{s}_o(\phi)}^{\tilde{s}_1(\phi)} \{f_V(\underline{\eta}^* + \underline{\nu}, s) - f_V(\underline{\eta}^*, s)\} \, ds d\phi \tag{4.17}$$

We note, in particular, that $\tilde{\eta}$, $\eta^*$, $\nu$ and $\tilde{s}_i$, i=0,1 will satisfy the requirements a) - d) of Section 2 and further that, since $w(s) = w''(s_i)(s-s_i)^2/2 + 0(s-s_i)^3$ in the neighbourhood of $s = s_i$, i = 0,1, it holds

$$\begin{aligned} d(\tilde{\Sigma}) &\leq d(\Sigma) \\ d(\eta^*) &\leq C_1 d(\Sigma) \\ d(\tilde{\eta}) &\leq C_1 \{d(\eta) + d(\Sigma)\} \\ d(\nu) &\leq C_1 \{d(\eta) + d(\Sigma)\} \end{aligned} \tag{4.18}$$

if only $d(\eta) + d(\Sigma) \leq d_1$, where $C_1$ and $d_1$ are some $\eta$-independent constants. Also, as in (3.6) the integrands in (4.16) and (4.17) are analytic in the arguments $\eta^*$, $\eta^*_s$, $\eta^*_\phi$ and $\nu$, $\nu_s$, $\nu_\phi$ in some region $|\underline{\eta}^*| + |\underline{\nu}| \leq d_2$ where $d_2$ is an $\eta$-independent constant. By (4.18) then, we may Taylor expand the integrands in (4.16) and (4.17) at all points of $\tilde{\Sigma}$ where $\underline{\eta}^*$ and $\underline{\nu}$ are continuous, if only $d(\eta) + d(\Sigma) \leq d_3$, where $d_3$ is some $\eta$-independent constant. We obtain

$$\begin{aligned} &f_E(\underline{\eta}^* + \underline{\nu}, s) - f_E(\underline{\eta}^*, s) \\ &= f_{E\underline{\nu}}(\underline{\eta}^*, s)^T \cdot \underline{\nu} + \frac{1}{2} \underline{\nu}^T f_{E\underline{\eta}\underline{\eta}}(\underline{0}, s) \underline{\nu} + h_E(\underline{\eta}^*, \underline{\nu}, s) \end{aligned} \tag{4.19}$$

and

$$f_V(\underline{\eta}^* + \underline{\nu}, s) - f_V(\underline{\eta}^*, s) = \frac{\partial f_V}{\partial \eta}(\underline{0}, s) \cdot \nu + h_V(\underline{\eta}^*, \underline{\nu}, s) \tag{4.20}$$

Where, by (4.18) and noting from (1.9) that $f_{E\underline{\eta}}(\underline{0},s) = \underline{0}$,

$$|h_E(\underline{\eta}^*,\underline{\nu},s)| \leq C_2\{d(\eta) + d(\Sigma)\}(\nu_s^2 + \nu_\phi^2 + \nu^2) \tag{4.21}$$

$$|h_V(\underline{\eta}^*,\underline{\nu},s)| \leq C_2\{d(\eta) + d(\Sigma)\}(|\nu_s| + |\nu_\phi| + |\nu|) \tag{4.22}$$

if only $d(\eta) + d(\Sigma) \leq d_4$, where $d_4$ and $C_2$ are some $\eta$-independent positive constants.

Now, by (1.8), (1.9) and (4.8), the first term to the right in (4.19) is of the form

$$f_{E\underline{\eta}}(\underline{\eta}^*,s)^T \cdot \underline{\nu} = \begin{cases} 0 \text{ in } \Sigma_o \\ \\ f_{E\underline{\eta}}(\underline{w},s)^T \cdot \underline{\nu} \end{cases}$$

$$= \{A(s) + D_A(s)\}w'(s)\nu_s + \{C(s) + D_C(s)\}w(s)\nu \quad \text{in } \Sigma_+ \tag{4.23}$$

where $A(s) = \sigma R(s)$ and $C(s)$ are the functions introduced in (1.14) and where

$$|D_A(s)| + |D_C(s)| \leq C_3\{|w(s)| + w'(s)^2\} \tag{4.24}$$

if only $d(\Sigma) \leq d_5$, where $d_5$ and $C_3$ are some positive, $\eta$-independent constants. Further, $D_A(s)$ is continuously differentiable in the interior of $\Sigma_+$ if $w''(s)$ is continuous there.

Now consider the contribution of the terms in (4.23) to the energy integral (4.16):

$$\int_0^{2\pi}\int_{\tilde{s}_o(\phi)}^{\tilde{s}_1(\phi)} f_{E\underline{\eta}}(\underline{\eta}^*,s)^T \cdot \underline{\nu}\, ds d\phi = \int_0^{2\pi}\int_{\tilde{\Delta}\phi} f_{E\underline{\eta}}(\underline{w},s)^T \cdot \underline{\nu}\, ds d\phi \tag{4.25}$$

$$= \int_0^{2\pi}\int_{\tilde{\Delta}\phi} \{\{A(s) + D_A(s)\}w'(s)\nu_s + \{C(s) + D_C(s)\}w(s)\nu\} ds d\phi .$$

By partial integration of the first term over $\tilde{\Delta}\phi = (\tilde{s}_o(\phi), s_o) \cup (s_1, \tilde{s}_1(\phi))$, noting that $w'(s_i) = 0$, $i=0,1$, and that $\nu(\tilde{s}_i(\phi),\phi) = 0$, $0 \le \phi \le 2\pi$ by (4.15) we get

$$\int_0^{2\pi} \int_{\tilde{s}_o(\phi)}^{\tilde{s}_1(\phi)} f_{E\underline{\eta}}(\underline{\eta}^*, s)^T \cdot \underline{\nu}\, ds d\phi$$

$$= \int_0^{2\pi} \int_{\tilde{\Delta}\phi} \left\{ -\frac{d}{ds}\left\{(A(s) + D_A(s))w'(s)\right\} + \left\{C(s) + D_C(s)\right\} w(s) \right\} \nu ds d\phi \,. \tag{4.26}$$

Note that it holds in $\tilde{\Delta}\phi$, if $d(\Sigma)$ is sufficiently small,

$$\begin{aligned} &A(s) = \sigma R(s) \ge R_o > 0 \\ &w(s) = \tfrac{1}{2} w''(s_i)(s - s_i)^2 + O(s - s_i)^3 \,, \\ &\nu(s,\phi) \ge 0 \text{ (with strict inequality in interior points)} \,, \\ &\tilde{s}_o(\phi) \le s_o \text{ and } s_1 \le \tilde{s}_1(\phi) \quad , \quad 0 \le \phi \le 2\pi \,. \end{aligned} \tag{4.27}$$

The last two formulas follow from (4.15) and (4.12), respectively. Using (4.27) and (4.24) we then see that <u>since $w''(s_i) < 0$, $i=0,1$, the last integrand in (4.26) is non-negative in $\tilde{\Delta}\phi$</u> (with $-A(s) \cdot w''(s) \cdot \nu(s,\phi)$ as the dominating term), if only $d(\Sigma)$ is sufficiently small. Consequently,

$$\int_0^{2\pi} \int_{\tilde{\Delta}\phi} f_{E\underline{\eta}}(\underline{\eta}^*, s)^T \cdot \underline{\nu}\, ds d\phi \ge 0 \tag{4.28}$$

if only $d(\Sigma) \le d_6$ where $d_6$ is some $\eta$-independent constant. (4.16) and (4.19) then give, using the notation of (1.14)

$$\delta E(\eta) \ge \frac{1}{2} \int_0^{2\pi} \int_{\tilde{s}_o(\phi)}^{\tilde{s}_1(\phi)} \left\{ A(s)\nu_s^2 + B(s)\nu_\phi^2 + C(s)\nu^2 + 2h_E(\underline{\eta}^*, \underline{\nu}, s) \right\} ds d\phi \tag{4.29}$$

where $\nu(s,\phi)$ satisfies the volume constraint $\delta V = 0$, which by (4.17) and (4.20) is of the form

$$\int_0^{2\pi} \int_{\tilde{s}_o(\phi)}^{\tilde{s}_1(\phi)} A(s) \cdot \nu ds d\phi = -\sigma \cdot \int_0^{2\pi} \int_{\tilde{s}_o(\phi)}^{\tilde{s}_1(\phi)} h_V(\underline{\eta}^*, \underline{\nu}, s)\, ds d\phi \tag{4.30}$$

Again, the functions $h_E$ and $h_V$ of (4.29) and (4.30) will satisfy (4.21) and (4.22), if only $d(\eta) + d(\Sigma) \leq d_7$, where $d_7$ is some $\eta$-independent constant.

In order to relate (4.29) - (4.30) to the properties (4.4) - (4.7) of the quadratic form $Q_o$, we proceed as in the proof of Theorem 3.1 by introducing a change of variable:

$$\begin{cases} s = s(s',\phi) = \tilde{s}_o(\phi) + \dfrac{s' - s_o}{s_1 - s_o}(\tilde{s}_1(\phi) - \tilde{s}_o(\phi)) & (4.31) \\ \\ \mu(s',\phi) = \nu(s(s',\phi),\phi) & (4.32) \end{cases}$$

(4.31) takes $\tilde{\Sigma}$ onto the rectangle $\Sigma_o$ and the transformation satisfies (3.19) (with $\eta$ replaced by $\nu$) and (3.20). Furthermore, by (4.15) and (4.32), $\mu(s',\phi)$ will satisfy (4.7). Using, in addition, (4.21) and (4.22) we obtain in the same way as for (3.21) and (3.24),

$$\delta E(\eta) = \int_0^{2\pi} \int_{s_o}^{s_1} \frac{1}{2}\{(A + \delta A)\mu_{s'}^2 + (B + \delta B)\mu_\phi + (C + \delta C)\mu^2\} ds d\phi\,, \tag{4.32}$$

where $\delta A(s',\phi)$, $\delta B(s',\phi)$, $\delta C(s',\phi)$ are bounded and integrable on $\Sigma_o$ with

$$|(\dot{A},\mu)_o| \leq C_4\{d(\eta) + d(\Sigma)\}\{\|\mu_{s'}\|_o + \|\mu_\phi\|_o + \|\mu\|_o\}, \tag{4.33}$$

$$\|\delta A\|_\infty + \|\delta B\|_\infty + \|\delta C\|_\infty \leq C_4\{d(\eta) + d(\Sigma)\} \tag{4.34}$$

if $d(\eta) + d(\Sigma) \leq d_8$, where $C_4$ and $d_8$ are some positive constants, independent of $\eta$. We can then apply Lemma 2.3 to conclude by (4.4), that e.g.

$$\delta E(\eta) \geq \frac{\lambda_o}{3}\|\mu\|_o^2 \tag{4.35}$$

if only $d(\eta) + d(\Sigma) \leq d_o$, where $d_o$ is some $\eta$-independent, positive constant Since, furthermore, by (4.11), (4.14) and (4.15) $\nu \equiv 0$ in $\tilde{\Sigma}$ if and only if $\eta \equiv 0$ in $\Sigma$ and since by (4.32) $\|\mu\|_o = 0$ if and only if $\nu \equiv 0$ in $\tilde{\Sigma}$, (4.35) completes the proof of Theorem 4.1.

## 5. EXPLICIT FORM OF THE JACOBI EQUATIONS. CONCLUDING REMARKS.

The functions A(s), B(s) and C(s) of (1.14) are found by straightforward manipulations from (1.8) to be (we put R = R(s), Z = Z(s) for brevity):

$$A(s) = \sigma R(s)$$

$$B(s) = \sigma / R(s)$$

$$C(s) = -2\sigma R'' + \rho g\{RR' - ZZ' + ZR(R''Z' - Z''R')\}$$

$$+ \lambda\{Z' - R(R''Z' - Z''R')\} \tag{5.1}$$

Using (5.1) the Jacobi differential equations (1.17) become (putting $B_o = \rho g/\sigma$ and $H_o = \lambda/\sigma$ as in (1.11)):

$$R\mu_{ik}'' + R'\mu_{ik}' - \left\{\frac{k^2}{R} - 2R'' + B_o\{RR' - ZZ'\right.$$

$$\left. + ZR(R''Z' - Z''R')\} + H_o\{Z' - R(R''Z' - Z''R')\}\right\}\mu_{ik}$$

$$= \lambda_{ik}\mu_{ik} \qquad ; \qquad \begin{aligned} k &= 0,1,2... \\ i &= 1,2,3... \\ s_o &\leq s \leq s_1 \quad , \end{aligned} \tag{5.2}$$

with the boundary conditions

$$(-1)^i \tan\gamma\, \mu'(s_i) = \{\sin^2\gamma(R''Z' - Z''R') - \cos^2\gamma w''\}_{s=s_i} \cdot \mu(s_i)$$

$$i=0,1. \tag{5.3}$$

Note that (5.3) tends formally to $\mu(s_i) = 0$ as $\gamma \to 0$, <u>if $w''(s_i) \neq 0$, $i=0,1$,</u> which is the case covered by Theorem 4.1.

Finally we remark that the conditions b) and d) of Section 2 may probably be slightly relaxed by introducing concepts from the theory of Lebesque

integrals. With regard to the physical background of the problem, however, such extensions of the set of permissible perturbations do not seem very meaningful.

## ACKNOWLEDGMENTS

The writer wishes to thank Dr. Paul Concus of the LBL and Dr. Robert Finn of the Mathematics Department, Stanford University, for stimulating discussions related to the subject of this paper.

This work was done with support from the Energy Research and Development Administration and from the National Aeronautics and Space Administration.

REFERENCES

[1] T. Kato, "Perturbation Theory for Linear Operators," Springer-Verlag, Inc., New York, 1966.

[2] W. C. Reynolds, M. A. Saad, H. M. Satterlee, "Capillary Hydrostatics and Hydrodynamics at Low g," Technical Report Number LG-3, Mechanical Engineering Department, Stanford University, September 1, 1964.

[3] O. Bolza, "Lectures on the Calculus of Variations," Dover Publications, Inc., New York, 1904, 1961.

[4] R. Gillette, "The Stability of Axisymmetric Fluid Interfaces," Ph.D. Thesis in Chemical Engineering, Houston, Texas, November, 1970.

[5] P. Concus, G. E. Crane, K. W. Satterlee, "Small Amplitude Lateral Sloshing in Spheroidal Containers under Low-Gravitational Conditions," NASA CR-72500 Lewis Research Center, Cleveland, Ohio, February, 1969.

[6] S. Agmon, "Lectures on Elliptic Boundary Value Problems," Van Nostrand Company, Inc., 1965.

[7] P. Concus, I. Karasalo, "A Numerical Study of Capillary Stability in a Circular Cylindrical Container with a Concave Spheroidal Bottom," (to appear).

APPENDIX II

# STABILITY OF AXISYMMETRIC, ANNULAR FLUID INTERFACES AT ZERO CONTACT ANGLE

by

Ilkka Karasalo

To appear in Archive for Rational Mechanics and Analysis

# STABILITY OF AXISYMMETRIC, ANNULAR FLUID INTERFACES AT ZERO CONTACT ANGLE

Ilkka Karasalo


## ABSTRACT

We study the stability, in terms of minimal total potential energy, of liquid configurations in axisymmetric containers, such that the liquid-vapor interface is annular and meets the container walls at zero contact angle. The proper limits of sufficient and necessary conditions for stability, respectively, as the contact angle tends to zero, are formulated in terms of the Jacobi accessory differential equations. The stability is shown to depend crucially on whether the equilibrium liquid-vapor interface stays inside the container or not when continued analytically past the three-phase contact lines.

## 1. INTRODUCTION

We shall study in this paper the stability of certain configurations of liquid partially filling an axially symmetric tank in a gravitational field directed along the axis of symmetry. We require, that the tank shape and the liquid volume are such that the liquid-vapor interface is annular, i.e. it does not intersect the axis of symmetry, cf. figure 1:

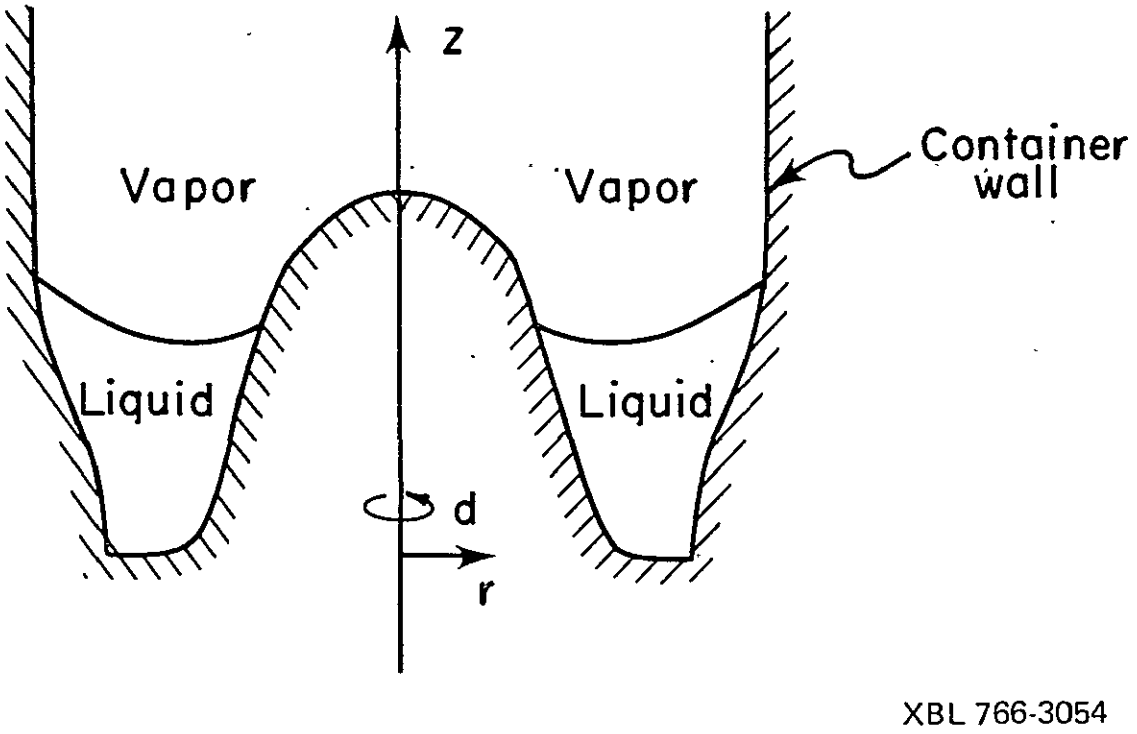


Figure 1: Example of permissible liquid-tank configuration and associated coordinate system.

A configuration is in stable equilibrium if and only if it strictly minimizes the total static potential energy of the system,

$$E = \sigma \cdot (A_f - \cos \gamma \cdot A_w) + E_g \tag{1.1}$$

among all nearby configurations with the same liquid volume V. Here $\sigma > 0$ (the liquid-vapor surface tension) and $0 \leq \gamma \leq \pi$ (the contact angle between the liquid-vapor surface and the container wall) are constants, $A_f$ and $A_w$ are the areas of the liquid-vapor and the liquid-wall interfaces, respectively, and $E_g$ is the gravitational potential energy of the liquid. This constrained minimization problem has received much attention in the literature, see e.g. Huh [5] and Gillette [4] for extensive lists of references. By a suitable choice of variables, it may be viewed as a variable-endpoint problem of variational calculus ([4] p. 21 and p. 145). When $\gamma > 0$, this approach results in conditions which distinguish between stable and unstable cases in a rather satisfactory way. There appear to be fewer rigorous results, however, concerning to what extent these stability conditions also apply to the limiting case $\gamma = 0$ (cf. [4], p. 23). The purpose of this paper is to analyze this limiting case for axially symmetric liquid configurations of the above kind. More specifically, we shall look at necessary and sufficient conditions, respectively, for minimum of E based on the Jacobi accessory minimization problem for the second variation of E (see e.g. Akhiezer [1], p. 69), as $\gamma \to 0$. The formal limits, as $\gamma \to 0$, of the boundary conditions associated with the Jacobi accessory differential equations depend crucially on

whether the curvatures of the equilibrium liquid-vapor interface and the container wall coincide or not at the three-phase contact lines. In the latter case these limiting boundary conditions will be of the fixed end-point type (when using a parametric representation of the surfaces, see further Section 2.1 below).

We will show, firstly (Theorems 3.1 and 3.2) that the stability conditions (sufficient and necessary, respectively) based on the fixed end-point boundary conditions in fact apply to (1.1) with $\gamma = 0$ if only the analytic continuation of the equilibrium liquid-vapor interface does not penetrate the container walls at the three-phase contact lines. Secondly (Theorem 3.3), we show that if the analytic continuation of the equilibrium liquid-vapor interface does penetrate the wall at either of the contact lines, the configuration will be unstable regardless of the conditions on the second variation of E.

## 2. NOTATION AND SOME PRELIMINARY RESULTS

### 2.1 The Euler-Lagrange and Jacobi Conditions

It will suffice to consider (1.1) at small perturbations from axially symmetric configurations. We will use a parametric arc-length, normal displacement representation of the surfaces (see e.g. Reynolds, Saad, Satterlee [8]). Thus the unperturbed liquid-vapor interface is described by

$$\begin{cases} r = R(s) \\ z = Z(s) \end{cases} \quad ; \quad \begin{matrix} s_o \leq s \leq s_1 \\ 0 \leq \phi \leq 2\pi \end{matrix} \tag{2.1}$$

in the polar co-ordinate system of figure 1, where s is the arc-length along the curve of intersection between the interface and any plane $\phi$ = constant. Then the equations

$$\begin{cases} r = R(s) - \eta(s,\phi)Z'(s) \\ z = Z(s) + \eta(s,\phi)R'(s) \end{cases} \quad ; \quad \begin{matrix} s_o(\phi) \leq s \leq s_1(\phi) \\ 0 \leq \phi \leq 2\pi \end{matrix} \tag{2.2}$$

describe a surface obtained by moving each point of the surface (2.1) the distance $\eta(s,\phi)$ in the direction of the normal at $(s,\phi)$. (In general, since we want the perturbed surface (2.2) to intersect the container walls, the functions R and Z of (2.1) must be continued to some open interval containing $[s_o,s_1]$. A convenient way of doing this, which we will use in the sequel, is provided by the differential equations (2.9) below). Similarly, in some neighborhood of the unperturbed contact lines ($s = s_o$ and $s = s_1$ in (2.1)), the container

wall will be given by

$$\begin{cases} r = R(s) - w(s)Z'(s) \\ \\ z = Z(s) + w(s)R'(s) \end{cases} \quad ; \quad 0 \leq \phi \leq 2\pi. \tag{2.3}$$

Then, denoting by $\delta E(\eta)$ and $\delta V(\eta)$ the increments of the energy (1.1) and the liquid volume at the perturbation (2.2), we obtain in a straightforward way

$$\delta E(\eta) = \int_0^{2\pi} \int_{s_o(\phi)}^{s_1(\phi)} \left\{ f_A(\underline{\eta},s) - f_A(\underline{0},s) + f_g(\underline{\eta},s) \right\} ds d\phi$$

$$- \int_0^{2\pi} \int_{\Delta\phi} \left\{ \cos\gamma \cdot f_A(\underline{w},s) - f_A(\underline{0},s) + f_g(\underline{w},s) \right\} ds d\phi \tag{2.4}$$

$$\delta V(\eta) = \int_0^{2\pi} \int_{s_o(\phi)}^{s_1(\phi)} f_V(\underline{\eta},s) ds d\phi - \int_0^{2\pi} \int_{\Delta\phi} f_V(\underline{w},s) ds d\phi \tag{2.5}$$

where we have put

$$\begin{aligned} \underline{\eta} &= \underline{\eta}(s,\phi) = (\eta(s,\phi), \eta_s(s,\phi), \eta_\phi(s,\phi))^T \\ \underline{w} &= \underline{w}(s) = (w(s), w'(s), 0)^T \\ \Delta_\phi &= \text{the interval } (s_o(\phi), s_o) \cup (s_1, s_1(\phi)) \end{aligned} \tag{2.6}$$

and, denoting $R = R(s)$, $Z = Z(s)$,

$$f_A(\underline{\eta},s) = \sigma \cdot \{(R - \eta Z')^2(\eta_s^2 + (1 + \eta(R''Z' - Z''R'))^2)$$

$$+ \eta_\phi^2(1 + \eta(R''Z' - Z''R'))^2\}^{1/2}$$

$$f_V(\underline{\eta},s) = \eta\{1 + \frac{\eta}{2}(R''Z' - Z''R')\}(R - \frac{\eta}{2}Z')$$

$$f_g(\underline{\eta},s) = \rho g \cdot (Z + \frac{\eta}{2}R') \cdot f_V(\underline{\eta},s) \qquad (2.7)$$

Here $\rho$ is the constant liquid density and g is the gravitation constant with $g > 0$ if the gravitation force acts towards the negative z-axis in figure 1.

The condition, that all first order $\eta$-terms in $\delta E(\eta)$ should vanish for all $\eta$ such that $\delta V(\eta) = 0$ then leads to

$$\left.\begin{aligned} &\frac{\partial f_A}{\partial \eta}(\underline{0},s) + \frac{\partial f_g}{\partial \eta}(\underline{0},s) - \lambda\frac{\partial f_V}{\partial \eta}(\underline{0},s) = 0 \\ &\text{in } s_o \leq s \leq s_1, \text{ with the boundary conditions} \\ &\cos\gamma\, f_A(\underline{w}(s_i),s_i) - f_A(\underline{0},s_i) = 0 \quad ; \quad i=0,1\ , \end{aligned}\right\} \qquad (2.8)$$

where $\lambda$ is a constant (the Lagrange multiplier). Putting $B_o = \rho g/\sigma$, $H_o = \lambda/\sigma$, using (2.6), (2.7) and the identity $R'(s)^2 + Z'(s)^2 \equiv 1$, (2.8) becomes the Euler-Lagrange boundary value problem

$$\left.\begin{aligned} R'' &= -Z'(B_oZ - H_o - Z'/R) \\ Z'' &= R'(B_oZ - H_o - Z'/R) \\ w(s_i) &= 0 \\ w'(s_i) &= (-1)^{i+1}\tan\gamma \quad ; \quad i=0,1. \end{aligned}\right\} \qquad (2.9)$$

(Without loss of generality we have excluded the contact angles $\pi - \gamma$ allowed by (2.8)).

Assuming now that (2.9) is satisfied, the condition, that all second order $\eta$-terms should give a non-negative contribution to $\delta E(\eta)$ for all $\eta$ such that $\delta V(\eta) = 0$, takes the form

$$Q_o(\underline{\mu}) = \int_0^{2\pi}\int_{s_o}^{s_1} \{A(s)\mu_s^2 + B(s)\mu_\phi^2 + C(s)\mu^2\}\, ds d\phi$$
$$+ \int_0^{2\pi} \{\alpha_o \mu(s_o,\phi)^2 + \alpha_1 \mu(s_1,\phi)^2\}\, d\phi \geq 0 \qquad (2.10)$$

for all $\mu(s,\phi)$ such that

$$\int_0^{2\pi}\int_{s_o}^{s_1} R(s)\mu(s,\phi) ds d\phi = 0 \ . \qquad (2.11)$$

Here we have put

$$f_{A\underline{\eta\eta}}(\underline{0},s) + f_{g\underline{\eta\eta}}(\underline{0},s) - f_{V\underline{\eta\eta}}(\underline{0},s) = \mathrm{diag}\{C(s),A(s),B(s)\} \ , \qquad (2.12)$$

$$\frac{(-1)^i}{\tan^2\gamma} \cdot \frac{d}{ds}\left\{\cos\gamma\, f_A(\underline{w}(s),s) - f_A(\underline{0},s) + f_g(\underline{w}(s),s) - \lambda f_V(\underline{w}(s),s)\right\}_{s=s_i}$$
$$= \alpha_i \ , \quad i=0,1. \qquad (2.13)$$

By (2.12) and (2.7), the A, B and C of (2.10) are

$$A(s) = \sigma R(s)$$
$$B(s) = \sigma/R(s)$$
$$C(s) = -2\sigma R'' + \rho g\{RR' - ZZ' + ZR(R''Z' - Z''R')\}$$
$$+ \lambda\{Z' - R(R''Z' - Z''R')\} \qquad (2.14)$$

By (2.9), since $R(s) \geq R_{min} > 0$ in $s_o \leq s \leq s_1$, A, B and C will be smooth (in fact analytic) in some open interval containing $[s_o, s_1]$ and $A(s) \geq A_{min} > 0$, $B(s) \geq B_{min} > 0$ will hold there. By standard results for symmetric, semibounded quadratic forms in Hilbert space (see e.g. Kato [7], p. 322 and 352-353), (2.10) may be analyzed in terms of the eigenvalues and eigenfunctions of an associated selfadjoint differential operator:

$$T\mu = -\frac{\partial}{\partial s}(A(s)\mu_s) - \frac{\partial}{\partial \phi}(B(s)\mu_\phi) + C(s)\mu$$

in $s_o \leq s \leq s_1$, $0 \leq \phi \leq 2\pi$, with the boundary conditions, that $\mu$ should be periodic in $\phi$ with period $2\pi$ and

$$A(s_i)\mu_s(s_i,\phi) = (-1)^i \alpha_i \mu(s_i,\phi) \quad , \quad 0 \leq \phi \leq 2\pi \qquad i = 0,1 \ .$$

T has a complete, orthogonal system of eigenfunctions of the form

$$\{\mu_{ik}(s) \cos k\phi\}_{i=1,k=0}^{\infty} \quad , \quad \{\mu_{ik}(s) \sin k\phi\}_{i=1,k=1}^{\infty}$$

with associated eigenvalues $\{\kappa_{ik}\}_{i=1,k=0}^{\infty}$ (ordered increasingly in the index i), determined from the boundary value problems

$$\begin{cases} -\frac{d}{ds}(A(s)\mu_{ik}(s)) + \{k^2 \cdot B(s) + C(s)\}\mu_{ik}(s) = \kappa_{ik}\mu_{ik}(s) \\ A(s_j)\mu'_{ik}(s_j) = (-1)^j \alpha_j \mu_{ik}(s_j) \quad ; \quad \begin{matrix} j=0,1 \\ i=1,2,3,\ldots \\ k=0,1,2,\ldots \end{matrix} \end{cases} ; \qquad (2.15)$$

We notice, that all eigenfunctions but those with k = 0 satisfy the constraint (2.11) and that, since B(s) > 0 in $s_o \leq s \leq s_1$, the eigenvalues $\kappa_{ik}$ are increasing functions of k. It then follows that (2.10) with the side-condition (2.11) holds for all $\mu$ in the class of continuous functions in $s_o \leq s \leq s_1$, $0 \leq \phi \leq 2\pi$, which are periodic in $\phi$ with period $2\pi$ and have square integrable first derivatives (see e.g. Kato [7], p. 322-323, Cor. 2.3) if and only if

$$\kappa_o = \min\{\beta_1^2\kappa_{10} + \beta_2^2\kappa_{20}, \kappa_{11}\} \geq 0 \tag{2.16}$$

where, denoting $(f,g)_o = \int_0^{2\pi}\int_{s_o}^{s_1} f(s,\phi)g(s,\phi)dsd\phi$, $\beta_1^2$ and $\beta_2^2$ are the solutions to

$$\begin{cases} \beta_1^2(\mu_{10},R)_o^2 - \beta_2^2(\mu_{20},R)_o^2 = 0 \\ \beta_1^2(\mu_{10},\mu_{10})_o + \beta_2^2(\mu_{20},\mu_{20})_o \end{cases} \tag{2.17}$$

with $\beta_2 = 0$ if the solutions are non-unique.

(2.15) - (2.17) are(the equivalent of)the Jacobi accessory boundary value problems for our constrained minimization problem. By (2.13), (2.6) and (2.7), the boundary conditions are

$$\begin{aligned} &(-1)^i \tan\gamma\, \mu'_{ik}(s_j) \\ &= \{\sin^2\gamma\,(R''Z' - Z''R') - \cos^2\gamma\, w''\}_{s=s_j} \cdot \mu_{ik}(s_j) \qquad j=0,1. \end{aligned} \tag{2.18}$$

We notice, that <u>if $w''(s_j) \neq 0$, j=0,1, (2.18) converges formally to</u>

$$\mu_{ik}(s_j) = 0 \quad , \quad j=0,1 \quad , \tag{2.19}$$

as $\gamma \to 0$.

## 2.2 Permissible Perturbations. Two Lemmas.

By the contact lines of the liquid-vapor interface we mean the two closed curves within the container wall, any open neighborhoods of which intersects the interiors of both the liquid and the vapor inside the container (cf. fig. 1). The contact lines determine by (2.2) a closed region $s_o(\phi) \leq s \leq s_1(\phi)$, $0 \leq \phi \leq 2\pi$ in the $(s,\phi)$-plane. We denote this region with $\Sigma$ and require the following regularity properites from $\Sigma$ and the associated function $\eta$:

a) $\eta$ is continuous in $\Sigma$ and periodic in $\phi$ with period $2\pi$.

b) $\eta_s$ and $\eta_\phi$ are continuous in $\Sigma$ except possibly at finitely many isolated points or finitely many piecewise smooth curves with finite length. In particular, $\eta_s$ is piecewise continuous as function of $s$ for all $0 \leq \phi \leq 2\pi$.

c) $$d(\eta) = \sup|\eta(s,\phi)| + \sup|\eta_s(s,\phi)| + \sup|\eta_\phi(s,\phi)| < \infty, \tag{2.20}$$

where the supremum is taken over all points of $\Sigma$ where $\eta_s$ and $\eta_\phi$ are continuous.

d) $s_i(\phi)$, $i=0,1$ are continuous and such that $s_i(\phi) - s_i$, $i=0,1$, change sign at most finitely many times in $0 \leq \phi \leq 2\pi$. $s_i'(\phi)$, $i=0,1$, are continuous except possibly at finitely

many points in $0 \leq \phi \leq 2\pi$ and

$$d(\Sigma) = \sum_{i=0}^{I} (\sup|s_i(\phi) - s_i| + \sup|s_i'(\phi)|) < \infty \qquad (2.21)$$

where the supremum is taken over all points of $0 \leq \phi \leq 2\pi$ where $s_o'(\phi)$ and $s_I'(\phi)$ are continuous.

Remark: The sufficient conditions to be considered below will ensure the stability of the surface (2.1) with respect to all perturbations (2.2) which satisfy a) - d) above and for which $d(\eta) + d(\Sigma)$ is sufficiently small. Thus in terms of variational calculus (see e.g. Bolza [2], p. 68-70) the extremum will be "weak". The detailed assumptions under b) and d) are introduced for simplicity in what follows, and could be relaxed slightly by introducing more advanced concepts from the theory of Lebesque integrals. With regard to the physical background, however, nothing essential is lost by the above.

We will denote the closed rectangle $s_o \leq s \leq s_1$, $0 \leq \phi \leq 2\pi$ by $\Sigma_o$ and use, for any $f(s,\phi)$ which is square integrable on $\Sigma_o$,

$$\|f\|_o^2 = (f,f)_o \qquad (2.22)$$

where $(\ ,\ )_o$ is defined as in (2.17). Then the following result will be useful:

Lemma 2.1: *Let $\mu(s,\phi)$ satisfy the requirements a)-c) on $\Sigma_o$ and the condition*

$$\mu(s_o,\phi) = \mu(s_1,\phi) = 0 \quad , \quad 0 \leq \phi \leq 2\pi. \tag{2.23}$$

*Let $Q_o(\underline{\mu})$ be defined as in (2.10) and assume that $A_{max} \geq A(s) \geq A_{min} > 0$, $B_{max} \geq B(s) \geq B_{min} > 0$ and $|C(s)| \leq C_{max}$ hold in $s_o \leq s \leq s_1$. Then there exist positive constants $K_o$, $K_1$, $L_o$ and $L_1$, depending on $s_o$, $s_1$, $A_{min}$, $A_{max}$, $B_{min}$, $B_{max}$ and $C_{max}$ but not on $\mu$, such that*

$$K_o Q_o(\underline{\mu}) - L_o \|\mu\|_o^2 \leq \|\mu_s\|_o^2 + \|\mu_\phi\|_o^2 \leq K_1 Q_o(\underline{\mu}) + L_1 \|\mu\|_o^2 \ . \tag{2.24}$$

(2.24) follows from the mean value theorem in a straightforward way and the proof is omitted. (By use of a Sobolev-type inequality (see e.g. Kato [7], p. 193), condition (2.23) could in fact be omitted, and this stronger result could be used for a similar treatment of the case $\gamma > 0$, Karasalo [6]).

Before stating our second Lemma we need some further notation. For any $\mu(s,\phi)$ satisfying a) - c) on $\Sigma_o$ and (2.23) we put, for clarity

$$Q_o(A,B,C,\underline{\mu}) = Q_o(\underline{\mu}) \tag{2.25}$$

where $Q_o(\underline{\mu})$ is defined in (2.10). Further, if $\delta A(s,\phi)$, $\delta B(s,\phi)$ and $\delta C(s,\phi)$ are bounded and integrable on $\Sigma_o$ and $\varepsilon$ is a positive constant, we put

$$\Phi = \Phi(\delta A,\delta B,\delta C,\varepsilon) = \inf Q_o(A + \delta A, B + \delta B, C + \delta B, \underline{\mu}) \tag{2.26}$$

over all $\mu$ satisfying a) - c) on $\Sigma_o$, (2.23) and the conditions

$$\|\mu\|_o = 1 \ , \tag{2.27}$$

$$|(R,\mu)_o| \leq \varepsilon(\|\mu_s\|_o + \|\mu_\phi\|_o + \|\mu\|_o). \tag{2.28}$$

If $f(s,\phi)$ is bounded on $\Sigma_o$, we will let, as usual, $\|f\|_\infty$ denote the supremum of $|f(s,\phi)|$ over $(s,\phi)$ in $\Sigma_o$. Then we have

Lemma 2.2: *Let $A(s)$, $B(s)$ and $C(s)$ satisfy the requirements in Lemma 2.1 and let $\delta A(s,\phi)$, $\delta B(s,\phi)$ and $\delta C(s,\phi)$ be bounded and integrable on $\Sigma_o$. Let $\varepsilon > 0$, define $\Phi$ as in (2.25) - (2.28), denote $\Phi_o = \Phi(0,0,0,0)$ and put*

$$\delta = \|\delta A\|_\infty + \|\delta B\|_\infty + \|\delta C\|_\infty + \varepsilon \ . \tag{2.29}$$

*Then there exist positive constants $C$ and $\delta_o$, independent of $\delta A$, $\delta B$, $\delta C$ and $\varepsilon$, such that*

$$|\Phi - \Phi_o| \leq C \cdot \delta \tag{2.30}$$

*holds true, if only $\delta \leq \delta_o$.*

Proof: Throughout this proof, $M_i$, $N_i$, $\delta_i$, i=1,2,3,... will denote positive constants, independent of $\delta A$, $\delta B$, $\delta C$, $\varepsilon$ and $\mu$. Let $\mu$ satisfy conditions a) - c) on $\Sigma_o$, (2.23) and (2.27). With the notation of (2.25), put for brevity, $\delta Q_o(\underline{\mu}) = Q_o(\delta A, \delta B, \delta C, \underline{\mu})$. ($\delta Q_o$ will be well defined because of the assumptions.) Then there exist $M_1$, $M_2$, $N_1$ and $N_2$, such that

$$\begin{aligned}(1 - M_1\delta)Q_o(\underline{\mu}) - N_1\delta &\leq Q_o(\underline{\mu}) + \delta Q_o(\underline{\mu}) \\ &\leq (1 + M_1\delta)Q_o(\underline{\mu}) + N_1\delta\end{aligned} \tag{2.31}$$

because of Lemma 2.1 and the mean value theorem. Noting by (2.26) and (2.28), that $\Phi$ is a non-increasing function of $\epsilon$ and that, by (2.10) and (2.25), $Q_o(A,B,C,\underline{\mu})$ is a linear function of A, B and C we obtain from (2.31)

$$\Phi \leq (1 + M_1\delta)\Phi_o + N_1\delta \tag{2.32}$$

It follows, that we need only consider those $\mu$ which satisfy, e.g., the additional condition $Q_o(\underline{\mu}) + \delta Q_o(\underline{\mu}) \leq (1 + 2M_1\delta)|\Phi_o| + 2N_1\delta$ when forming the infimum in (2.26). By (2.31) and Lemma 2.1, however, for all such $\mu$

$$\|\mu_s\|_o^2 + \|\mu_\phi\|_o^2 \leq M_2|\Phi_o| + N_2 = M_3 \tag{2.33}$$

if only, e.g., $\delta \leq \delta_1 = \frac{1}{2M_1}$. Let $\mu$ be any function satisfying a) - c) on $\Sigma_o$, (2.23), (2.27), (2.28) and (2.33). Put

$$f^*(s,\phi) = (s - s_o)(s_1 - s)$$

$$\tilde{\mu} = C_1(\mu - C_2 f^*)$$

where $C_1$ and $C_2$ are chosen so as to make $\tilde{\mu}$ satisfy (2.27) and (2.28) with $\epsilon = 0$, i.e. $C_2 = (R,\mu)_o/(R,f^*)_o$, $C_1 = 1/\|\mu - C_2 f^*\|_o$. Noting that $(R,f^*)_o$ is a positive constant, dependent only on $s_o$, $s_1$ and R(s), it follows from (2.27) - (2.29) and (2.33) that

$$|C_2| \leq M_4\delta \quad ; \quad \frac{1}{C_1} \geq 1 - M_5\delta \tag{2.34}$$

Furthermore, since $f^*$ vanishes on $s = s_o$ and $s = s_1$, $\tilde{\mu}$ satisfies (2.23).

Then form

$$Q_o(\tilde{\underline{\mu}}) - \{Q_o(\underline{\mu}) + \delta Q_o(\underline{\mu})\}$$

$$= (C_1^2 - 1)Q_o(\underline{\mu}) + C_1^2 C_2^2 Q_o(\underline{f}^*) - \delta Q_o(\underline{\mu})$$

$$- 2C_1^2 C_2 \int_0^{2\pi} \int_{s_o}^{s_1} \{A(s)\mu_s f_s^* + C(s)\mu f^*\}\, ds d\phi \quad .$$

Here we use Lemma 2.1, (2.31), (2.33), (2.34), the mean value theorem and the Schwartz inequality to find upper bounds for the terms to the right. We obtain, that for some $M_6$, $\delta_2$

$$Q_o(\tilde{\underline{\mu}}) - \{Q_o(\underline{\mu}) + \delta Q_o(\underline{\mu})\} \leq M_6 \cdot \delta \tag{2.35}$$

holds true, if only $\delta \leq \delta_2$. Hence

$$\Phi_o - \Phi \leq M_6 \cdot \delta \tag{2.36}$$

if $\delta \leq \delta_2$. The statement of the lemma follows by combining (2.32) and (2.36).

## 3. STABILITY RESULTS AT $\gamma = 0$.

Our first statement concerns sufficient conditions for stability at zero contact angle:

Theorem 3.1: *Let $\gamma = 0$ in (1.1) and assume that the unperturbed surface satisfies the Euler-Lagrange equations with the associated boundary conditions (2.9), and does not intersect the z-axis. Assume further that the function $w(s)$ of (2.3) is twice continuously differentiable and that*

$$w(s) \leq 0 \text{ in some open neighborhoods of } s = s_o \text{ and } s = s_1 . \quad (3.1)$$

*Let $\kappa_o$ be defined as in (2.15) - (2.17) but with the boundary conditions in (2.15) replaced by the fixed end-point conditions (2.19), and assume that $\kappa_o > 0$. Let $d(\eta)$ and $d(\Sigma)$ be defined as in (2.20) and (2.21). Then there exists a constant $d_o > 0$, such that in (2.4)*

$$\delta E(\eta) \geq 0 \text{ with equality iff } \eta = 0 \text{ in } \Sigma \quad (3.2)$$

*holds for all $\eta$ satisfying the volume constraint $\delta V(\eta) = 0$ in (2.5), the conditions a) - d) of Section 2.2 and the condition*

$$d(\eta) + d(\Sigma) \leq d_o . \quad (3.3)$$

Remark: When $\gamma = 0$, both the energy (1.1) and the liquid volume remain unchanged if the liquid-vapor interface is continued past the contact lines by "wetting" dry parts of the container walls. Thus, when $\gamma = 0$, any configuration is neutrally unstable with respect to

such "wetting" perturbations. With our notation, however, the region $\Sigma$ is unchanged at "wetting" (see the beginning of Section 2.2), and there is no ambiguity in (3.2) in this respect.

Proof of Theorem 3.1: Let $Q_o$ be defined as in (2.10). Then, by (2.15) - (2.17) and the representation theorem for quadratic forms in Hilbert space (see e.g. Kato [7], p. 322-323):

$$\inf Q_o(\underline{\mu}) = \kappa_o > 0 \tag{3.4}$$

where the infimum is taken over all $\mu$ satisfying in $\Sigma_o$ the conditions a) - c) of Section 2.2, (2.11), (2.23) and (2.27).

Using the notation of (2.7) we put

$$f_E(\underline{\eta},s) = f_A(\underline{\eta},s) - f_A(\underline{0},s) + f_g(\underline{\eta},s) - \lambda f_V(\underline{\eta},s) \tag{3.5}$$

where $\lambda$ is the constant in (2.8). Then, by (2.4) and (2.5),

$$\delta E(\eta) = \int_0^{2\pi} \int_{s_o(\phi)}^{s_1(\phi)} f_E(\underline{\eta},s)\, ds d\phi$$

$$- \int_0^{2\pi} \int_{\Delta\phi} f_E(\underline{w},s)\, ds d\phi \tag{3.6}$$

for all $\eta$ satisfying the volume constraint $\delta V(\eta) = 0$. For convenience in the following we denote

$\Sigma_+$ = complement of $(\Sigma \cap \Sigma_o)$ w.r.t. $\Sigma$,

$\Sigma_-$ = complement of $(\Sigma \cap \Sigma_o)$ w.r.t. $\Sigma_o$ and

$$\tilde{\Sigma} = \Sigma \cup \Sigma_o = \Sigma_o \cup \Sigma_+ = \Sigma \cup \Sigma_- \tag{3.7}$$

and define a function $\tilde{\eta}(s,\phi)$ on $\tilde{\Sigma}$ by

$$\tilde{\eta}(s,\phi) = \begin{cases} \eta(s,\phi) & , \quad (s,\phi) \in \Sigma \\ \\ w(s) & , \quad (s,\phi) \in \Sigma_- \end{cases} , \tag{3.8}$$

(i.e. $\tilde{\eta}$ is obtained by extending $\eta$ by wetting those parts of the wall which dried because of the perturbation $\eta$). By (2.6) and (3.7), $\tilde{\Sigma}$ has the boundaries

$$\begin{cases} \tilde{s}_o(\phi) = \min\{s_o(\phi), s_o\} \\ \\ \tilde{s}_1(\phi) = \max\{s_1(\phi), s_1\} \end{cases} ; \quad 0 \leq \phi \leq 2\pi . \tag{3.9}$$

Putting further

$$\eta^*(s,\phi) = \begin{cases} 0 & , \quad (s,\phi) \in \Sigma_o \\ \\ w(s) & , \quad (s,\phi) \in \Sigma_+ \end{cases} , \tag{3.10}$$

$$\nu(s,\phi) = \tilde{\eta}(s,\phi) - \eta^*(s,\phi) \quad , \quad (s,\phi) \in \tilde{\Sigma} , \tag{3.11}$$

we obtain by (3.6) and (2.5), noting that $f_E(\underline{0},s) = 0$ and $f_V(\underline{0},s) = 0$,

$$\delta E(\eta) = \int_0^{2\pi} \int_{\tilde{s}_o(\phi)}^{\tilde{s}_1(\phi)} f_E(\underline{\tilde{\eta}},s)\, dsd\phi - \int_0^{2\pi} \int_{\underline{\tilde{\Delta}}\phi} f_E(\underline{w},s)\, dsd\phi$$

$$= \int_0^{2\pi} \int_{\tilde{s}_o(\phi)}^{\tilde{s}_1(\phi)} \{f_E(\underline{\eta}^* + \underline{\nu},\, s) - f_E(\underline{\eta}^*,s)\}\, dsd\phi \quad , \tag{3.12}$$

for all $\eta$ satisfying the volume constraint

$$\delta V(\eta) = \int_0^{2\pi} \int_{\tilde{s}_o(\phi)}^{\tilde{s}_1(\phi)} \{f_V(\underline{\eta}^* + \underline{\nu},s) - f_V(\underline{\eta}^*,s)\}\, dsd\phi = 0. \tag{3.13}$$

In the sequel $M_i$, $N_i$ and $d_i$, $i=1,2,3,\ldots$, will denote positive constants, independent of $\mu$, $\eta$, $\Sigma$, $s$ and $\phi$. By (3.8) - (3.11), $\tilde{\eta}$, $\eta^*$, $\nu$ and $\tilde{s}_i(\phi)$ will satisfy the requirements a) - d) of Section 2.2. Furthermore, since $w(s) = 0(s - s_i)^2$ in the neighborhood of $s = s_i$, we may find some $M_1$ and $d_1$, such that

$$d(\tilde{\Sigma}) + d(\eta^*) + d(\tilde{\eta}) + d(\nu) \leq M_1\{d(\Sigma) + d(\eta)\} \tag{3.14}$$

if only $d(\Sigma) + d(\eta) \leq d_1$.

By (2.9) and since $R(s) > 0$ in $s_o \leq s \leq s_1$, the functions R and Z can be continued analytically to some open interval containing $[s_o,s_1]$ and it will hold $R(s) \geq R_{min} > 0$ there. It then follows from (2.7), (3.5) and (3.9) that there exist some $d_2$ and $d_3$, such that $f_E(\underline{\eta},s)$ and $f_V(\underline{\eta},s)$ are analytic functions of the arguments $\eta$, $\eta_s$, and $\eta_\phi$ in the region $|\eta| + |\eta_s| + |\eta_\phi| \leq d_2$ at all points of $\tilde{\Sigma}$, if only $d(\Sigma) \leq d_3$. Hence, putting in (3.12) and (3.13)

$$f_E(\underline{\eta}^* + \underline{\nu},s) - f_E(\underline{\eta}^*,s)$$

$$= f_{E\underline{\eta}}(\underline{\eta}^*,s)^T\underline{\nu} + \frac{1}{2}\underline{\nu}^T f_{E\underline{\eta}\underline{\eta}}(\underline{0},s)\underline{\nu} + h_E(\underline{\eta}^*,\underline{\nu},s) \qquad (3.15)$$

and

$$f_V(\underline{\eta}^* + \underline{\nu},s) - f_V(\underline{\eta}^*,s) = \frac{\partial f_V}{\partial \eta}(\underline{0},s)\nu + h_V(\underline{\eta}^*,\underline{\nu},s) \qquad (3.16)$$

there will exist some $M_2$ and $d_4$, such that

$$|h_E(\underline{\eta}^*,\underline{\nu},s)| \leq M_2\{d(\eta) + d(\Sigma)\}(\nu_s^2 + \nu_\phi^2 + \nu^2)$$

$$|h_V(\underline{\eta}^*,\underline{\nu},s)| \leq M_2\{d(\eta) + d(\Sigma)\}(|\nu_s| + |\nu_\phi| + |\nu|) \qquad (3.17)$$

holds at all points of $\tilde{\Sigma}$ where $\underline{\eta}^*$ and $\underline{\nu}$ are continuous, if only $d(\eta) + d(\Sigma) \leq d_4$.

We now observe, that since $w(s) \leq 0$ in some open neighborhoods of $s = s_0$ and $s = s_1$, the first term to the right in (3.15) gives a non-negative contribution to $\delta E(\eta)$. To see this, first note that $f_{E\underline{\eta}}(\underline{\eta}^*,s) = 0$ in $\Sigma_o$, by (3.10), (3.5), (2.7) and (2.8). Second, when $(s,\phi) \in \Sigma_+$ we have by (3.10), (2.12) and (2.14)

$$f_{E\underline{\eta}}(\underline{\eta}^*,s)^T\underline{\nu} = \{\sigma R(s) + D_R(s)\}w'(s)\nu_s + \{C(s) + D_C(s)\}w(s)\nu \qquad (3.18)$$

where, for some $M_3$ and $d_5$,

$$|D_R(s)| + |D_C(s)| \leq M_3\{|w(s)| + w'(s)^2\}$$

if only $d(\Sigma) \leq d_5$. Furthermore, since $w''(s)$ is continuous in $\Sigma_+$, $D_R$ will be continuously differentiable there. Hence, after partial integration of the first term in (3.18) noting that $\nu(s,\phi)w'(s) = 0$ on the boundaries of $\Sigma_+$, we obtain

$$\int_0^{2\pi}\int_{\tilde{s}_o(\phi)}^{\tilde{s}_1(\phi)} f_{E\underline{\eta}}(\underline{\eta}^*,s)^T \cdot \underline{\nu}\, ds d\phi$$

$$= \int_0^{2\pi}\int_{\tilde{\Delta}\phi} \left\{-\sigma R(s)w''(s) + D(s)\right\}\nu\, ds d\phi \qquad (3.19)$$

where, for some $d_6$, $M_4$, $|D(s)| \leq M_4|w'(s)|$ if only $d(\Sigma) \leq d_6$. Now by (3.1), since $w(s_i) = w'(s_i) = 0$, $i=0,1$, $w''(s) \leq 0$ in some open neighborhoods of $s = s_o$ and $s = s_1$, whence the first factor of the last integrand will be non-negative, if only $d(\Sigma)$ is sufficiently small. Since further, by (3.8) - (3.11), $\nu(s,\phi) > 0$ at interior points of $\Sigma_+$, we can then find some $d_7$, such that for all permissible $\eta$ for which $\delta V(\eta) = 0$

$$\delta E(\eta) \geq \frac{1}{2}\int_0^{2\pi}\int_{\tilde{s}_o(\phi)}^{\tilde{s}_1(\phi)} \left\{A(s)\nu_s^2 + B(s)\nu_\phi^2 + C(s)\nu^2 + 2h_E(\underline{\eta}^*,\underline{\nu},s)\right\} ds d\phi\ , \qquad (3.20)$$

if only $d(\eta) + d(\Sigma) \leq d_7$. Furthermore, (3.20) holds with equality if $\Sigma_+$ is empty or if $w(s) \equiv 0$ in $\Sigma_+$.

In (3.13) and (3.20) we introduce a change of variable by putting

$$\begin{cases} s = s(s',\phi) = \tilde{s}_o(\phi) + \dfrac{s' - s_o}{s_1 - s_o}(\tilde{s}_1(\phi) - \tilde{s}_o(\phi)) & (3.21) \\ \mu(s',\phi) = \nu(s(s',\phi),\phi) \ . & (3.22) \end{cases}$$

(3.21) takes $\tilde{\Sigma}$ onto the rectangle $\Sigma_o$ in the $(s',\phi)$-plane. It follows by (3.17), (3.21), (3.22) and the smoothness properties of A, B and C that in the notation of (2.25)

$$\delta E(\eta) \geq \frac{1}{2} Q_o (A + \delta A, B + \delta B, C + \delta C, \underline{\mu})$$

where $\delta A(s',\phi)$, $\delta B(s',\phi)$ and $\delta C(s',\phi)$ are bounded and integrable on $\Sigma_o$ and such that for some $M_5$ and $d_8$

$$\|\delta A\|_\infty + \|\delta B\|_\infty + \|\delta C\|_\infty \leq M_5\{d(\eta) + d(\Sigma)\}$$

if $d(\eta) + d(\Sigma) \leq d_8$. Similarly, by (3.13), (3.16), (3.17) and (2.7), there exist $M_6$ and $d_9$, such that

$$|(R,\mu)_o| \leq M_6\{d(\eta) + d(\Sigma)\}\{\|\mu_s\|_o + \|\mu_\phi\|_o + \|\mu\|_o\}$$

if $d(\eta) + d(\Sigma) \leq d_9$. Furthermore, $\mu(s',\phi)$ satisfies (2.23) and requirements a) - c) of Section 2.2 on $\Sigma_o$. We may then use (3.4) and Lemma 2.2 to conclude that there exists some $d_o$ such that, e.g.,

$$\delta E(\eta) \geq \frac{\kappa_o}{3} \|\mu\|_o^2$$

for all $\eta$ satisfying the volume constraint, if only $d(\eta) + d(\Sigma) \leq d_o$. Since, by (3.7) - (3.11) and (3.21) - (3.22). $\|\mu\|_o = 0$ if and only if

$\eta \equiv 0$ in $\Sigma$, this completes the proof of Theorem 3.1.

The second statement of this section is concerned with necessary conditions for stability at zero contact angle, based on the fixed end-point conditions (2.19). As may be expected, these will apply regardless of the additional condition (3.1):

Theorem 3.2: *Let $\gamma = 0$ and assume that the unperturbed surface satisfies (2.9) and does not intersect the z-axis. Let $\kappa_o$ be defined as in (2.15) - (2.17) but with the boundary conditions (2.19) and assume that $\kappa_o < 0$. Then, for any $d_o > 0$ we may find a function $\eta$ satisfying a) - d) of Section 2.2, the volume constraint $\delta V(\eta) = 0$ in (2.5) and the condition $d(\eta) + d(\Sigma) \leq d_o$, such that in (2.4)*

$$\delta E(\eta) < 0 \ . \tag{3.23}$$

Proof: We note that the infimum $\kappa_o$ in (3.4) under the conditions stated there is attained for $\mu = \hat{\mu}$ where $\hat{\mu}$ is either $\mu_{11}$ or $\beta_1\mu_{10} + \beta_2\mu_{20}$ in the notation of (2.15) - (2.17). We can use $\hat{\mu}$ to construct a function $\eta$ with the properties required in the theorem as follows: Let e.g. $s_{00} = 2s_o/3 + s_1/3$, $s_{10} = s_o/3 + 2s_1/3$ and put

$$g(s) = \begin{cases} (s - s_{00})(s_{10} - s) \quad , & s_{00} \leq s \leq s_{10} \\ \\ 0 \qquad \text{otherwise} \ . \end{cases} \tag{3.24}$$

Then put

$$\eta(s,\phi) = \varepsilon\hat{\mu}(s,\phi) + a(\varepsilon)g(s) \tag{3.25}$$

where $a(\varepsilon)$ is chosen so as to make $\eta(s,\phi)$ satisfy the volume constraint. Using (2.5), the assumption $(R,\hat{\mu})_o = 0$ and the contraction mapping theorem it can be shown that $a(\varepsilon)$ is well defined when $|\varepsilon|$ is small and that $a(\varepsilon) = o(\varepsilon)$, $\varepsilon \to 0$. Since $\hat{\mu}$ and $g$ are zero on $s = s_o$ and $s = s_1$, $\Sigma_+$ as defined in (3.7) will be empty. Hence, by putting

$$\eta^*(s,\phi) = \begin{cases} 0 \quad ; \quad (s,\phi) \in \Sigma \\ \\ w(s) - \varepsilon\hat{\mu}(s,\phi) \quad ; \quad (s,\phi) \in \Sigma_- \end{cases} \tag{3.26}$$

we obtain by (3.6)

$$\delta E(\eta) = \int_0^{2\pi}\int_{s_o}^{s_1} f_E(\varepsilon\underline{\hat{\mu}} + \underline{\eta}^* + a(\varepsilon)\underline{g},s)\, dsd\phi \tag{3.27}$$

if only $\varepsilon$ is small enough for $g(s)$ to be zero within $\Sigma_-$, cf. (3.24), (3.25). Noting that $|\eta^*(s,\phi)| \leq |\varepsilon\hat{\mu}(s,\phi)|$ in $\Sigma_-$ and that the area of $\Sigma_-$ tends to zero as $\varepsilon \to 0$, we get from (3.27)

$$\delta E(\eta) = \varepsilon^2 \int_0^{2\pi}\int_{s_o}^{s_1} \frac{1}{2}\underline{\hat{\mu}}^T f_{E\underline{\eta\eta}}(\underline{0},s)\underline{\hat{\mu}}\, dsd\phi + o(\varepsilon^2)$$

$$= \frac{\varepsilon^2}{2}(\kappa_o + o(1)) \quad , \quad \varepsilon \to 0.$$

Since $\kappa_o < 0$, the statement of Theorem 3.2 follows.

Finally, the following theorem states that if the analytic continuation of the equilibrium liquid-vapor interface penetrates

the container walls at either of the three-phase contact lines, the configuration is unstable:

Theorem 3.3: *Let $\gamma = 0$ and assume that the unperturbed surface satisfies (2.9) and does not intersect the z-axis. Assume further, that for i=0 or i=1 the function w(s) in (2.3) changes sign at $s = s_i$ and that w''(s) is continuous and monotone in some open neighbourhood of that point. Then, for any $d_0 > 0$, we may find a function $\eta$ satisfying a) - d) of Section 2.2, the volume constraint $\delta V(\eta) = 0$ in (2.5) and the condition $d(\eta) + d(\Sigma) \leq d_0$, such that in (2.4)*

$$\delta E(\eta) < 0 \ .$$

Proof: Assume e.g. i=1. Then, by the mean-value theorem, we may find some $s_2 > s_1$ such that e.g.

$$|w'(s)| \leq (s-s_1)w''(s)$$
$$|w(s)| \leq (s-s_1)^2 w''(s)$$

holds for $s_1 \leq s \leq s_2$. Hence, noting the upper bound for $|D(s)|$ in the integrand in (3.19), for any given $d_0 > 0$ there exists a $k > 0$ such that

$$k \leq \tfrac{1}{3} d_0 \ , \tag{3.28}$$

$$\max \{|w(s)|, |w'(s)|\} \leq \tfrac{1}{6} d_0 \ ; \quad s_1 \leq s \leq s_1 + k \ , \tag{3.29}$$

$$-\sigma R(s) w''(s) + D(s) < 0 \ ; \quad s_1 < s \leq s_1 + k \ . \tag{3.30}$$

Now consider the set of axially symmetric perturbations $\eta = \eta(s)$ for which, cf. (2.2),

$$s_0(\phi) = s_0 \ ; \quad s_1(\phi) = s_1 + k \ ; \quad 0 \leq \phi \leq 2\pi \ .$$

Let $\nu(s)$ be defined as in (3.7)-(3.11) and, keeping k fixed, let $d(\nu) \to 0$ (i.e. let the perturbation tend to the unperturbed surface extended by wetting the portion $s_1 < s \leq s_1 + k$ of the container wall). By (3.30) the integral (3.19) will be negative and linear in $\nu$ while by (3.12), (3.15) and (3.17) other contributions to $\delta E(\eta)$ are of higher order in $\nu$. Hence, proceeding as in the proof of Theorem 3.2 to satisfy the volume constraint, for any given $d_1 > 0$ we may choose a function $\eta(s)$ suitably to satisfy $\delta V(\eta) = 0$ and

$$d(\nu) \le d_1 \quad , \tag{3.31}$$

$$\delta E(\eta) < 0 \quad .$$

Since, by (3.28) and (3.29), using the definitions (2.20), (2.21) and (3.7)-(3.11),

$$d(\Sigma) = k \le \tfrac{1}{3} d_0$$

$$\lim_{d(\nu)\to 0} d(\eta) = \sup_{s_1 \le s \le s_1+k} |w(s)| + \sup_{s_1 \le s \le s_1+k} |w'(s)| \le \tfrac{1}{3} d_0 \quad ,$$

the statement of the theorem follows by choosing $d_1$ in (3.31) sufficiently small.

Remark: We note that the instability stated in Theorem 3.3 is present regardless of the stability conditions based on the second variation of (1.1). The method of proof suggests that the instability should show by a thin layer of liquid building up past the contact line $s = s_i$. A verification of this kind of instability by experiments would of course be virtually impossible because of the several idealizing assumptions inherent in the model (cf. however [3] where a series of low-gravity experiments performed at the NASA Lewis Research Center are studied computationally).

ACKNOWLEDGEMENTS

The investigations reported in this paper arose in connection with a computational study made for the National Aeronautics and Space Administration (NASA) while the writer was a visitor at the Lawrence Berkeley Laboratory. The writer wishes to thank Dr. Paul Concus of the LBL and Dr. Robert Finn of Stanford University for enlightening discussions related to the subject of this paper.

# REFERENCES

[1] Akhiezer, N. I., The Calculus of Variations. Blaisdell Publishing Company 1962.

[2] Bolza, O., Lectures on the Calculus of Variations. Dover Publications, Inc. 1904/1961.

[3] Concus, P., and Karasalo, I., A Numerical Study of Capillary Stability in a Circular Cylindrical Container with a Concave Spheroidal Bottom. LBL 6144, February 1977.

[4] Gillette, R., The Stability of Axisymmetric Fluid Interfaces. Ph.D. Thesis, 1970, (Dept. of Chemical Engineering, Rice University).

[5] Huh, C., Capillary Hydrodynamics: Interfacial Instability and the Solid/Liquid/Fluid Contact Line. Ph.D. Thesis, 1969, (Dept. of Chemical Engineering, University of Minnesota).

[6] Karasalo, I., Sufficient Conditions for Stability of Axisymmetric Annular Liquid Interfaces. LBL 4898, June 1976.

[7] Kato, T., Perturbation Theory for Linear Operators. New York: Springer Verlag 1966.

[8] Reynolds, W. C., Saad, M. A., and Satterlee, H. M., Capillary Hydrostatics and Hydrodynamics at Low g. Technical Report, No. LG-3, September 1, 1964, (Mechanical Engineering Dept., Stanford University).

APPENDIX III

# A NUMERICAL STUDY OF CAPILLARY STABILITY IN A CIRCULAR CYLINDRICAL CONTAINER WITH A CONCAVE SPHEROIDAL BOTTOM

by

Paul Concus and Ilkka Karasalo

To appear in Computer Methods in Applied Mechanics and Engineering

# A NUMERICAL STUDY OF CAPILLARY STABILITY IN A CIRCULAR CYLINDRICAL CONTAINER WITH A CONCAVE SPHEROIDAL BOTTOM

P. Concus*

I. Karasalo**

## ABSTRACT

We study computationally the stability, under gravitational and surface forces, of a liquid in a circular cylindrical container with a concave spheroidal bottom, for the case in which the volume of liquid is sufficiently small so that the bottom is not covered entirely. We assume the gravitational field to be directed along the axis of symmetry of the container, and for a specific container shape we compute the critical Bond number as a function of liquid volume for contact angles $\gamma = 0°$, $1°$, $2°$, and $4°$. For the case $\gamma = 0°$ we present graphically several critical equilibrium configurations and corresponding perturbation modes.

* Lawrence Berkeley Laboratory, University of California, Berkeley, CA 94720.

**Lawrence Berkeley Laboratory, University of California, Berkeley, CA 94720. Now at KDT, ASEA, S-721 83 Västerås, Sweden.

## 1. STATEMENT OF THE PROBLEM

In this paper we present the results of a computational study of the stability of a liquid in a rotationally symmetric container subject to gravitational and surface forces. We consider vertical right circular cylindrical containers with concave spheroidal bottoms, for the case in which the volume of liquid is sufficiently small so that liquid lies only in an annular region of the container (Fig. 1). We are interested specifically in the case for which the contact angle $\gamma$ is zero, or nearly zero, and our numerical results are obtained for a container currently used for the storage of liquid fuels in National Aeronautics and Space Administration Centaur space vehicles, for which the axial ratio of the bottom is $b/a = 0.724$.

A vertical section through the axis of the container is depicted in Fig. 1, along with the associated cylindrical coordinate system. The container may be in motion, but the net external gravitational force is assumed to be uniform and directed parallel to the axis of symmetry. It is well known, that even if the gravitational force is directed upward, liquid may be in stable equilibrium at the container bottom because of the effect of surface forces. For a given liquid volume, stable configurations of this kind are possible only if the magnitude of the upward-directed gravitational force does not exceed a certain critical value. This critical value depends on physical parameters such as the liquid-vapor surface tension coefficient, the difference in liquid and vapor densities, the liquid-container contact angle,

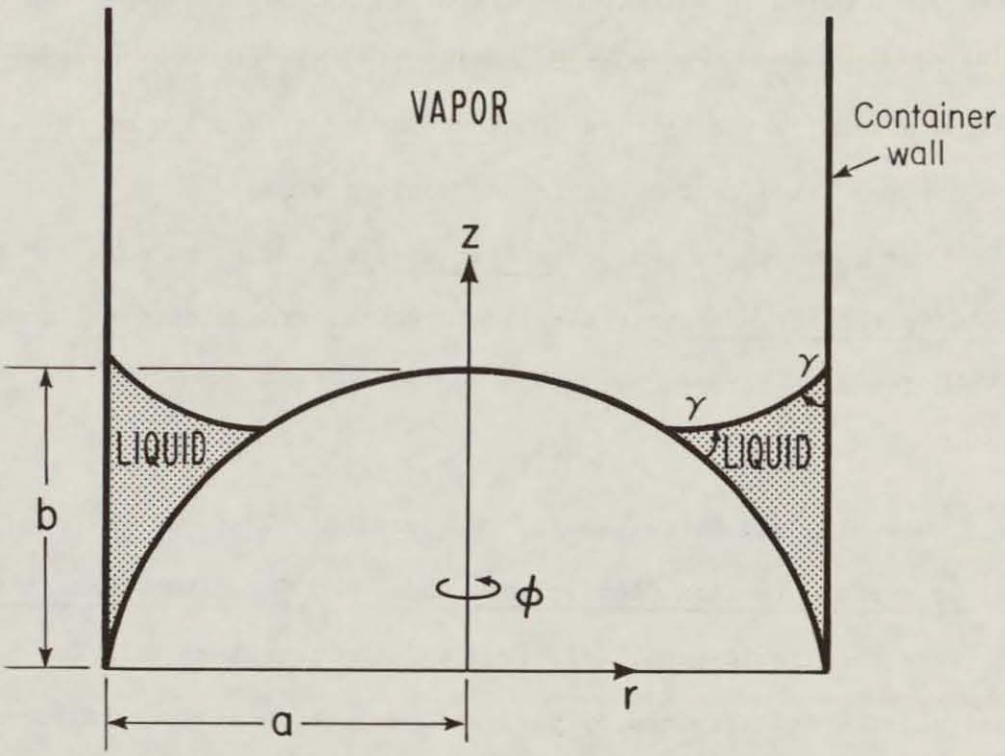


XBL 773-583

Figure 1: The container and the associated cylindrical coordinate system. The bottom has the shape of an ellipsoid of revolution with axial ratio b/a.

and geometrical parameters such as the container size and shape. The combined effect of certain of these parameters may be represented by the dimensionless Bond number (see (2.11) below), whose critical value for our problem is a function only of the container shape, the liquid volume, and the contact angle. In this study we determine computationally the critical Bond number as a function of the liquid volume for fixed contact angle and container shape.

Our approach is that of static analysis, i.e. we consider the total potential energy of the liquid-container system (in a container-fixed frame of reference), given by

$$E = \sigma(A_f - A_w \cos\gamma) + E_g \tag{1.1}$$

(cf. Reynolds and Satterlee [3], p. 394-396). Here $\sigma > 0$ (the liquid-vapor surface tension coefficient) and $0 \leqslant \gamma \leqslant \pi$ (the contact angle between the liquid vapor interface and the container wall and bottom) are constants determined by physical properties of the liquid and the container, $A_f$ and $A_w$ are the areas of the liquid-vapor and the liquid-container interfaces, respectively, and $E_g$ is the gravitational potential energy of the liquid. A configuration of liquid is in stable equilibrium if and only if the total potential energy (1.1) is minimal compared with that of any nearby configuration having the same liquid volume. Thus the critical Bond number for a certain volume of liquid is the one at which E in (1.1) ceases to have a strict local minimum with respect to all perturbations that conserve the liquid volume. In Section 2 below we give a summary of an analysis of this constrained minimization problem using methods of variational calculus.

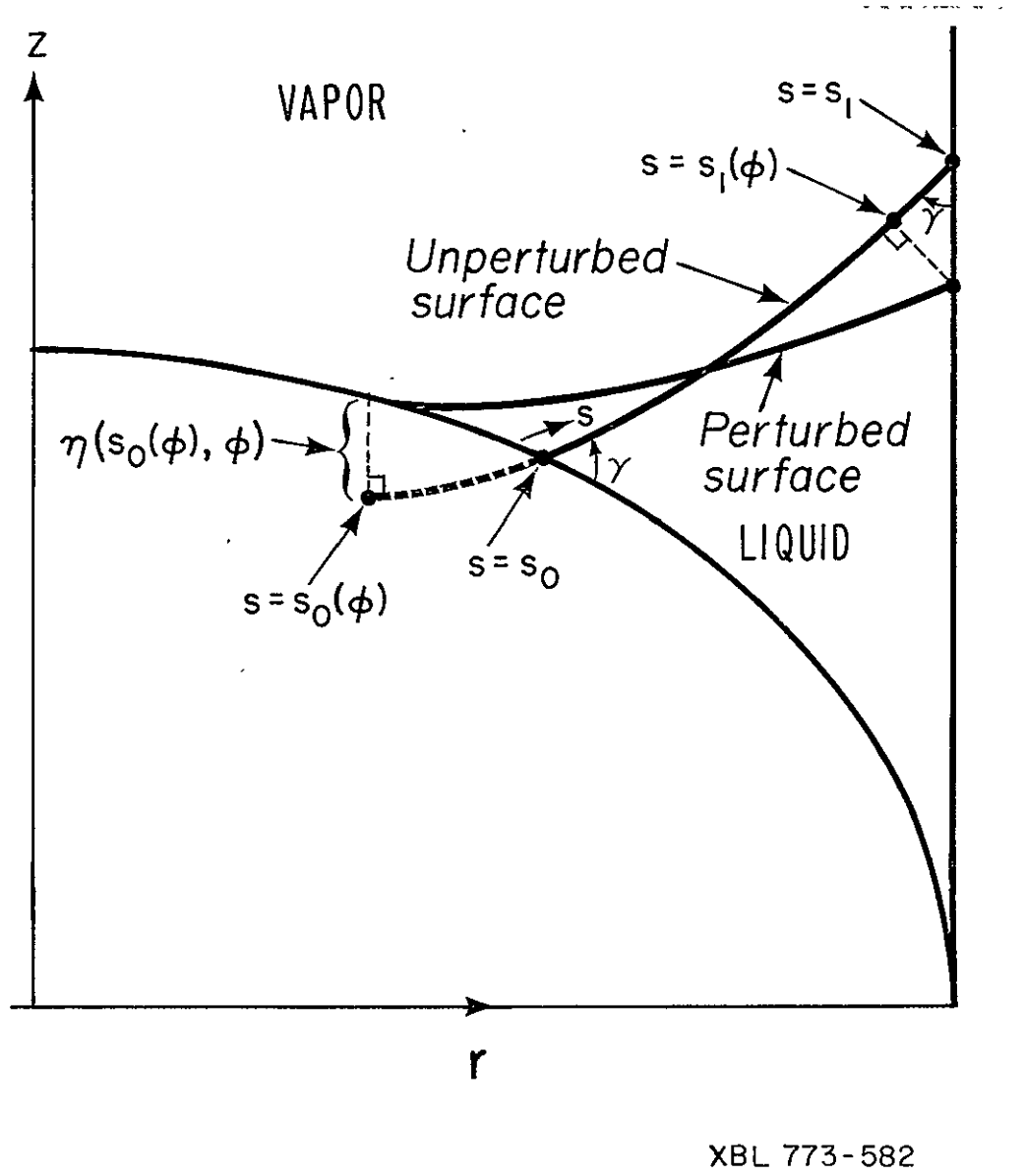


Figure 2: The arc-length, normal-displacement coordinate system.

continuation of the unperturbed surface to the left in Fig. 2. (The continuation may be done in several ways, perhaps most conveniently by using the fact that R(s) and Z(s) will be analytic functions for equilibrium configurations, cf. (2.9) below.)

In a way similar to (2.2), the container wall and bottom are described by

$$\begin{cases} r = R(s) - w(s)Z'(s) \\ z = Z(s) + w(s)R'(s) \end{cases} \qquad 0 \leqslant \phi \leqslant 2\pi \tag{2.3}$$

in some neighborhoods of the unperturbed contact lines $s = s_0$ and $s = s_1$. Then clearly $w(s_0) = w(s_1) = 0$. The function $w(s)$ will depend on the shape of the container wall and bottom and, implicitly, the shape of the unperturbed liquid-vapor interface. The representation (2.3) is convenient for the purpose of deriving the differential equations; however, in the actual computations we must, of course, make use of the known, configuration-independent shape of the container, cf. (3.4) and (3.5) below.

The increments of the total potential energy E and the liquid volume V caused by the perturbation $\eta(s,\phi)$ in (2.2) may then be computed. We obtain in a straightforward way

$$\begin{aligned} \delta E(\eta) &= \sigma(\delta A_f - \delta A_w \cos\gamma) + \delta E_g \\ &= \int_0^{2\pi} \int_{s_0(\phi)}^{s_1(\phi)} \left\{ \sigma(f_A(\underline{\eta},s) - f_A(\underline{0},s)) + \rho g\, f_g(\underline{\eta},s) \right\} ds\, d\phi \\ &\quad - \int_0^{2\pi} \int_{\Delta_\phi} \left\{ \sigma(\cos\gamma \cdot f_A(\underline{w},s) - f_A(\underline{0},s)) + \rho g\, f_g(\underline{w},s) \right\} ds\, d\phi \,, \end{aligned} \tag{2.4}$$

$$\delta V(\eta) = \int_0^{2\pi} \int_{s_0(\phi)}^{s_1(\phi)} f_V(\underline{\eta},s)\, ds\, d\phi \; - \int_0^{2\pi} \int_{\Delta_\phi} f_V(\underline{w},s)\, ds\, d\phi\,, \tag{2.5}$$

where we have put

$$\begin{aligned} \underline{\eta} &= \underline{\eta}(s,\phi) = (\eta(s,\phi),\ \eta_s(s,\phi),\ \eta_\phi(s,\phi))^T\,, \\ \underline{w} &= \underline{w}(s) = (w(s),\ w'(s),\ 0)^T \\ \Delta_\phi &= \text{the interval } (s_0(\phi),\ s_0) \cup (s_1,\ s_1(\phi))\,, \end{aligned} \tag{2.6}$$

and where the functions $f_A(\underline{\eta},s)$, $f_V(\underline{\eta},s)$, and $f_g(\underline{\eta},s)$ are given by (denoting $R = R(s)$, $Z = Z(s)$, and $C = Z''R' - R''Z'$ for brevity)

$$\begin{aligned} f_A(\underline{\eta},s) &= \left\{(R - \eta Z')^2(\eta_s^2 + (1 - \eta C)^2) + \eta_\phi^2(1 - \eta C)^2\right\}^{\frac{1}{2}} \\ f_V(\underline{\eta},s) &= \eta\left\{R - \tfrac{1}{2}(Z' + RC)\eta + \tfrac{1}{3}Z'C\eta^2\right\} \\ f_g(\underline{\eta},s) &= \eta\left\{RZ + \tfrac{1}{2}(RR' - ZZ' - RZC)\eta - \right. \\ &\qquad \left. - \tfrac{1}{3}((RR' - ZZ')C + R'Z')\eta^2 + \tfrac{1}{4}R'Z'C\eta^3\right\} \end{aligned} \tag{2.7}$$

In (2.4) $\rho$, the liquid density (or, more precisely, the difference between the liquid and vapor densities), is assumed to be constant, and $g$ is the gravitational constant (which may assume any value) defined so that $g > 0$ if the gravitational force pulls toward the negative z-axis.

The condition, that all first-order $\eta$-terms in $\delta E(\eta)$ as given by (2.4) should vanish for all $\eta$ such that $\delta V(\eta) = 0$ in (2.5) is then

$$\sigma \frac{\partial f_A}{\partial \eta}(\underline{0},s) + \rho g \frac{\partial f_g}{\partial \eta}(\underline{0},s) - \lambda \frac{\partial f_V}{\partial \eta}(\underline{0},s) = 0$$

in $s_0 \leqslant s \leqslant s_1$ , with the side-conditions (2.8)

$$\cos\gamma \cdot f_A(\underline{w}(s_i),s_i) - f_A(\underline{0},s_i) = 0,\ i = 0,\ 1,$$

where $\lambda$ is a constant (the Lagrange multiplier). Putting here $B = \rho g/\sigma$, $H = \lambda/\sigma$, and using (2.7) and the identity

$$R'(s)^2 + Z'(s)^2 = 1$$

(which holds because s is the arc-length) (2.8) becomes the Euler - Lagrange boundary value problem for the equilibrium liquid-vapor interface

$$\begin{cases} R'' = -Z'(BZ - H - Z'/R) \\ Z'' = R'(BZ - H - Z'/R) \\ w(s_0) = w(s_1) = 0, \\ w'(s_0) = -\tan\gamma,\ w'(s_1) = \tan\gamma \end{cases} \tag{2.9}$$

In general, the requirement that (2.9) should have a solution for a given container shape will restrict the B, H, and V - values to some two-dimensional subset of the (B,H,V) - space.

The equations (2.9) have the following invariance property: if $\ell$ is any positive constant and if we put

$$\overline{R}(s) = \frac{1}{\ell} R(\ell s),\quad \overline{Z}(s) = \frac{1}{\ell} Z(\ell s),\quad \overline{w}(s) = \frac{1}{\ell} w(\ell s) \tag{2.10}$$

then $\overline{R}$ and $\overline{Z}$ will satisfy (2.9) with B replaced by $\overline{B} = B\ell^2$, H replaced by $\overline{H} = H\ell$ and w replaced by $\overline{w}$. The transformation (2.10) means simply that $\overline{R}$, $\overline{Z}$, and $\overline{w}$ describe a liquid-tank configuration obtained by uniformly enlarging the original one by a factor $1/\ell$. Therefore, if we define dimensionless constants $B_0$ and $H_0$ by

$$B_0 = B\,a^2 = \frac{a^2\rho g}{\sigma}\quad ,\quad H_0 = H\,a = \frac{a\lambda}{\sigma} \tag{2.11}$$

where a is the container radius, $B_0$ (the Bond number) and $H_0$ will be invariant under uniform re-scalings of equilibrium liquid-tank configurations. We will therefore present the results of our computations below in terms of the $B_0$ in (2.11) in order to facilitate their use for arbitrary-sized containers.

We assume now that the liquid-vapor interface (2.1) satisfies the Euler-Lagrange equations (2.9). Then the condition, that all second order $\eta$-terms give a non-negative contribution to $\delta E(\eta)$ in (2.4) for all $\eta$ such that in (2.5) $\delta V(\eta) = 0$, may be written as

$$\int_0^{2\pi}\int_{s_0}^{s_1} \left\{ R(s)\eta_s^2 + \frac{1}{R(s)}\eta_\phi^2 + A(s)\eta^2 \right\} ds\, d\phi$$

$$+ \int_0^{2\pi} \left\{ \alpha_0 \eta(s_0,\phi)^2 + \alpha_1 \eta(s_1,\phi)^2 \right\} d\phi \quad \geq 0 \tag{2.12}$$

for all $\eta = \eta(s,\phi)$ such that

$$\int_0^{2\pi}\int_{s_0}^{s_1} R(s)\,\eta(s,\phi)\, ds\, d\phi = 0 \tag{2.13}$$

In (2.12) we have denoted

$$A(s) = -2R'' + B\{RR' - ZZ' + ZR(R''Z' - Z''R')\}$$
$$+ H\{Z' - R(R''Z' - Z''R')\} \tag{2.14}$$

and

$$\alpha_i = \frac{(-1)^i}{\tan^2\gamma} \frac{d}{ds} \Big\{ \cos\gamma \cdot f_A(\underline{w}(s),s) - f_A(\underline{0},s) + Bf_g(\underline{w}(s),s) -$$
$$- Hf_V(\underline{w}(s),s) \Big\}_{s=s_i}, \quad i = 0, 1 \tag{2.15}$$

It can be shown that if (2.12) (with the side-condition (2.13)) holds with strict inequality for all nonzero functions $\eta(s,\phi)$ then in fact E will be locally minimal at $\eta = 0$, i.e. the configuration described by the R(s) and Z(s) in (2.9) is a stable one. It can further be shown that if (2.12) (under (2.13)) does not hold for all $\eta$, then E cannot be locally minimal at $\eta = 0$ and the configuration is an unstable one. Thus the critical value of B will be the value at which the transition between these two cases occurs (provided that the corresponding solutions R(s), Z(s) to (2.9) describe an equilibrium liquid-vapor interface that is physically realizable, which may not always be the case - see the end of this Section). When B is critical in this sense, (2.12) still holds (under (2.13)) but there exists some non-zero $\eta = \eta(s,\phi)$ for which (2.12) holds with equality.

The inequality (2.12)-(2.13) may be analysed in terms of an associated sequence of eigenfunctions of the form

$$\{\mu_{ik}(s)\ \cos k\phi\}_{i=1,k=0}^{\infty} \tag{2.16}$$

with eigenvalues $\{\lambda_{ik}\}_{i=1,k=0}^{\infty}$. These are given by the solutions to the eigenvalue problems

$$\begin{cases} -\frac{d}{ds}\{R(s)\mu_{ik}'(s)\} + \left\{\frac{k^2}{R(s)} + A(s)\right\}\mu_{ik}(s) = \lambda_{ik}\mu_{ik}(s) \\ R(s_j)\mu_{ik}'(s_j) = (-1)^j\alpha_j\mu_{ik}(s_j) \qquad \begin{matrix} j = 0, 1 \\ k = 0, 1, 2, \ldots \\ i = 1, 2, 3, \ldots \end{matrix} \end{cases} \tag{2.17}$$

where $A(s)$, $\alpha_0$, and $\alpha_1$ were introduced in (2.14)-(2.15). It can be shown from (2.17) that the eigenvalues increase with the index $k$. It further follows from (2.16) that all eigenfunctions but those with $k = 0$ in (2.16) satisfy trivially the condition (2.13). Then it follows, that (2.12) under the side-condition (2.13) holds if and only if (assuming $\lambda_{ik}$ to be ordered increasingly with i)

$$\min \left\{ \lambda_{11}, \sum_{i=1}^{\infty} \hat{\beta}_i^2 \lambda_{i0} \right\} \geqslant 0 \ , \tag{2.18}$$

where, because of (2.13), $\{\hat{\beta}_i\}_{i=1}^{\infty}$ are solutions to:

$$\begin{aligned} &\text{Minimize} \sum_{i=1}^{\infty} \beta_i^2 \lambda_{i0} \text{ under the constraints} \\ &\sum_{i=1}^{\infty} \beta_i^2 = 1 \qquad \text{and} \\ &\sum_{i=1}^{\infty} \beta_i (\mu_{i0}, R) = 0 \ . \end{aligned} \tag{2.19}$$

In (2.19) we have denoted

$$(f,g) = \int_0^{2\pi} \int_{s_0}^{s_1} f(s,\phi)\, g(s,\phi)\, ds\, d\phi \ ,$$

and assumed $\{\mu_{i0}\}_{i=1}^{\infty}$ to be normalized to $(\mu_{i0}, \mu_{i0}) = 1$, $i = 1,2,3,\ldots$ .

In all the cases studied below it will in fact hold $|(\mu_{10},R)| >> |(\mu_{i0},R)|$, $i = 2,3,\ldots$ and $(\lambda_{20} - \lambda_{10}) >> (\lambda_{11} - \lambda_{10}) > 0$, so that the minimum in (2.18) is attained at $\lambda_{11}$. Thus, the critical value of B is determined by the condition $\lambda_{11} = 0$ (with the above mentioned restriction concerning non-realizable equilibrium configurations). By (2.14), (2.15), and (2.17), we obtain that this condition is equivalent to requiring that the Jacobi-Legendre boundary value problem

$$\begin{cases} -R\mu''(s) - R'\mu'(s) + \left\{\frac{1}{R} - 2R'' + B\{RR' - ZZ' + ZR(R''Z' - Z''R')\} + \right. \\ \qquad \left. + \; H\{Z' - R(R''Z' - Z''R')\}\right\}\mu(s) = 0, \quad s_0 \leq s \leq s_1 \qquad (2.20) \\ (-1)^i \tan\gamma\cdot\mu'(s_i) = \{\sin^2\gamma\cdot(R''Z' - Z''R') - \cos^2\gamma\cdot w''\}_{s=s_i}\cdot\mu(s_i) \\ \qquad\qquad i = 0, 1, \qquad (2.21) \end{cases}$$

should have a non-trivial solution $\mu(s)$.

We remark that the formulas (2.12) and (2.15) in the above discussion are meaningful only if the contact angle $\gamma$ is strictly positive. However, one of our principal interests is the limiting case $\gamma = 0$. Therefore a special analysis is needed in order to determine the proper limiting form of the above conditions (2.19)-(2.20) when $\gamma \to 0$. It can be shown (Karasalo [4]) that if $w''(s_i) < 0$, $i = 0, 1$, then the differential equation (2.20) with the fixed end-point boundary conditions

$$\mu(s_0) = \mu(s_1) = 0 \qquad (2.22)$$

is the correct one to use when $\gamma = 0$. Furthermore it holds when $\gamma = 0$ that if in the set of solutions $R(s)$, $Z(s)$ to (2.9) obtained by keeping the volume fixed and varying B (and H, cf. the comment after (2.9) above) $w''(s_0)$ or $w''(s_1)$ change sign as functions of B at some value of B, then this B-value is critical even if (2.20)-(2.22) lacks nontrivial solutions. This is so because only solutions $R(s)$, $Z(s)$ for which $w''(s_0) \leq 0$ and $w''(s_1) \leq 0$ hold are permissible for $\gamma = 0$ due to the constraints imposed by the container geometry. Our computations show, in fact, for the Centaur space vehicle example, that small liquid

volumes become unstable because of the conditions (2.20)-(2.22), whereas the stability of large liquid volumes is decided by the constraint $w''(s_1) \leqslant 0$. The transition between these two conditions occurs at a certain well defined volume, cf. (3.6)-(3.7) below.

## 3. COMPUTATIONAL PROCEDURE

With a given liquid volume in a given container of the shape shown in Fig. 1 we associate a dimensionless fill height, defined as follows: let $z_V$ be such that the given volume V coincides with the volume bounded by the container wall and bottom and the plane $z = z_V$. Then the fill height for the volume V in the container with radius a is

$$h_V = z_V/a = \frac{1}{a}\left(\frac{3b^2V}{\pi a^2}\right)^{1/3}. \tag{3.1}$$

We shall compute the critical Bond number $B_{0c}$ (cf.(2.11)) as a function of $h_V$. Obviously, by (2.10)-(2.11) and (3.1), these quantities are invariant under uniform re-scalings of the container, and we can therefore restrict our computations to a container with a specific radius, e.g. a = 1. We are interested only in the fill-height range $0 < h_V < b/a$, i.e. only in volumes that are smaller than that of the annular crevice at the container bottom.

Before describing our computational algorithm in detail we shall give the explicit form of the boundary conditions (2.21) at $s = s_0$ and $s = s_1$, respectively. In a neighborhood of $s = s_0$ there holds by (2.3), since the bottom is an ellispoid of revolution (cf. Figs.1 and 2)

$$\frac{(R(s) - w(s)Z'(s))^2}{a^2} + \frac{(Z(s) + w(s)R'(s))^2}{b^2} = 1 . \qquad (3.2)$$

Similarly, in a neighborhood of $s = s_1$ we have

$$R(s) - w(s)Z'(s) = a \qquad (3.3)$$

By differentiating these expressions twice and using (2.9), (2.21) becomes after some straightforward manipulations (we put $Z_i = Z(s_i)$, $R_i = R(s_i)$, $i = 0, 1$, for brevity)

$$\sin\gamma\cdot\mu'(s_0) = \left\{\frac{a^4b^4}{(a^4Z_0^2 + b^4R_0^2)^{3/2}} + \cos\gamma\cdot(BZ_0 - H - \frac{Z_0'}{R_0})\right\}\cdot\mu(s_0) \qquad (3.4)$$

$$\sin\gamma\cdot\mu'(s_1) = -\cos\gamma\cdot(BZ_1 - H - \frac{\cos\gamma}{a})\,\mu(s_1) . \qquad (3.5)$$

Our computations are carried out for the case $b/a = 0.724$ and proceed in two principal steps. In the first of these (which requires the main part of the computational effort) we determine successively some 50-60 points on the curve $B_{0c} = B_{0c}(h_V)$ at non-equidistant values of $h_V$. Each of these points is obtained in the following manner:

a) We choose a fixed point $R = a = 1$, $Z = Z_1$ at the cylindrical container wall and "guess" a corresponding pair of values for $B_0$ and $H_0$ in a way to be specified below.

b) We put $R(s_1) = a = 1$, $Z(s_1) = Z_1$, $R'(s_1) = \sin\gamma$, $Z'(s_1) = \cos\gamma$ to satisfy the boundary conditions at $s = s_1$ in (2.9) (we may choose $s_1$ arbitrarily, e.g. $s_1 = 1$). We further choose a pair of values $\mu'(s_1)$, $\mu(s_1)$, not both zero, consistent with the boundary condition

(3.5) (except for the large $h_V$ cases for $\gamma = 0$, cf. (3.6) below).

c) We solve simultaneously the differential equations (2.9) and (2.20) numerically, integrating from $s = s_1$ backwards with a standard fourth-order Runge-Kutta scheme. The stepsize of the integration is kept constant except for the last step which is adjusted (using a secant method) so as to make the last computed point of the solution to (2.9) lie on the container bottom profile (for the case $\gamma = 0$ we adjust the last step so as to make the normal of the computed solution to (2.9) at $s = s_0$ intersect the bottom profile at an angle of $\pi/2$). Thus we have ensured $w(s_0) = 0$ ($w'(s_0) = 0$ in the case $\gamma = 0$).

d) We compute the discrepancies in the boundary condition (3.4) and the remaining boundary condition at $s = s_0$ in (2.9). We adjust $B_0$ and $H_0$ (using eventually a Newton-type method to obtain the corrections) and repeat from b) above until the corrections in $B_0$ and $H_0$ are less than a prescribed tolerance.

e) We make a final integration computing this time also the liquid volume V, simply by adding the appropriate extra differential equation to the others. Then the corresponding $h_V$-value is obtained using (3.1).

We repeat the steps a)-e), using a set of some 50-60 regularly spaced $Z_1$-values. To obtain the initial "guesses" for $B_0$ and $H_0$ in a), we extrapolate the functions $B_{0c} = B_{0c}(Z_1)$ and $H_{0c} = H_{0c}(Z_1)$ to the next $Z_1$-value, fitting two quadratic polynomials in $Z_1$ through the three closest previously computed values of $\log|B_{0c}|$ and $\log|H_{0c}|$, respectively.

The functions $\log|B_{0c}(Z_1)|$ and $\log|H_{0c}(Z_1)|$ turn out to be close to linear in $Z_1$, and the accuracy in the guessed values was found to be very good (the "guesses" have in general 3-4 correct decimals when the spacing of the $Z_1$-values is 0.02a).

For all the contact angles studied, the computed points on the curve $B_{0c} = B_{0c}(h_V)$ indicate that $\log|B_{0c}|$ is only mildly nonlinear as a function of $h_V$. The second main step of our computation is to fit a cubic spline through the computed points on the curve $\log|B_{0c}| = \log|B_{0c}(h_V)|$. In this way we obtain a convenient and satisfactorily accurate representation of the sought function $B_{0c} = B_{0c}(h_V)$ throughout the entire $h_V$-interval of interest.

We have studied the contact angle values $\gamma = 4°$, $2°$, $1°$, and $0°$, the last of these values being the case of main interest. In the case $\gamma = 0$ we find that the above algorithm must be modified in the following way: When, in step a) above, $Z_1 > Z_1^*$ (corresponding to $h_V > h_V^*$, where $Z_1^* = 0.7014$ and $h_V^* = 0.5031$ with four correct decimals), then the condition

$$w''(s_1) \leqslant 0 \tag{3.6}$$

(which expresses the condition that the equilibrium liquid-vapor interface must lie inside the container for $s < s_1$, cf. the discussion at the end of Section 2) places a more restrictive bound on $B_0$ than the conditions under d) above. By (3.3), (3.6) is equivalent to

$$R''(s_1) = -(B_0 Z_1 - H_0 - 1) \leqslant 0 \tag{3.7}$$

Hence, when $\gamma = 0$ and $Z_1 > Z_1^*$ we solve, in steps b) and c) above, only the differential equations (2.9) and adjust, in step d), $B_0$ and $H_0$ so as to satisfy $w(s_0) = 0$ and $B_0 Z_1 - H_0 - 1 = 0$ (using again a Newton-like method to obtain the corrections).

## 4. NUMERICAL RESULTS

Table 1 shows the cubic spline approximations to the functions $B_{0c} = B_{0c}(h_V)$ for the contact angle values $\gamma = 0°$, $1°$, $2°$, and $4°$ (for the case $b/a = 0.724$). The relative error in each entry shown is less than $10^{-4}$, as estimated from repeated computations with different step-sizes in the numerical integration and different spacings for the $Z_1$-values used in step a) in the computational algorithm (cf. Section 3).

Figures 3-6 show graphs of the functions in Table 1. For practical reasons we use a logarithmic scale on the $B_{0c}$-axis, for which the curves are close to linear. Figure 7, showing all the graphs from Figures 3-6 simultaneously, illustrates the almost insignificant dependence on $\gamma$ in this range.

In Figure 8 we show the equilibrium surfaces at critical Bond number for the fill heights $h_V = 0.2(0.1)0.7$ for the case $\gamma = 0°$. The curves were plotted by numerical integration from starting points at the cylindrical wall using the subroutine package GRAFPAC available at LBL for graphical display of the results. The starting points for the integrations were obtained using cubic spline fitting to the points on the curve $Z_1 = Z_1(h_V)$, which are known as a "by product" of the $B_{0c} = B_{0c}(h_V)$ - calculation (cf. steps a) - e) of the algorithm described in Section 3).

The graphs of Figure 9 represent solutions to the Jacobi-Legendre equation (2.20) in the cases corresponding to the equilibrium configurations shown in Figure 8. The functions shown in Figure 9 are of the form

$$\nu(s) = \frac{\mu(s)}{R'(s)} \tag{4.1}$$

where $\mu(s)$ is a solution to (2.20) satisfying $\mu(s_0) = 0$. The function $\nu(s)$ depicts the radial dependence of the perturbation $\mu(s)\cos\phi$, but in terms of vertical displacement (whereas $\mu(s)$ is the radial perturbation profile in terms of displacement normal to the unperturbed surface, cf. (2.2)). The abscissa of the graphs in Figure 9 is R(s) and the functions are normalized so that $d\nu/dR \approx 1$ at the left end points. Theoretically, for $h_V > h_V^* \approx 0.5031$ (see (3.6)) the functions $\nu(s)$ defined in (4.1) have a singularity at $s = s_1$, i.e., at $R = 1$, while for $h_V < h_V^*$ $\nu(s_1)$ is nonzero but finite. Hence the graph corresponding to $h_V = 0.5$ in Figure 9 in fact intersects the line $R = 1$, whereas the two graphs above it do not.

Finally, in Figures 10-15 we show the equilibrium liquid-vapor interfaces of Figure 8 (solid lines) together with the equilibrium liquid-vapor interfaces superimposed by a small multiple of the corresponding $\nu(s)$ as given by (4.1). These curves are of some interest because, theoretically, when $B_0 = B_{0c}$ and $h_V < h_V^*$ the only possible initial shape of an unstable perturbation is given by $\nu(s)\cos\phi$ (in terms of vertical displacement). For $h_V > h_V^*$ it can in fact be shown (Karasalo [5]) that the configurations are unstable at $B_0 = B_{0c}$ for,

e.g., perturbations that build up some suitably chosen, axially symmetric layer of liquid above the unperturbed contact line at the cylindrical wall. Notice, however, that the dashed curves in Figures 14 and 15 do not show such a perturbation, but they are nevertheless included here for completeness. These results on the initial perturbation shape rely, of course, on several idealizing assumptions, such as that (1.1) holds exactly, that it represents all boundary constraints, that viscosity effects need not be included, etc., and the conclusions from Figures 10-15 should not be drawn too far.

The numerical results presented here have been found to be consistent with preliminary experimental results obtained at the NASA Lewis Research Center [6].

## 5. ACKNOWLEDGMENTS

We wish to thank Eugene P. Symons for initiating our interest in this problem by means of the remarkable color movies of stability experiments carried out at the NASA Lewis Zero Gravity Facility for the container depicted in Figure 1, and for his continued interest and sharing of experimental data with us during the course of our study. This work was supported in part by the National Aeronautics and Space Administration and by the Energy Research and Development Administration.

REFERENCES

1. R.F. Lacovic, Centaur zero gravity coast and engine restart on the Titan/Centaur (TC-2) extended mission, NASA TM X - 71821, Lewis Research Center, Cleveland, Ohio, October 1975.

2. P. Concus, G.E. Crane, H.M. Satterlee, Small amplitude lateral sloshing in spheroidal containers under low gravitational conditions. NASA CR - 72500, Lewis Research Center, Cleveland, Ohio, February 1969.

3. N. Abramson (editor), The dynamic behavior of liquid in moving containers, NASA SP 106, U.S. Government Printing Office, Washington, D.C., 1966.

4. I. Karasalo, Sufficient conditions for stability of axisymmetric annular fluid interfaces, LBL 4898, Lawrence Berkeley Laboratory, Berkeley, California, June 1976.

5. I. Karasalo, Stability of axisymmetric, annular fluid interfaces at zero contact angle, Preprint LBL 5318, Lawrence Berkeley Laboratory, Berkeley, California, June 1976 (to appear in Arch. Rat. Mech. Anal.).

6. E.P. Symons (private communication), 1976.

Table 1. Critical Bond number, $B_{0c}$, as function of fill height, $h_V$, at $\gamma = 0°$, 1°, 2°, and 4°.

| $h_V$ | $\gamma = 0°$ | $\gamma = 1°$ | $\gamma = 2°$ | $\gamma = 4°$ |
|---|---|---|---|---|
| 0.200 | -480.4283 | -480.3526 | -480.1183 | -479.1676 |
| 0.210 | -412.6934 | -412.6251 | -412.4212 | -411.5999 |
| 0.220 | -356.8787 | -356.8212 | -356.6472 | -355.9423 |
| 0.230 | -310.4444 | -310.3955 | -310.2463 | -309.6393 |
| 0.240 | -271.5210 | -271.4787 | -271.3503 | -270.8253 |
| 0.250 | -238.6539 | -238.6178 | -238.5075 | -238.0536 |
| 0.260 | -210.7102 | -210.6795 | -210.5850 | -210.1928 |
| 0.270 | -186.8042 | -186.7783 | -186.6978 | -186.3599 |
| 0.280 | -166.2339 | -166.2123 | -166.1443 | -165.8546 |
| 0.290 | -148.4377 | -148.4200 | -148.3635 | -148.1170 |
| 0.300 | -132.9638 | -132.9499 | -132.9038 | -132.6967 |
| 0.310 | -119.4456 | -119.4352 | -119.3990 | -119.2280 |
| 0.320 | -107.5834 | -107.5765 | -107.5497 | -107.4123 |
| 0.330 | -97.1310 | -97.1274 | -97.1098 | -97.0041 |
| 0.340 | -87.8844 | -87.8843 | -87.8757 | -87.8004 |
| 0.350 | -79.6741 | -79.6776 | -79.6781 | -79.6321 |
| 0.360 | -72.3581 | -72.3654 | -72.3752 | -72.3581 |
| 0.370 | -65.8171 | -65.8287 | -65.8482 | -65.8598 |
| 0.380 | -59.9504 | -59.9666 | -59.9965 | -60.0369 |
| 0.390 | -54.6722 | -54.6937 | -54.7349 | -54.8046 |
| 0.400 | -49.9096 | -49.9374 | -49.9908 | -50.0906 |
| 0.410 | -45.6000 | -45.6353 | -45.7024 | -45.8332 |
| 0.420 | -41.6896 | -41.7341 | -41.8166 | -41.9796 |
| 0.430 | -38.1320 | -38.1879 | -38.2878 | -38.4843 |
| 0.440 | -34.8869 | -34.9574 | -35.0769 | -35.3082 |
| 0.450 | -31.9190 | -32.0084 | -32.1502 | -32.4173 |
| 0.460 | -29.1976 | -29.3120 | -29.4786 | -29.7822 |
| 0.470 | -26.6956 | -26.8433 | -27.0371 | -27.3775 |
| 0.480 | -24.3887 | -24.5813 | -24.8043 | -25.1807 |
| 0.490 | -22.2554 | -22.5086 | -22.7615 | -23.1725 |
| 0.500 | -20.2759 | -20.6107 | -20.8925 | -21.3355 |
| 0.510 | -18.4509 | -18.8751 | -19.1830 | -19.6544 |
| 0.520 | -16.8150 | -17.2908 | -17.6204 | -18.1156 |
| 0.530 | -15.3484 | -15.8474 | -16.1930 | -16.7068 |
| 0.540 | -14.0314 | -14.5345 | -14.8900 | -15.4170 |
| 0.550 | -12.8467 | -13.3417 | -13.7013 | -14.2359 |
| 0.560 | -11.7792 | -12.2587 | -12.6174 | -13.1545 |
| 0.570 | -10.8157 | -11.2756 | -11.6291 | -12.1641 |
| 0.580 | -9.9447 | -10.3828 | -10.7281 | -11.2570 |
| 0.590 | -9.1561 | -9.5717 | -9.9065 | -10.4259 |

Table 1. (cont.)

| | | | | |
|---|---|---|---|---|
| 0.600 | -8.4411 | -8.8342 | -9.1571 | -9.6644 |
| 0.610 | -7.7920 | -8.1630 | -8.4730 | -8.9662 |
| 0.620 | -7.2017 | -7.5517 | -7.8483 | -8.3259 |
| 0.630 | -6.6644 | -6.9942 | -7.2773 | -7.7384 |
| 0.640 | -6.1746 | -6.4854 | -6.7551 | -7.1990 |
| 0.650 | -5.7276 | -6.0204 | -6.2770 | -6.7035 |
| 0.660 | -5.3192 | -5.5951 | -5.8390 | -6.2481 |
| 0.670 | -4.9456 | -5.2057 | -5.4373 | -5.8291 |
| 0.680 | -4.6035 | -4.8487 | -5.0686 | -5.4435 |
| 0.690 | -4.2898 | -4.5212 | -4.7299 | -5.0884 |
| 0.700 | -4.0020 | -4.2204 | -4.4185 | -4.7610 |

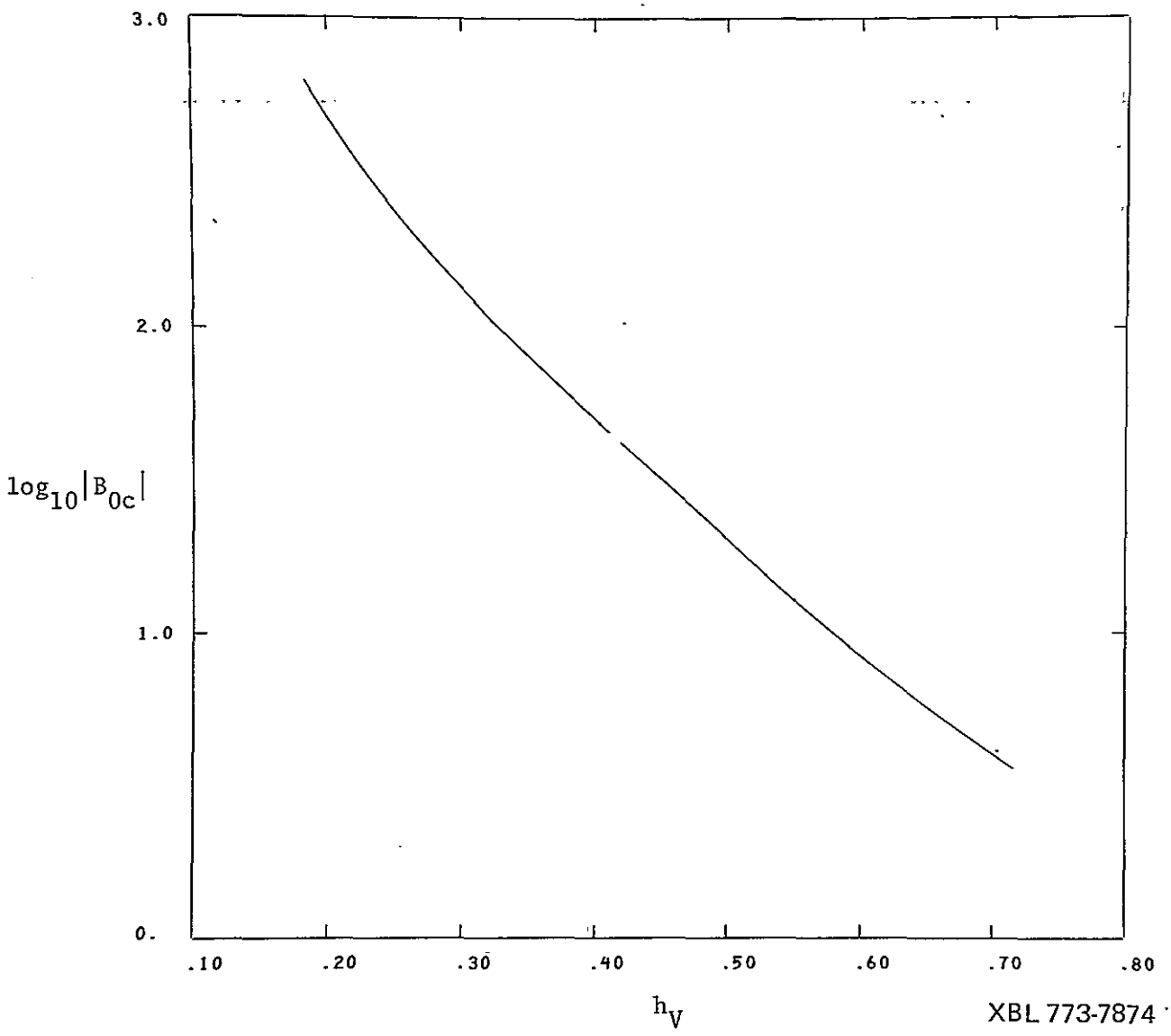


Figure 3: $B_{0c}$ as a function of $h_V$ for $\gamma = 0°$.

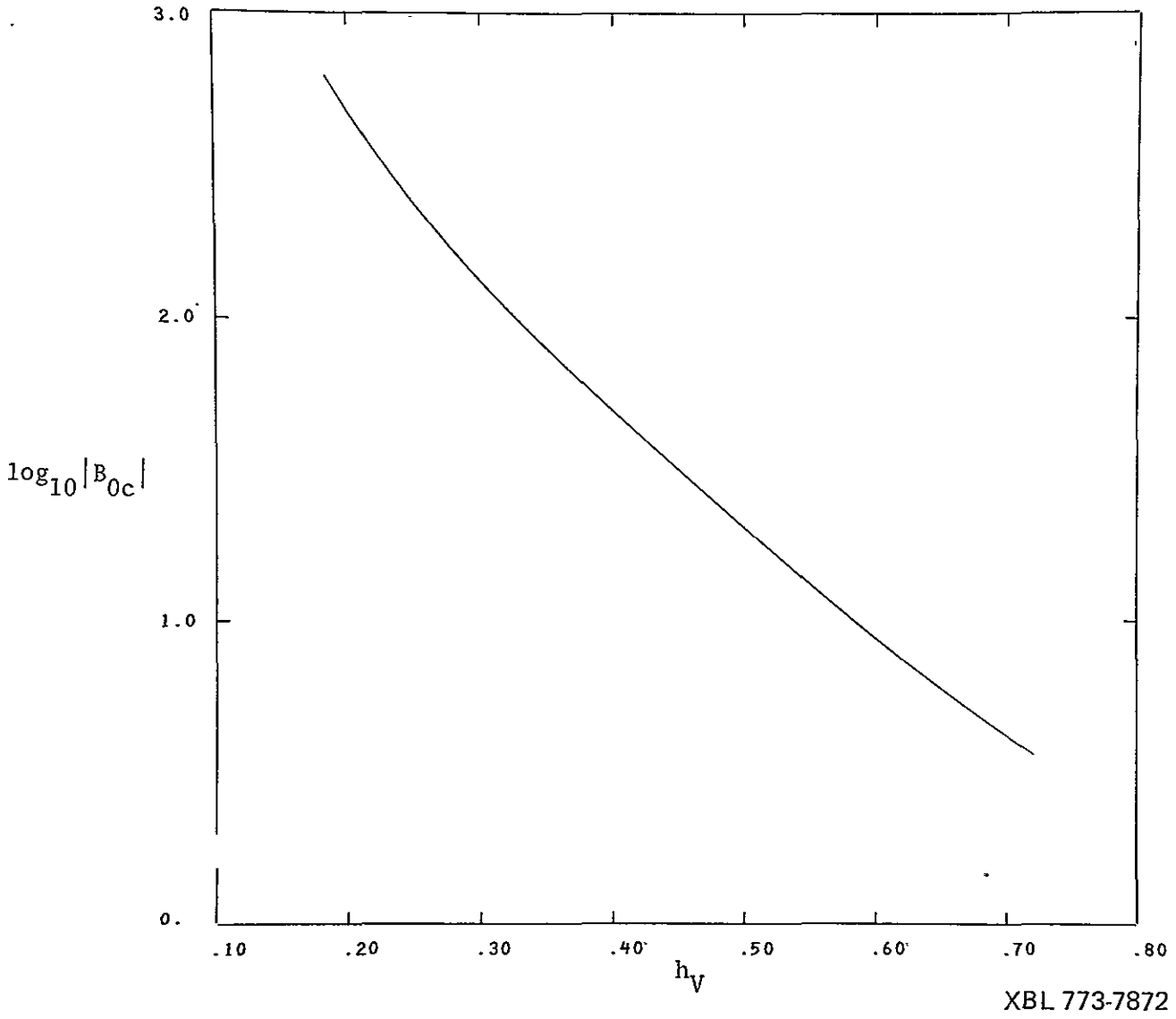


Figure 4: $B_{0c}$ as a function of $h_v$ for $\gamma = 1°$.

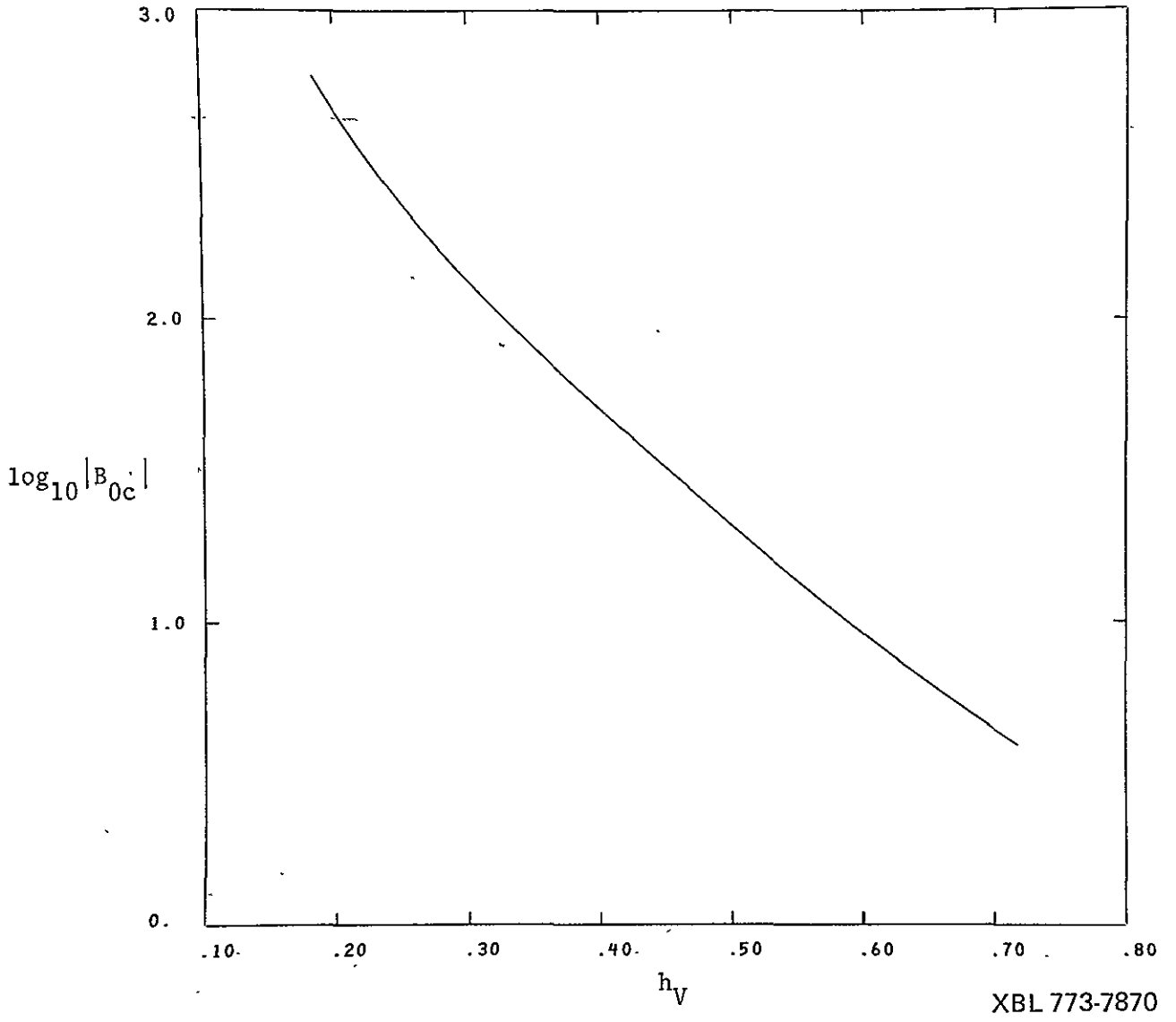


Figure 5: $B_{0c}$ as a function of $h_V$ for $\gamma = 2°$.

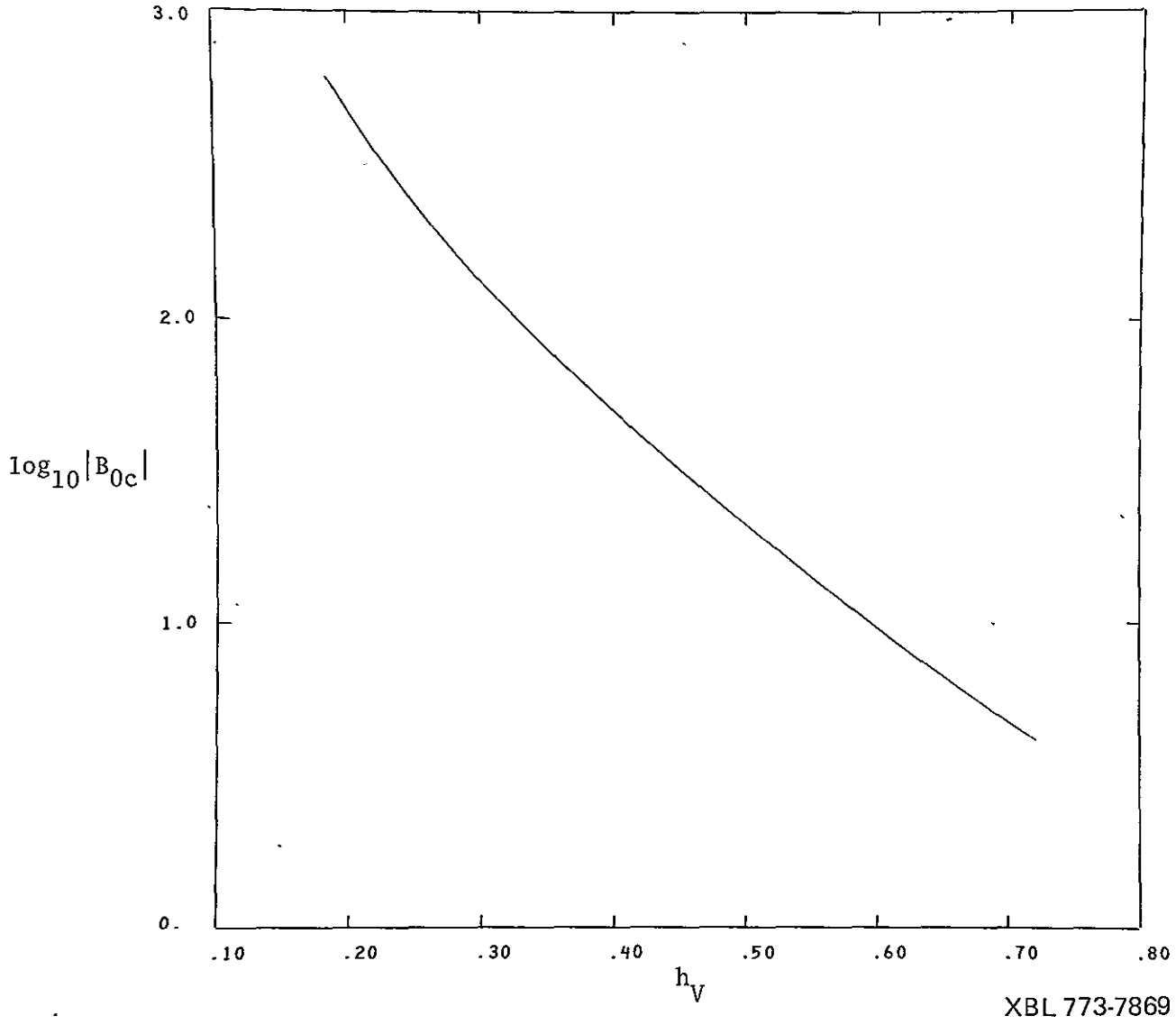


Figure 6: $B_{0c}$ as a function of $h_V$ for $\gamma = 4°$.

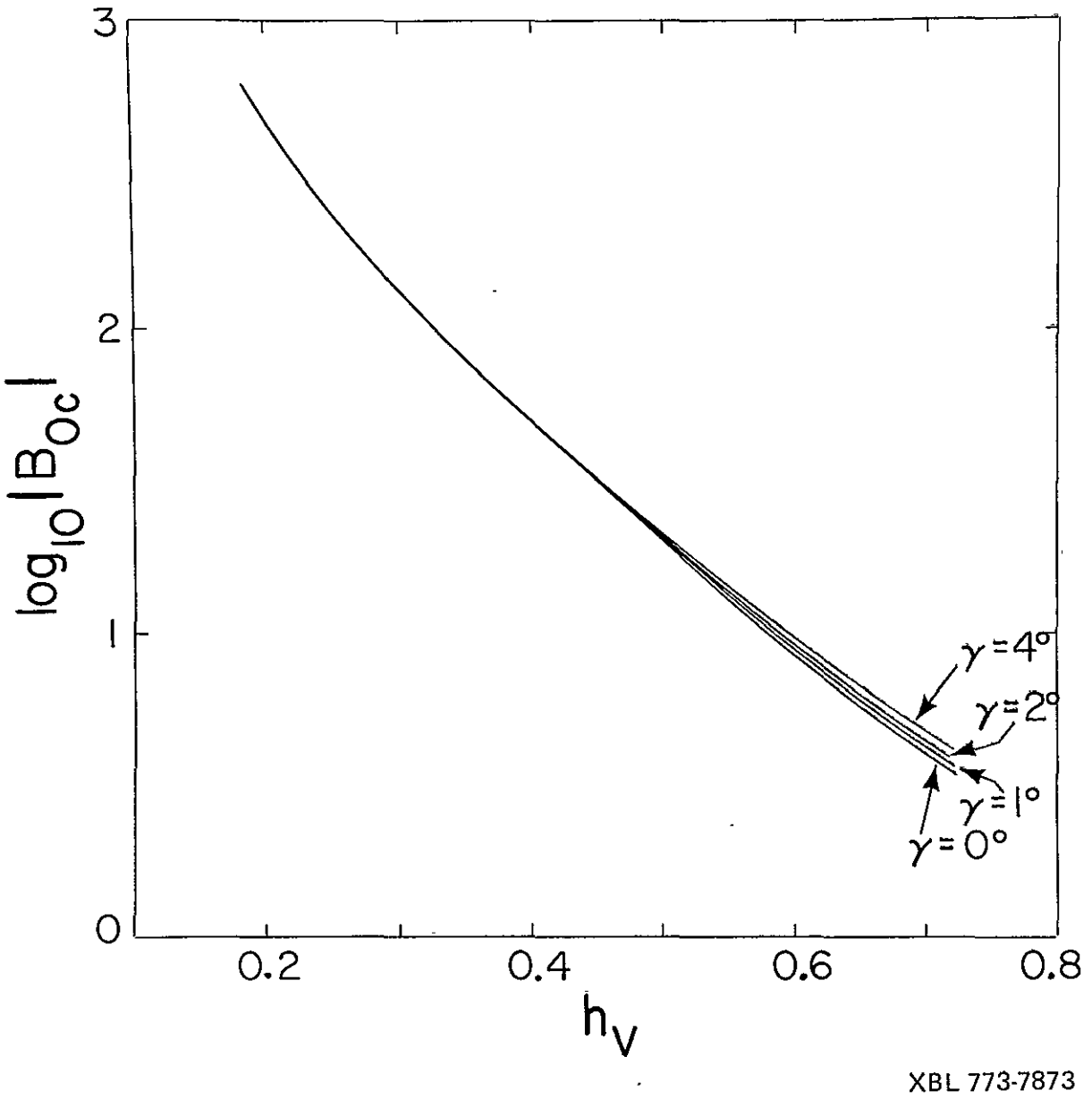


Figure 7: $B_{0c}$ as a function of $h_v$ for $\gamma = 0°$, $1°$, $2°$ and $4°$.

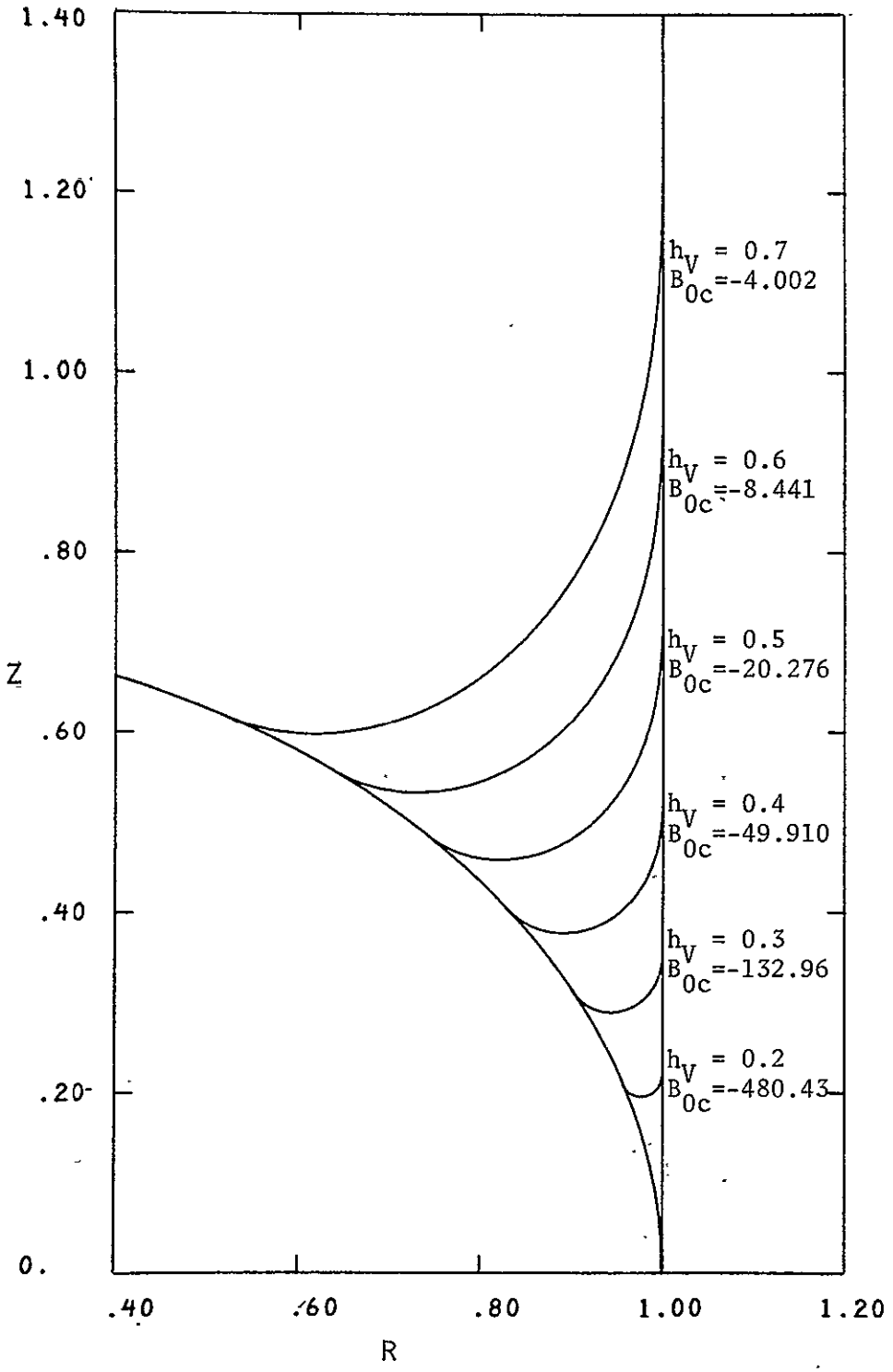


Figure 8: Equilibrium surfaces at critical Bond number for $\gamma = 0°$.

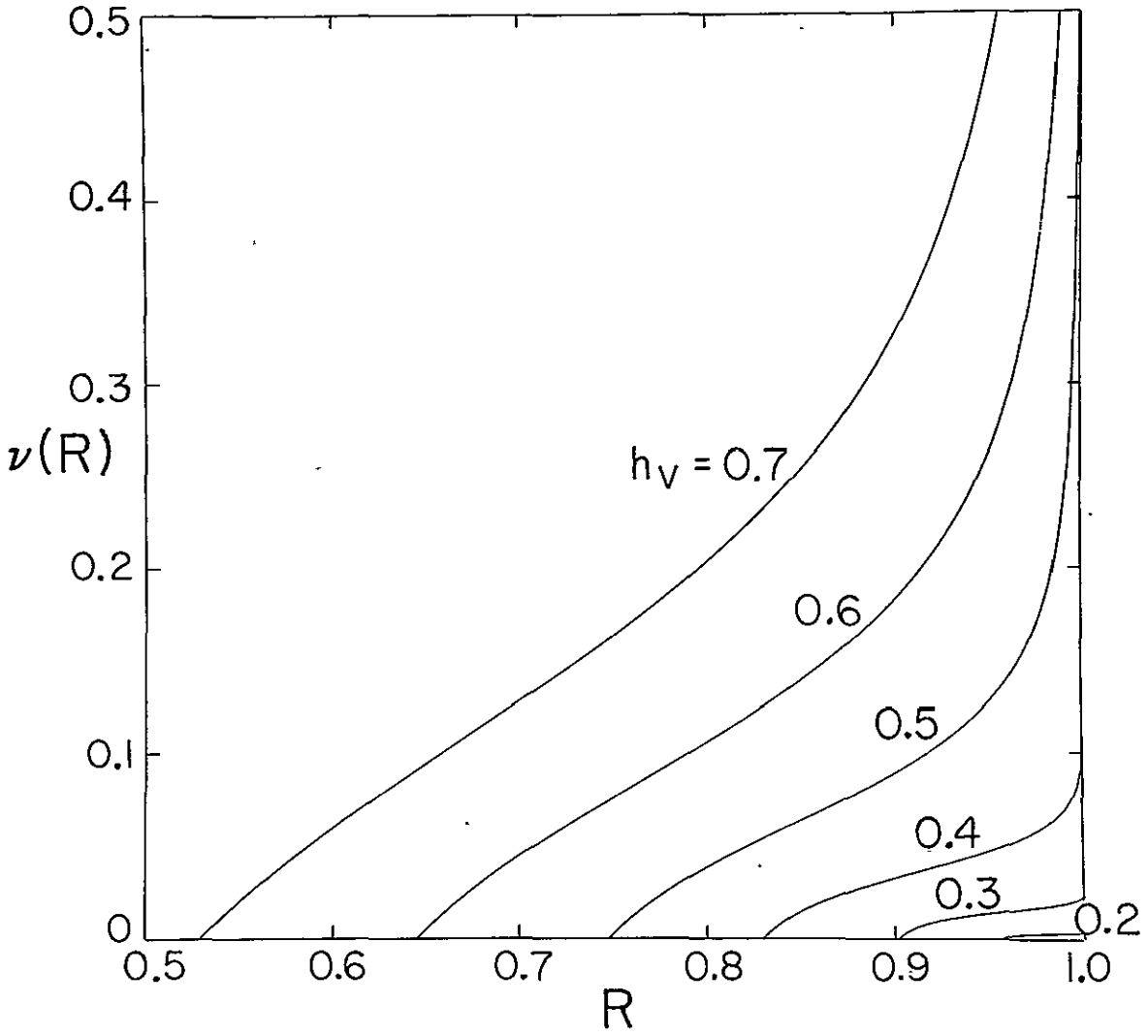


XBL 773-7879

Figure 9: Radial dependence of first angular perturbation modes in terms of vertical displacement. Curves normalized so that $\gamma(R_o) = 0$ and $(\frac{d}{dR})_{R_o} = 1$. ($R_o$ = left end point of curve.)

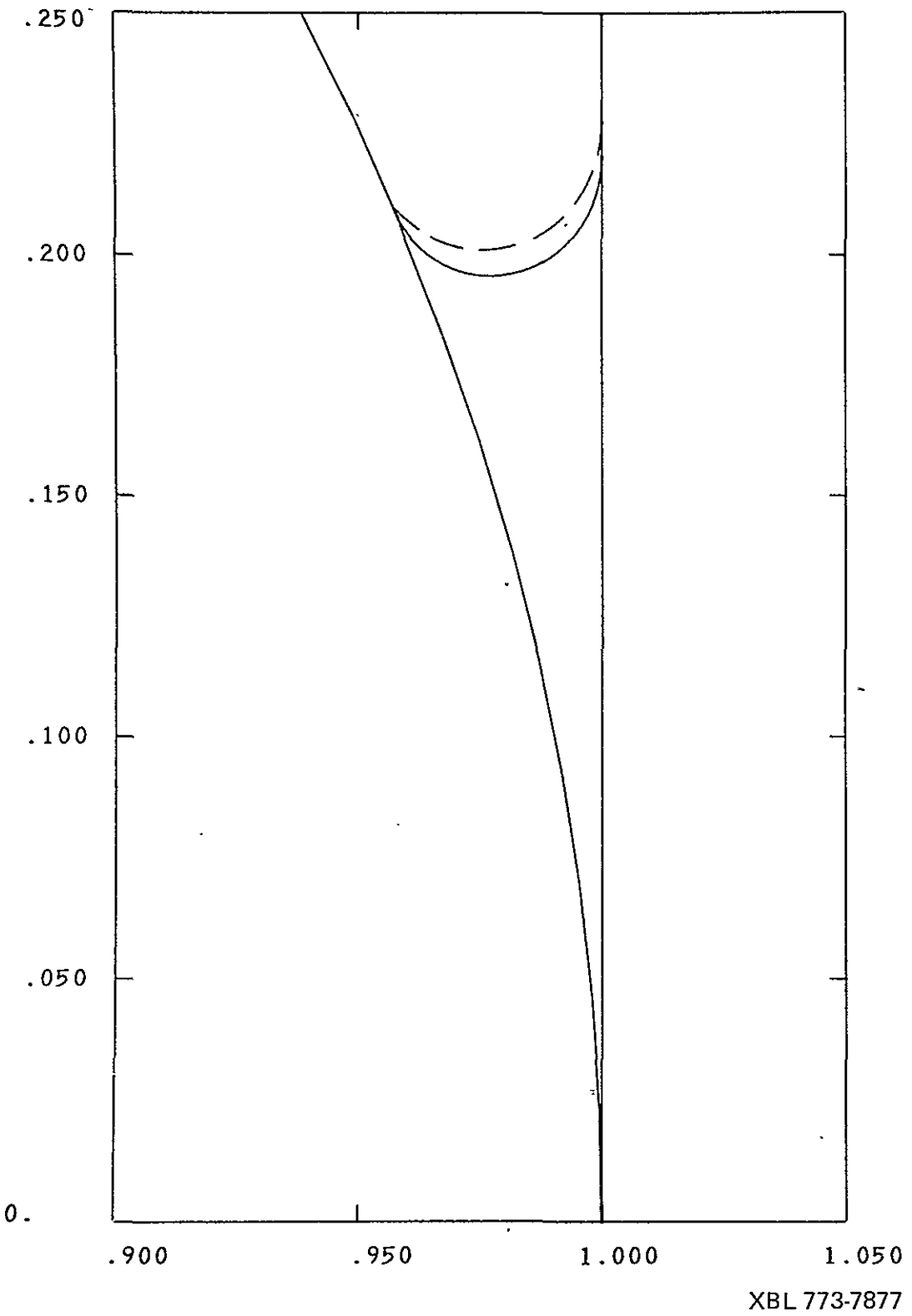


Figure 10: Solid Curve: Equilibrium surface at critical Bond number for $\gamma = 0°$ and $h_V = 0.2$.

Dashed Curve: Solid curve superimposed with the corresponding perturbant mode from Figure 9.

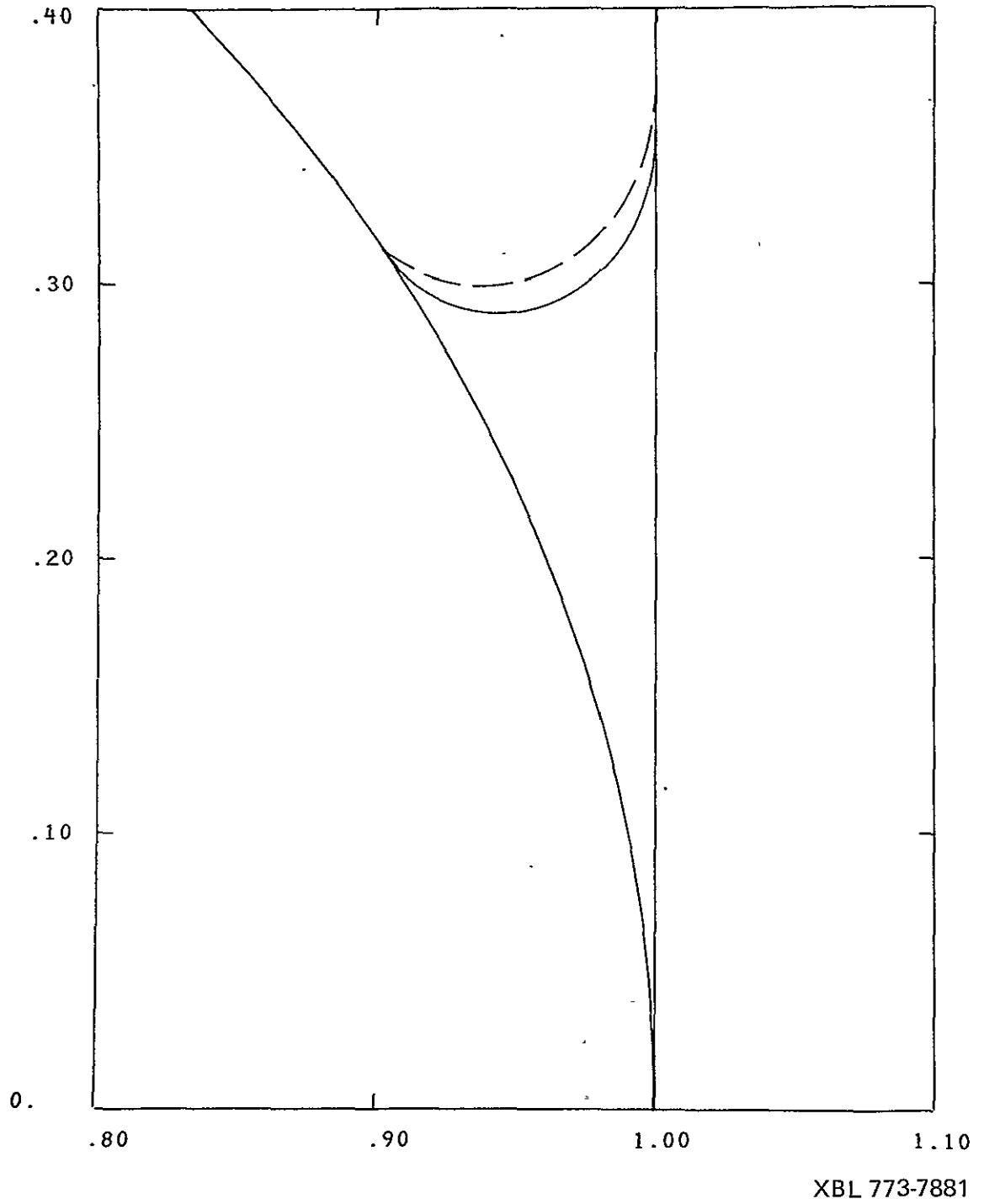


Figure 11: Solid Curve: Equilibrium surface at critical Bond number for $\gamma = 0°$ and $h_V = 0.3$.

Dashed Curve: Solid curve superimposed with the corresponding perturbation mode from Figure 9.

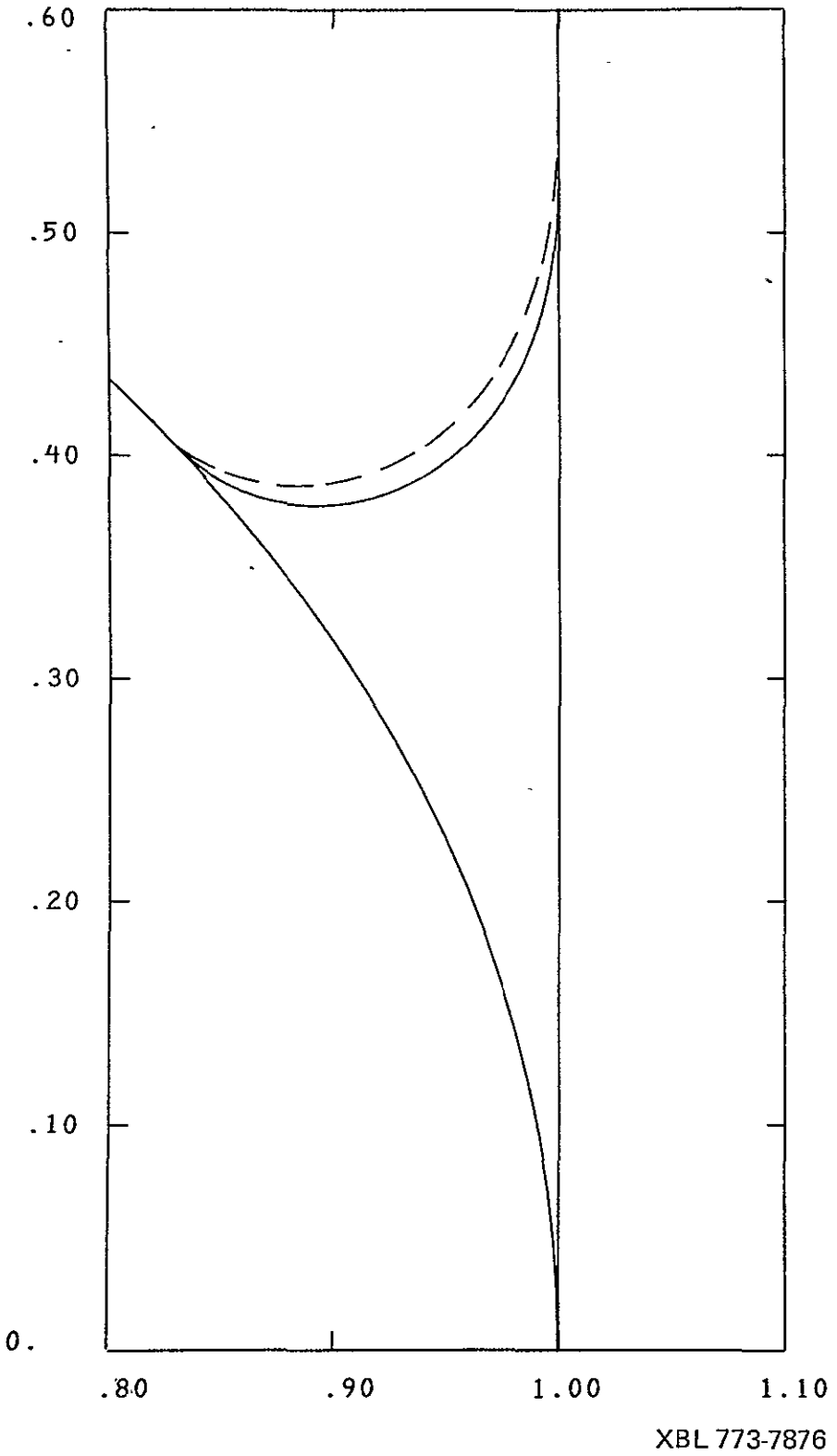


Figure 12: Solid Curve: Equilibrium surface at critical Bond number for $\gamma = 0°$ and $h_V = 0.4$.

Dashed Curve: Solid curve superimposed with the corresponding perturbation mode from Figure 9.

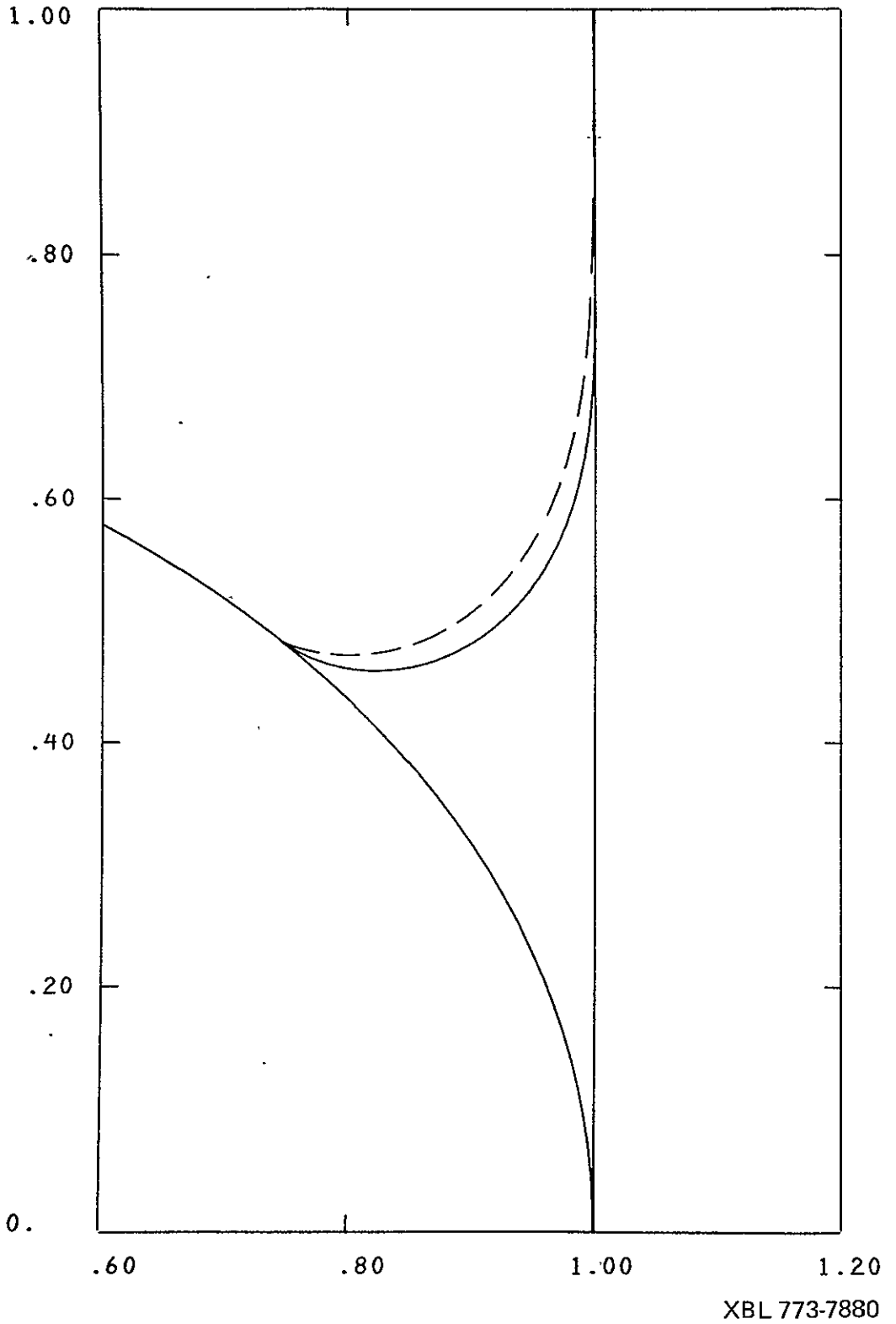


Figure 13: Solid Curve: Equilibrium surface at critical Bond number for $\gamma = 0°$ and $h_V = 0.5$.

Dashed Curve: Solid curve superimposed with the corresponding perturbation mode from Figure 9.

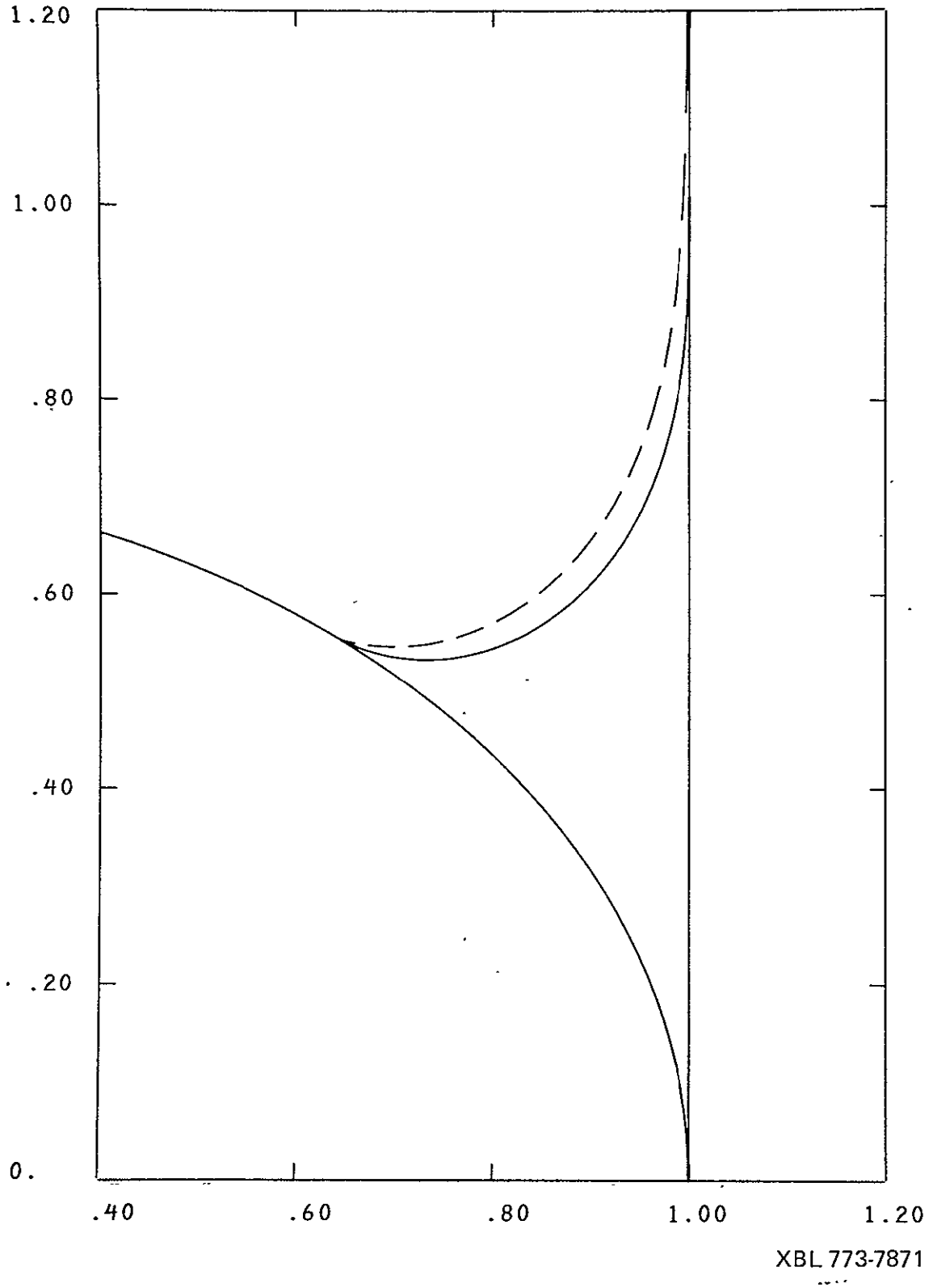


Figure 14: Solid Curve: Equilibrium surface at critical Bond number for $\gamma = 0°$ and $h_V = 0.6$.

Dashed Curve: Solid curve superimposed with the corresponding perturbation mode from Figure 9.

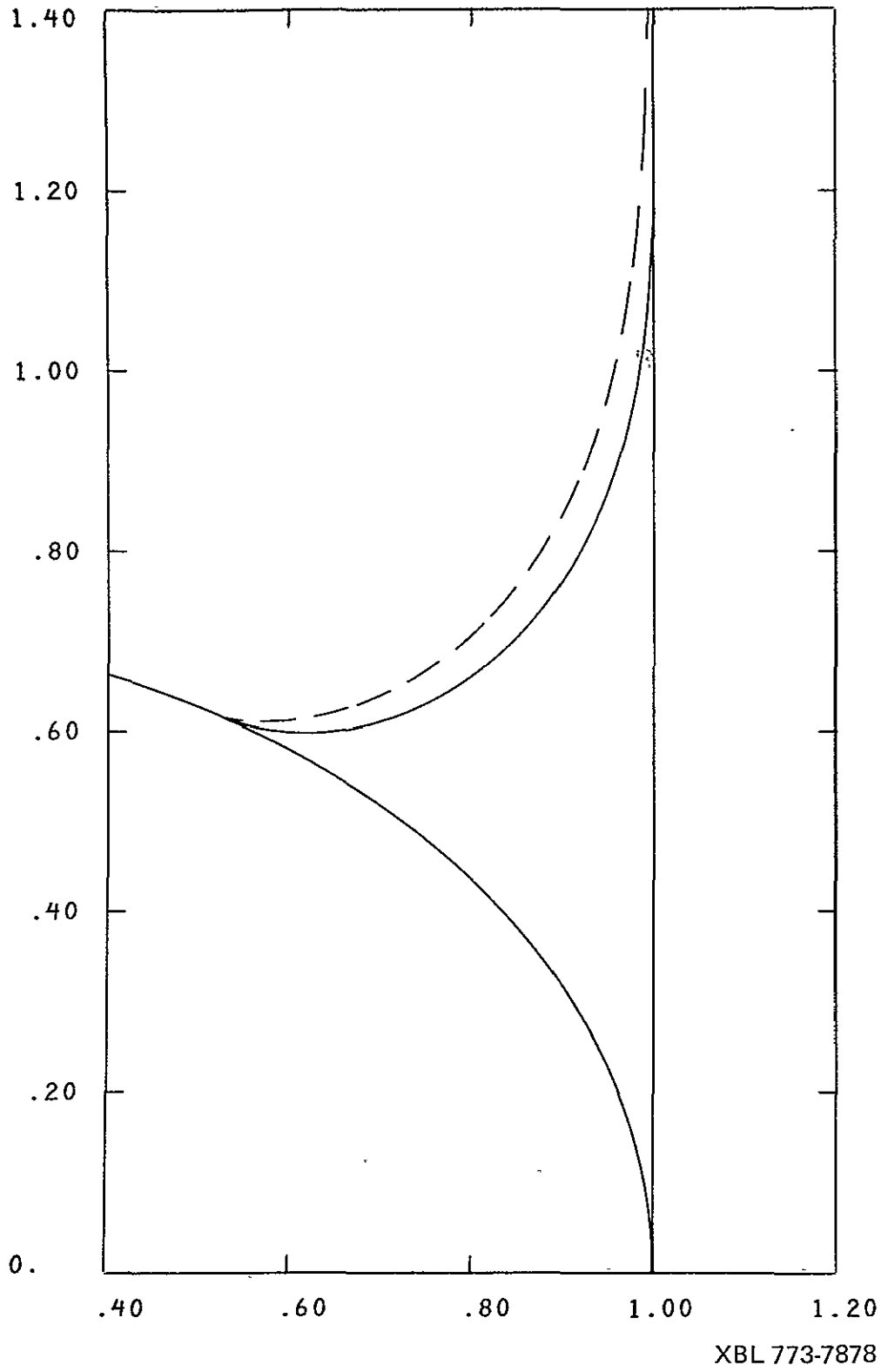


Figure 15: Solid Curve: Equilibrium surface at critical Bond number for $\gamma = 0^\circ$ and $h_V = 0.7$.

Dashed Curve: Solid curve superimposed with the corresponding perturbation mode from Figure 9.

APPENDIX IV

# SMALL AMPLITUDE PERIODIC SLOSHING MODES OF A LIQUID IN A VERTICAL RIGHT CIRCULAR CYLINDER WITH A CONCAVE SPHEROIDAL BOTTOM

by

Norman Albright and Paul Concus

Issued as Lawrence Berkeley Laboratory Report LBL-7204, November 1977

## ABSTRACT

In this paper we calculate the small-amplitude periodic sloshing modes of a liquid in a vertical right circular cylinder with a concave spheroidal bottom, for the case in which there is not sufficient liquid to cover the bottom entirely. Equilibrium free surfaces of the liquid were calculated by the program CAPIL for the case in which the ratio of the minor and major semi-axes of the spheroidal bottom was 0.724. Perturbations about these surfaces were calculated by the program SLOSH. For the fill heights that were studied, and to the accuracy of these calculations, we found the same critical Bond number, $B_{crit}$, for instability of the free surface as was found in the static analysis of P. Concus and I. Karasalo for the same test problem. Furthermore, in agreement with their calculation we also found no equilibrium surfaces for this problem for fill heights greater than 0.503 and for Bond numbers $B < B_{crit} < 0$. For fill heights ranging from 0.20 to 0.45 we found unstable equilibrium surfaces for a range of Bond numbers, $B_{conv} \leq B < B_{crit}$. Frequencies or growth rates were calculated for numerous equilibrium surfaces. Growth rates of the maximally unstable modes were calculated for fill height 0.30 and various Bond numbers.

## 1. Introduction

In this paper we calculate the small-amplitude, periodic sloshing modes of a liquid in a rotationally symmetric cylindrical container under the effect of surface and gravitational forces. We consider a right circular cylinder, oriented vertically, with a concave spheroidal bottom, for the case in which there is not sufficient liquid to cover the bottom entirely. This is the same configuration for which a stability study was carried out in [1]. Numerical results are obtained for a container currently used for the storage of liquid fuels in National Aeronautics and Space Administration Centaur space vehicles, for which the axial ratio of the bottom is $b/a = 0.724$. A vertical cross section of the cylinder and liquid is shown in Figure 1.

Equations describing the sloshing motion of liquids in rotationally symmetric containers are derived in [2] using a surface-normal polar coordinate system particularly suited to such problems. It is assumed there that the fluid flow is irrotational and incompressible and the free-surface boundary conditions are obtained from the time-dependent Bernoulli equation and the kinematic equation. The difference in pressure across the free surface at any point, due to the interfacial surface tension, is proportional to the mean curvature at that point. The edges of the surface satisfy time-independent contact angle conditions with the container bottom and the cylinder wall. We follow the derivation in [2] for obtaining the equations of motion for the case studied here, but we use a different technique for obtaining the numerical solution.

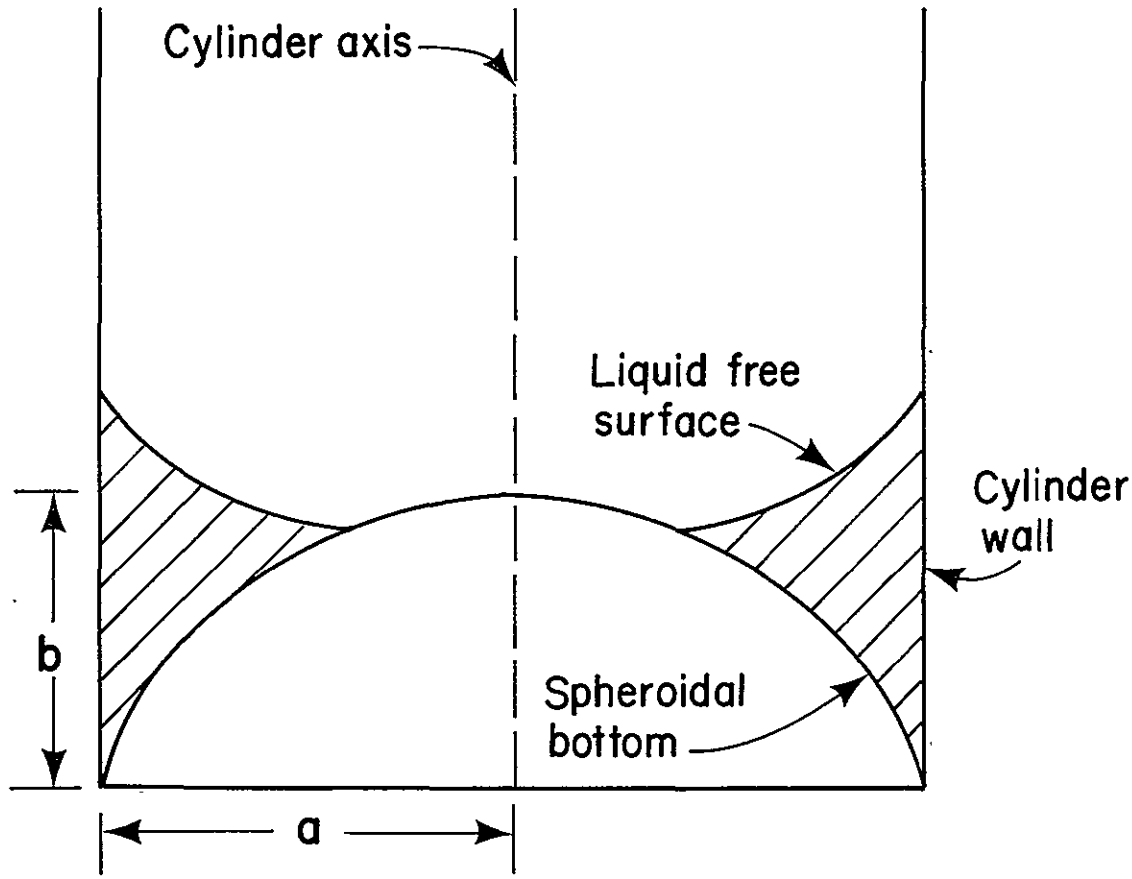


Figure 1. Vertical cross section of the cylinder and liquid.

XBL 781-103

2. Scaled Variables

We consider a circular cylindrical coordinate system with the z axis along the cylinder's axis of symmetry. It is convenient to define scaled length and time variables. Let symbols with a bar over them denote the corresponding physical, unscaled variables. Let

$$r = \bar{r}/a$$

$$z = \bar{z}/a$$

$$t = \bar{t}\,[(1+|B|)\,\sigma/\rho a^3]^{1/2}$$

$$H = \bar{H}\,a$$

$$B = \kappa a^2 = \rho g a^2/\sigma$$

$$2H_o = (p_g - p_o)\,a/\sigma$$

where $a$, the cylinder's radius, is the characteristic length used for scaling, $t$ is the time, $\rho$ is the difference in densities between the liquid and gas phases, $g$ is the acceleration due to gravity, considered positive when directed vertically downward, $\sigma$ is the gas-liquid surface tension, $\kappa$ is the capillary constant, $B$ is the Bond number, $H$ is the mean curvature at a point on the free surface, considered negative when the surface is concave upward, $p_g$ is the gas pressure, and $p_o$ is the liquid static pressure at the height $z = 0$.

The difference in pressure across the free surface satisfies the equation

$$p - p_g = -\,2H\,\sigma/a\ .$$

The liquid static pressure is given by

$$p - p_o = -\,\rho g z a\ .$$

From these equations it follows that the curvature H at any point on the equilibrium free surface is related to $H_o$, $B$, and $z$ by

$$2H = 2H_o + Bz\ .$$

3. Equilibrium Free Surface

We consider the vertical cross section through the axis of the cylinder shown in Figure 2. The cross section of the liquid is bounded by three curves: the meridians along the free surface, the cylinder wall, and the container bottom. Let $s$ be the arc length along this boundary, increasing clockwise. Let $s = 0$ be the intersection of the meridians on the free surface and the bottom, and let $s = S$ be the intersection of the meridians on the free surface and the cylinder wall.

The equilibrium free surface is rotationally symmetric about the axis of the cylinder. Its height is a function of $r$ only and not of $\Theta$. Thus the equilibrium surface can be described parametrically by the equations

$$r = R(s) \quad \text{and} \quad z = Z(s)$$

for $0 \leqslant s \leqslant S$ and $0 \leqslant \Theta < 2\pi$. Let $\psi$ be the angle in the cross-sectional plane between the tangent at a point on the free surface and the horizontal. Let $\psi$ be positive when the surface slopes upward in the direction of increasing $s$. Then

$$\tan \psi = Z_s/R_s ,$$

where the subscript $s$ denotes $d/ds$. Let the spheroidal bottom be described by

$$z = Z_B(r)$$

for $R(0) \leqslant r \leqslant 1$ and $0 \leqslant \Theta \leqslant 2\pi$. Let $\chi$ denote the angle in the cross-sectional plane between the tangent at a point on the bottom and the horizontal. Let $\chi$ be negative when the bottom slopes downward in

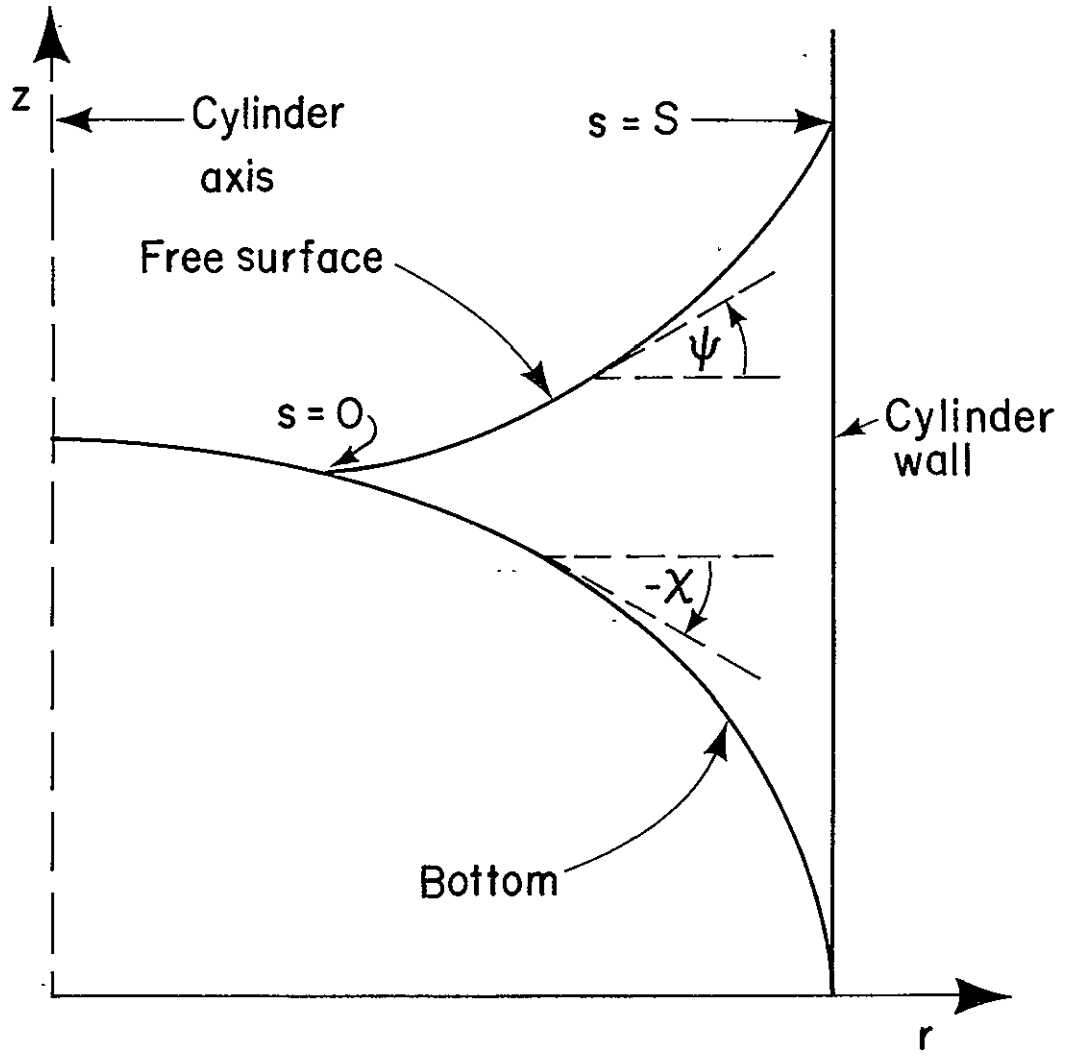


Figure 2. Vertical cross section of the liquid showing coordinates.

XBL 781-102

the direction of increasing $r$, as it does in our case. Then

$$\tan \chi = \frac{d}{dr} Z_B(r)$$

The equilibrium free surface is the solution of the time independent Bernoulli equation,

$$\psi_s = 2H_o + BZ - (\sin \psi)/R , \tag{3.1}$$

with

$$R_s = \cos \psi \tag{3.2}$$

$$Z_s = \sin \psi, \tag{3.3}$$

subject to the contact conditions,

$$Z(s) = Z_B(R(s)) \quad \text{at } s = 0 \tag{3.4}$$

$$R(s) = 1 \qquad \text{at } s = S \tag{3.5}$$

(the scaled radius of the cylinder is 1), and subject to the contact angle conditions,

$$\psi - \chi = \gamma \text{ at } s = 0 \tag{3.6}$$

$$\pi/2 - \psi = \gamma \text{ at } s = S , \tag{3.7}$$

where $\gamma$ is the contact angle. The volume of the liquid in the cylinder is

$$V = 2\pi \int_0^S [Z(s) - Z_B(R(s))]R(s) \cos \psi(s) \, ds . \tag{3.8}$$

This last equation determines implicitly the value of $H_o$ of V is given.

Equations (3.1) - (3.8) are the equations for the equilibrium free surface. The solution of these equations varies with the volume, the Bond number, the contact angle, and the shape of the bottom of the container. Depending on the values of these parameters, there may be

no, one, or more solutions of these equations [1]. If the equilibrium surface exists, it may be stable or unstable to small perturbations.

These equations are solved by the program CAPIL [3]. This program uses PASVA2 [4], a general-purpose finite difference solver for non-linear first-order systems of differential equations subject to two-point boundary conditions. PASVA2 solves these equations by iterating from an initial approximation to the surface. Either the user can supply the initial approximation, or the subroutine CYLCUR can generate it. When making calculations with the same fill for a sequence of Bond numbers, we let CYLCUR generate the initial approximation for the first case and use the output of each case as the initial approximation for the next case.

## 4. Small-Amplitude Periodic Sloshing Modes of the Liquid

The sloshing motion is treated as potential flow in an incompressible fluid. The fluid velocity $v$ at any point is the gradient of a potential function $\tilde{\phi}$

$$v = \nabla\tilde{\phi} .$$

Since the fluid is incompressible, $\nabla\cdot v = 0$, so $\tilde{\phi}$ satisfies Laplace's equation

$$\Delta\tilde{\phi} = 0 . \tag{4.1}$$

The boundary condition on $\tilde{\phi}$ along the cylinder wall and the bottom is

$$\tilde{\phi}_n = 0 , \tag{4.2}$$

where the subscript $n$ denotes the outward normal derivative.

The displacement of the free surface from its equilibrium will be described in surface polar normal coordinates $s$, $\Theta$ and $\eta$. The coordinate $s$ is the arc length along the equilibrium surface, and the coordinate $\eta$ is the displacement normal to this surface [1]. The perturbed surface is described by

$$\eta = \tilde{H}(s,\Theta,t) .$$

The time-dependent Bernoulli equation is linearized in the perturbation $\tilde{H}$. Since $\tilde{H}_t$ is the component of fluid velocity normal to the equilibrium surface, $\tilde{H}$ and $\tilde{\phi}$ are related by the kinematic equation on the eqiulibrium surface

$$\tilde{\phi}_n = \tilde{H}_t . \tag{4.3}$$

This is the boundary condition on $\tilde{\phi}$ along the free surface; it depends on the unknown function $\tilde{H}$.

The sloshing motion will be analyzed in terms of normal modes

$$\tilde{\phi} = \phi(r,z)\ \cos(m\theta)\ \cos(\omega t)\ ,$$

$$\tilde{H} = H(s)\ \cos(m\theta)\ \sin(\omega t)\ .$$

Equation (4.3) can be used to eliminate the function $\tilde{H}$ from the linearized time-dependent Bernoulli equation. The result is

$$-(R\phi_{ns})_s + RQ(s)\phi_n = \omega^2(1+|B|)R\phi\ , \tag{4.4}$$

where

$$Q(s) = BR_s + (m/R)^2 - [\psi_s{}^2 + (Z_s/R)^2]\ . \tag{4.5}$$

The solution of differential equation (4.3) gives the boundary condition on $\phi$ along the equilibrium surface. The boundary condition is specified by the contact angle conditions at $s = 0$ and $s = S$, which are assumed to be time independent. The perturbed surface and the equilibrium surface must have the same contact angle with the cylinder wall and the bottom.

These conditions relate $H_s$, $\psi_s$, and $\chi_r$ at $s = 0$ and $s = S$. In terms of the function $\phi$ these conditions are

$$\phi_{ns} \sin\gamma - \phi_n\ (\psi_s \cos\gamma - \chi_r \cos\chi) = 0 \quad \text{at} \quad s = 0 \tag{4.6}$$

$$\phi_{ns} \sin\gamma + \phi_n\psi_s \cos\gamma = 0 \quad \text{at} \quad s = S\ . \tag{4.7}$$

Equations (4.1), (4.2), and (4.4) - (4.7) determine the eigenfunctions $\phi$ and the corresponding eigenvalues $\omega$.

It will be convenient to let $\theta 0$, $\theta 1$, $\theta 2$, .... denote normal modes having $\cos(m\theta)$ dependence with the values $m = 0, 1, 2, \ldots$, respectively. We also shall let R0, R1, R2, ... denote normal modes having 0, 1, 2, ... radial nodes in the interval $0 < s < S$ (not counting the nodes, if any, at the endpoints of the interval).

## 5. Discrete Representation and the Solution of Laplace's Equation

The functions $\phi$ and $\phi_n$ on the boundary of the vertical cross section of the liquid will be represented by their values at $N + M$ points

$$\Phi = (\phi(s_1), \phi(s_2), \ldots, \phi(s_{N+M}))$$

and similarly for $\Phi_n$. These points are shown in Figure 3. The first N of these points will be along the meridian of the free surface in the cross-sectional plane. The remaining M will be on the meridians of the cylinder wall and the bottom in the cross-sectional plane. None of the $s_j$ are corner points of the boundary.

We shall partition the vectors $\Phi$ and $\Phi_n$ into two parts: $\Phi_1$ includes values of $\phi$ at points on the free surface, and $\Phi_2$ includes those on the cylinder wall and the bottom

$$\Phi = (\Phi_1, \Phi_2)$$

$$\Phi_1 = (\phi(s_1), \phi(s_2), \ldots, \phi(s_N))$$

$$\Phi_2 = (\phi(s_{N+1}), \ldots, \phi(s_{N+M}))$$

The boundary condition on $\phi$ along the cylinder wall and the bottom, Equation (4.2), becomes

$$\Phi_{2n} = 0 \ . \tag{5.1}$$

Because $\phi$ satisfies Laplace's equation, Green's formula yields an integral equation that relates $\phi$ and $\phi_n$ on the boundary of the vertical cross section of the liquid. This can be approximated by a matrix equation of the form:

$$W\Phi = C\Phi_n \ . \tag{5.2}$$

The calculation of the matrices W and C is described in [5].

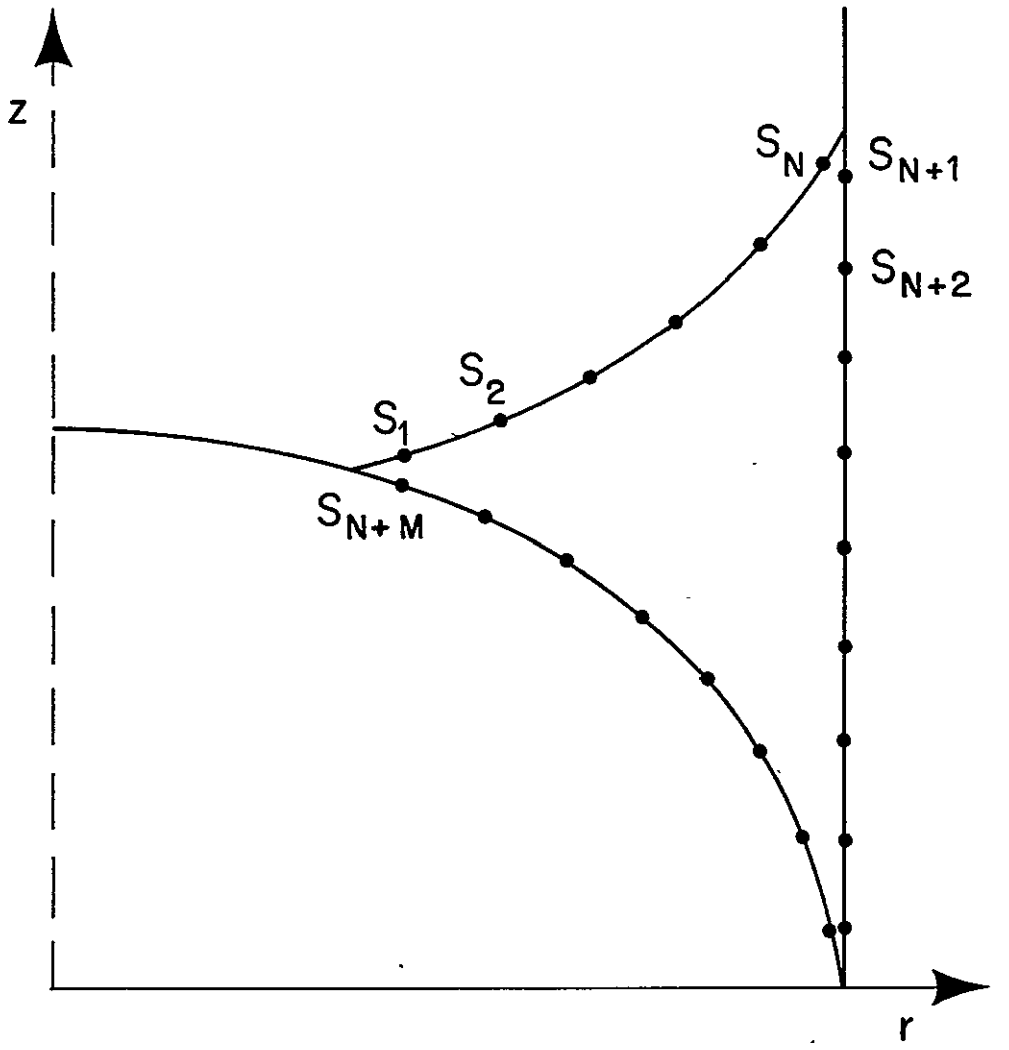


Figure 3. The discrete set of points on the boundary.

XBL 781-104

## 6. Discrete Representation of the Boundary Condition on the Free Surface

Using Equation (4.4) and the contact angle conditions (4.6) and (4.7), we will derive a discrete set of equations relating $\phi$ and $\phi_n$ at the points $s_1, s_2, \ldots s_N$ along the meridian of the free surface in the cross-sectional plane. Let this meridian be divided into N intervals. The $j^{th}$ interval has

$$t_j \leq s \leq t_{j+1} ,$$

where $t_1 = 0$ and $t_{N+1} = S$ . Let $s_j$ be the midpoint of the $j^{th}$ interval.

We integrate Equation (4.4) over the $j^{th}$ interval

$$R(t_j)\phi_{ns}(t_j) - R(t_{j+1})\phi_{ns}(t_{j+1}) + \int_{t_j}^{t_{j+1}} Q(s)R(s)\phi_n(s)\, ds$$

$$= \omega^2(1+|B|) \int_{t_j}^{t_{j+1}} R(s)\phi(s)\, ds . \qquad (6.1)$$

The integrals are approximated by

$$\phi_n(s_j) \int_{t_j}^{t_{j+1}} Q(s)\, R(s)\, ds$$

and

$$\phi(s_j) \int_{t_j}^{t_{j+1}} R(s)\, ds$$

If $t_j$ is not an endpoint of the meridian, we approximate $\phi_{ns}(t_j)$ by

$$\phi_{ns}(t_j) \approx \frac{\phi_n(s_j) - \phi_n(s_{j-1})}{s_j - s_{j-1}}$$

Substituting these approximations into Equation (6.1) gives

$$T_{j-1,j}\,\phi_n(s_{j-1}) + T_{jj}\phi_n(s_j) + T_{j,j+1}\phi_n(s_{j+1}) = \omega^2 A_{jj}\phi(s_j) \ , \quad (6.2)$$

where

$$A_{jj} = (1+|B|) \int_{t_j}^{t_{j+1}} R(s)\ ds$$

$$P_j = \int_{t_j}^{t_{j+1}} Q(s)R(s)\ ds \ ,$$

$$T_{j,j+1} = -R(t_{j+1})/(s_{j+1}-s_j)$$

and

$$T_{jj} = -T_{j-1,j} - T_{j,j+1} + P_j$$

For $t_1 = 0$ , the inner endpoint of the meridian, we approximate

$$\phi_{ns}(t_1) \approx \frac{\phi_n(s_1) = \phi_n(t_1)}{s_1 - t_1}$$

To eliminate the unknown $\phi_n(t_1)$ , we use the contact angle condition (4.6)

$$\phi_{ns}(t_1) \sin\gamma = L_1\,\phi_n(t_1) \ ,$$

where

$$L_1 = \psi_s(t_1)\cos\gamma - \chi_r(t_1)\cos\chi$$

These give

$$\phi_{ns}(t_1) = K_1\,\phi_n(s_1) \ ,$$

where

$$K_1 = L_1 / [\sin \gamma + (s_1 - t_1) L_1] .$$

Substituting this approximation into Equation (6.1) gives

$$T_{11} \phi_n(s_1) + T_{12} \phi_n(s_2) = \omega^2 A_{11} \phi(s_1) , \tag{6.3}$$

where

$$T_{11} = - T_{12} + K_1 R(t_1) + P_1 .$$

For $t_{N+1} = S$ , the outer endpoint of the meridian, we approximate

$$\phi_{ns}(t_{N+1}) \approx \frac{\phi_n(t_{N+1}) - \phi_n(s_n)}{t_{N+1} - s_N}$$

To eliminate the unknown $\phi_n(t_{N+1})$ , we use the contact angle condition (4.7)

$$\phi_{ns}(t_{N+1}) \sin \gamma = - L_2 \phi_n(t_{N+1}) ,$$

where

$$L_2 = \psi_s(t_{N+1}) \cos \gamma$$

These give

$$\phi_{ns}(t_{N+1}) = - K_1 \phi_n(s_N) ,$$

where

$$K_2 = L_2 / [\sin \gamma + (t_{N+1} - s_n) L_2]$$

Substituting this approximation into Equation (6.1) gives

$$T_{N-1,N} \phi_m(s_{N-1}) + T_{NN} \phi_n(s_N) = \omega^2 A_{NN} \phi(s_N), \tag{6.4}$$

where

$$T_{NN} = - T_{N-1,N} + K_2 R(t_{N+1}) + P_N$$

Equations (6.2) - (6.4) can be written in matrix form as

$$T\Phi_{1n} = \omega^2 A \Phi_1 \tag{6.5}$$

This is the boundary condition on $\phi$ along the meridian on the free surface. A is diagonal, and the diagonal elements are positive. T is tridiagonal and symmetric, and the off-diagonal elements are negative.

The set of Equations (5.1), (5.3), and (6.5) is the discrete version of the eigenvalue problem for the small-amplitude, periodic sloshing modes of a liquid in a vertical, rotationally symmetric cylinder.

## 7. Numerical Solution of the Discretized Eigenvalue Problem

We write the matrices W and C of equation (5.3) in block form: $W_{11}$, $W_{12}$, $W_{21}$, $W_{22}$, and similarly for C. Subscript 1 denotes the rows and columns corresponding to the N points along the free surface, and subscript 2 denotes those corresponding to the M points along the cylinder wall and bottom. Since $\Phi_{2n}$ is zero, Equation (5.3) can be written

$$\begin{aligned} W_{11}\,\Phi_1 + W_{12}\,\Phi_2 &= C_{11}\,\Phi_{1n}\ , \\ W_{21}\,\Phi_1 + W_{22}\,\Phi_2 &= C_{21}\,\Phi_{1n}\ . \end{aligned} \tag{7.1}$$

The matrix A is diagonal, so Equation (6.5) is easy to solve for $\Phi_1$, which we can eliminate from Equations (7.1).

Define

$$\begin{aligned} F_{11} &= W_{11}\,A^{-1}\,T\ , \\ F_{21} &= W_{21}\,A^{-1}\,T\ . \end{aligned} \tag{7.2}$$

Then Equations (7.1) give

$$\begin{aligned} F_{11}\,\Phi_{1n} &= \omega^2(C_{11}\Phi_{1n} - W_{12}\Phi_2), \\ F_{21}\,\Phi_{1n} &= \omega^2(C_{21}\Phi_{1n} - W_{22}\Phi_2) \end{aligned} \tag{7.3}$$

Equations (7.3) can be written as single matrix equation for the eigenvector $(\Phi_{1n}, \Phi_2)$

$$\begin{pmatrix} F_{11} & 0 \\ F_{21} & 0 \end{pmatrix} \begin{pmatrix} \Phi_{1n} \\ \Phi_2 \end{pmatrix} = \omega^2 \begin{pmatrix} C_{11} & -W_{12} \\ C_{12} & -W_{22} \end{pmatrix} \begin{pmatrix} \Phi_{1n} \\ \Phi_2 \end{pmatrix} \tag{7.4}$$

Equation 7.4 could be solved for the eigenvalues $\omega^2$; however, M of the eigenvectors have the eigenvalue $\omega^2 = 0$. A linearly independent

set of these eigenvectors is

$$\Phi_{1n} = 0 \qquad \Phi_2 = e_j \qquad j=1,2,\ldots M,$$

where $e_j$ is the vector with a one in the $j^{th}$ position and zeros elsewhere. These eigenvectors correspond to no motion of the free surface, since $\Phi_{1n}$ is zero. A computer program that calculates all the eigenvalues of a matrix, such as the IMSL routine EIGZF, will waste some time computing these unwanted eigenvalues.

We can avoid calculating the zero eigenvalues by eliminating $\Phi_2$ from the pair of Equations (7.3). Define

$$D = C_{11} - W_{11} W_{22}^{-1} C_{21} ,$$

$$E = F_{11} - W_{12} W_{22}^{-1} F_{21} = (W_{11} - W_{12} W_{22}^{-1} W_{21})A^{-1}T \tag{7.5}$$

Then Equations (7.3) combine to give

$$E\Phi_{1n} = \omega^2 D\Phi_{1n} \tag{7.6}$$

Equation (7.6) can be solved for its eigenvalue by the IMSL routine EIGZF, which uses a QZ algorithm to reduce E to upper Hessenberg form and D to upper triangular form.

The solution of Equation (7.6) is performed by the program SLOSH. The input to SLOSH is the set of points describing the equilibrium free surface calculated by CAPIL and parameters that define the cylinder wall and spheroidal bottom. SLOSH then calculates the matrices A, T, W, and C; uses the IMSL routine LINV1F to calculate $W_{22}$ inverse; calculates the matrices D and E; and uses EIGZF to calculate the eigenvalues. This method of solving the eigenvalue equation is not the most computationally efficient, but by using

the existing and reliable IMSL routines it requires the least amount of programming effort.

For comparison, the routine EIGZF was used to solve both Equation (7.6) and Equation (7.4) for a few cases. The numerical values of corresponding eigenvalues for these two methods were identical to the four figures that were printed out in each case.

## 8. Small-Amplitude Periodic Sloshing Modes of the Liquid between Two Concentric Right Circular Cylinders

In this section we solve the eigenvalue problem for the small-amplitude, periodic sloshing modes of the liquid contained between two concentric, vertically oriented, right circular cylinders of radii $r_0$ and $r_1$. A cross section is shown in Figure 4. The equilibrium surface is a horizontal plane when the contact angle is $90^\circ$. The normal mode problem for this case has an analytic solution. We can use this solution to test the accuracy of the program SLOSH.

Let $\mathcal{D}$ be the rectangular domain $r_0 \leq r \leq r_1$ and $0 \leq z \leq z_0$. Laplace's Equation for $\phi$ in the domain $\mathcal{D}$ is

$$\phi_{rr} + \frac{1}{r}\phi_r + \phi_{zz} - \frac{m^2}{r^2}\phi = 0 \ . \tag{8.1}$$

The boundary conditions are

$$\phi_r = 0 \qquad \text{at } r = r_0 \text{ and } r_1 \ ,$$

$$\phi_r = 0 \qquad \text{at } z = 0 \ .$$

Equation (4.4) for $\phi$ on the free surface, $z = z_0$, is

$$-\frac{1}{r}(r\phi_{rz})_r + Q(r)\phi_z = \omega^2(1+|B|)\phi \ , \tag{8.2}$$

where

$$Q(r) = B + (m/r)^2$$

The contact angle conditions, Equations (4.6) and (4.7), become

$$\phi_{rz} = 0 \qquad \text{at } (r_0,z_0) \text{ and } (r_1,z_0)$$

We solve these equations by separation of variables. Let

$$\phi(r,z) = X(r)\,U(z)$$

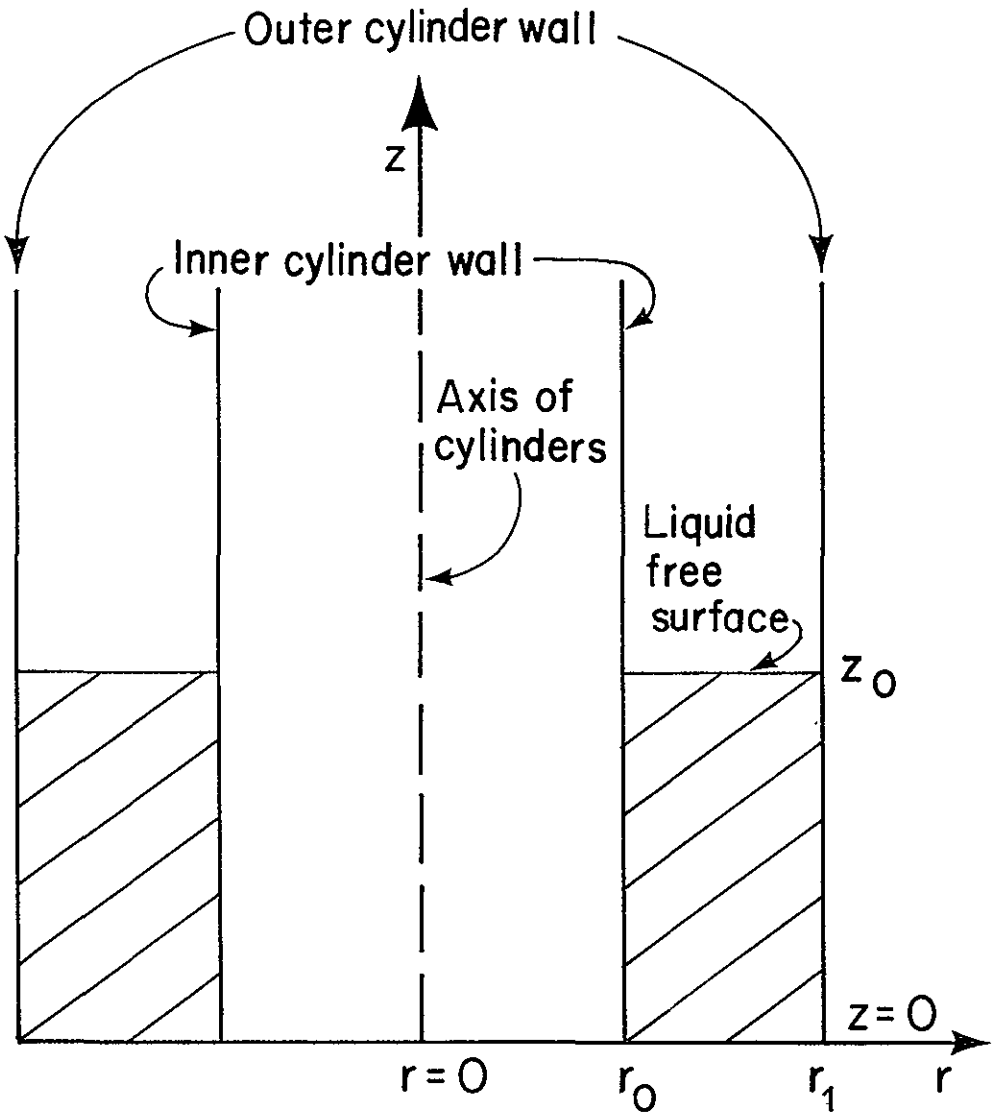


Figure 4. Cross section of two concentric cylinders or radii $r_0$ and $r_1$, respectively.

XBL 781-105

then (8.1) gives the pair of equations .

$$U'' = k^2 U \tag{8.3}$$

$$X'' + \frac{1}{r} X' + (k^2 - m^2/r^2)X = 0 \ , \tag{8.4}$$

with boundary conditions

$$U' = 0 \text{ at } z = 0 \ , \tag{8.5}$$

$$X' = 0 \text{ at } r = r_0 \text{ and } r_1 \tag{8.6}$$

The contact angle conditions will be automatically satisfied if Equation (8.6) is satisfied.

Equation (8.2) gives an equation for the eigenvalue

$$\omega^2 = \frac{(k^2 + B)}{(1 + |B|)} \quad \frac{U'(z_0)}{U(z_0)}$$

The solution of (8.3) and (8.5) is

$$U = \cosh (kz) \ .$$

Thus the eigenvalue is

$$\omega^2 = \frac{k(k^2 + B)}{(1 + |B|)} \quad \tanh (kz_0) \ . \tag{8.7}$$

The solution of (8.4) is

$$X(r) = c \, J_m(kr) + d \, Y_m(kr) \ ,$$

where $J_m$ and $Y_m$ are Bessel functions of the first and second kind of order m. Equation (8.6) requires

$$c \, J_m'(kr_0) + d \, Y_m'(kr_0) = 0 \ ,$$

$$c \, J_m'(kr_1) + d \, Y_m'(kr_1) = 0 \ .$$

These will have a nontrivial solution for c and d if

$$J_m'(kr_1) \, Y_m'(kr_0) - J'_m(kr_0) \, Y'_m(kr_1) = 0 \ . \tag{8.8}$$

Equation (8.8) gives the values of k for the normal modes. The first few values for the case $r_0 = 0.5$ and $r_1 = 1.0$ are listed in Table 1 to the accuracy indicated.

Table 1. k values for m = 0, 1, and 2.

| m = 0 | m = 1 | m = 2 |
|---|---|---|
| 0.0 | 1.3547 | 2.6812 |
| 6.3932 | 6.5649 | 7.0626 |
| 12.6247 | 12.7064 | 12.9494 |
| 18.8889 | 18.9427 | 19.1032 |
| 25.1624 | 25.2045 | 25.3224 |

The solution m = 0, k = 0.0 corresponds to no movement of the equilibrium surface or of the liquid.

## 9. Comparison of the Analytically and Numerically Calculated Solutions for the Normal Modes of the Liquid between Two Cylinders

Figure 4 shows the cross section of a liquid contained between two concentric right circular cylinders, oriented vertically. Each of the four sides of the cross section (the free surface, the bottom, and the two cylinder walls) was divided into $n$ intervals of equal length. The velocity potential $\phi$ on the perimeter of the cross section was represented by its values at the midpoints of these $4n$ intervals. These $4n$ values of $\phi$ are related by Equations (5.1), (5.3), and (6.5). Numerical solutions of these equations were computed for the case $r_0 = 0.5$, $r_1 = 1.0$, $z_0 = 0.9$, contact angle $90^o$, and Bond number 0 using the program SLOSH.

Numerically calculated squares of the frequencies for the modes θ1R0, θ1R1, and θ1R2 using n = 5, 10, and 20 points are shown in Table 2. The corresponding analytic values for the squares of the frequencies, calculated from Equation (8.7) and the k values of Table 1, are also shown.

Table 2. Squares of frequencies for various normal modes

| | θ1R0 | θ1R1 | θ1R2 |
|---|---|---|---|
| 5 points | 2.157 | 292.1 | 1965. |
| 10 points | 2.127 | 284.8 | 2080. |
| 20 points | 2.118 | 280.7 | 2072. |
| analytic | 2.087 | 282.9 | 2052. |

The relative errors of the numerically calculated squares of the frequencies $[\omega^2(\text{n points}) - \omega^2(\text{analytic})]/\ \omega^2\ (\text{analytic})$, are shown in Table 3.

Table 3. Relative errors of the squares of frequencies.

| | θ1R0 | θ1R1 | θ1R2 |
|---|---|---|---|
| 5 points | 0.034 | 0.033 | -0.042 |
| 10 points | 0.019 | 0.007 | 0.014 |
| 20 points | 0.015 | -0.008 | 0.010 |

Note that the relative errors of the frequencies are approximately half these values. The error decreases substantially between n = 5 and n = 10, but less so between n = 10 and n = 20. Even the errors for n = 5 are quite small, considering that only five radial modes can be represented by a 5-point approximation to the meridian on the free surface.

Numerically calculated squares of the frequencies for the modes θ0R0, θ0R1, θ0R2, θ2R0, θ2R1, and θ2R2 using n = 10 points are shown in Table 4. Corresponding analytic values are shown also.

Table 4. Squares of frequencies for various normal modes.

| | θ0R0 | θ0R1 | θ0R2 |
|---|---|---|---|
| 10 points | $0.7\ \ 10^{-12}$ | 265.4 | 2038. |
| analytic | 0.0 | 261.3 | 2012. |
| | θ2R0 | θ2R1 | θ2R2 |
| 10 points | 19.99 | 346.6 | 2201. |
| analytic | 18.97 | 352.3 | 2171. |

The relative errors of these squares of frequencies are shown in Table 5.

Table 5. Relative Errors of the squares of frequencies.

| | R0 | R1 | R2 |
|---|---|---|---|
| Θ0 modes | -- | 0.016 | 0.013 |
| Θ2 modes | 0.054 | -0.016 | 0.014 |

The relative errors of the squares of frequencies for n = 10 points, as shown in Tables 3 and 5, are typically from 0.01 to 0.02. These results show the program SLOSH calculates with satisfactory accuracy for our purposes the frequencies of the normal modes of a liquid contained between two concentric right circular cylinders.

10. Equilibrium Free Surfaces of a Liquid in a Vertical Right Circular Cylinder with a Concave Spheroidal Bottom

With a given volume of liquid in the cylindrical container we associate a dimensionless fill height defined as follows: let the given volume V equal the volume bounded by the container wall and bottom and the horizontal plane $z = z_v$. Then the fill height $h_v$ is $z_v$ divided by the container radius a.

$$h_v = z_v/a .$$

The axial ratio of the spheroidal bottom is $b/a = 0.724$.

Equilibrium free surfaces, approximated by 21 points on the meridian, were calculated by the program CAPIL for contact angle $\gamma = 0^o$ and for the fill heights: 0.20, 0.25, 0.30, 0.35, 0.40, 0.45, 0.50, 0.60, and 0.70. For each fill height equilibrium surfaces were calculated for a sequence of increasingly negative Bond numbers. The first surface for each fill height was calculated for Bond number $B = 0$. The initial approximation to this surface was generated by the subroutine CYLCUR. The equilibrium surface for each Bond number was used as the initial approximation to the surface for the next Bond number in that sequence.

The equilibrium surfaces that we have calculated are members of a family with two parameters B and $h_v$. Let $B_{eq}$ denote the critical value of the Bond number for the nonexistence of equilibrium surfaces of this family for a given fill height. Let $B_{crit}$ denote the critical value of the Bond number for the stability of equilibrium surfaces of this family for a given fill height. Stable equilibrium surfaces

exist for $B_{crit} \leq B$, unstable equilibrium surfaces exist for $B_{eq} \leq B < B_{crit} < 0$ if $B_{eq} \neq B_{crit}$, and no equilibrium surfaces of this family exist for $B < B_{eq}$. (Other equilibrium surfaces might exist, such as multiple-valued surfaces or surfaces with shapes very different from those of this family.) Concus and Karasalo showed that unstable equilibrium surfaces exist for $B$ infinitesimally lower than $B_{crit}$ and $h_v < h_v^* = 0.503$, but that no equilibrium surfaces of this family exist for $B < B_{crit}$ and $h_v \geq h_v^*$ [1]. Their result may be restated as $B_{eq} < B_{crit}$ for $h_v < h_v^*$, but $B_{eq} = B_{crit}$ for $h_v \geq h_v^*$. Our calculations agree with their result and provide an estimate of $B_{eq}$.

For each fill height we found a Bond number $B_{div}$, depending on $h_v$, for which the iteration for the equilibrium surface diverged. The iteration using $B_{div}$ was approached by a sequence of calculations using small decreases in $B$. Let $B_{conv}$ denote the Bond number immediately preceding $B_{div}$ in that sequence, $B_{div} < B_{conv} < 0$. For $B \geq B_{conv}$ the equilibrium surface changed only slowly with B. The equilibrium surface for each value of B was an excellent approximation to that for the next value of $B$ in the sequence. This indicates that the divergence for the case $B_{div}$ was caused not by the initial approximation but by the nonexistence of an equilibrium surface for this family. Thus $B_{div}$ is an approximation to $B_{eq}$. Table 6 shows $B_{conv}$ and $B_{div}$ as a function of $h_v$. It also shows $B_{crit}$ calculated to four decimal places by Concus and Karasalo [1].

Table 6. $B_{conv}$, $B_{div}$, and $B_{crit}$ for various fill heights.

| $h_v$ | $-B_{conv}$ | $-B_{div}$ | $-B_{crit}$ |
|---|---|---|---|
| 0.20 | 1310. | 1320. | 480.4283 |
| 0.25 | 488. | 492. | 238.6539 |
| 0.30 | 216. | 218. | 132.9638 |
| 0.35 | 107. | 108. | 79.6741 |
| 0.40 | 58.0 | 58.2 | 49.9096 |
| 0.45 | 33.4 | 33.6 | 31.9190 |
| 0.50 | 20.2759 | 20.2760 | 20.2759 |
| 0.60 | 8.42 | 8.43 | 8.4411 |
| 0.70 | 3.98 | 3.99 | 4.0020 |

The data of Table 6 are shown in Figure 5. The solid line is the graph of $B_{crit}$ and the dashed line is that of $B_{div}$. These lines divide the Bond-number, fill-height parameter space into three regions: one for which stable equilibrium surfaces exist, one for which unstable equilibrium surfaces exist, and one for which no equilibrium surfaces exist. (Growth rates for perturbations of the unstable equilibrium surfaces were calculated by the program SLOSH for various values of $B$ and $h_v$. These will be discussed in the next section of this report.)

Figure 5 also shows data points from stability experiments carried out at the NASA Lewis Zero Gravity Facility for the container shown in Figure 1 [6]. The experiments used three containers with radii 7 cm, 5.5 cm, and 2 cm, respectively. In the experiment the container had

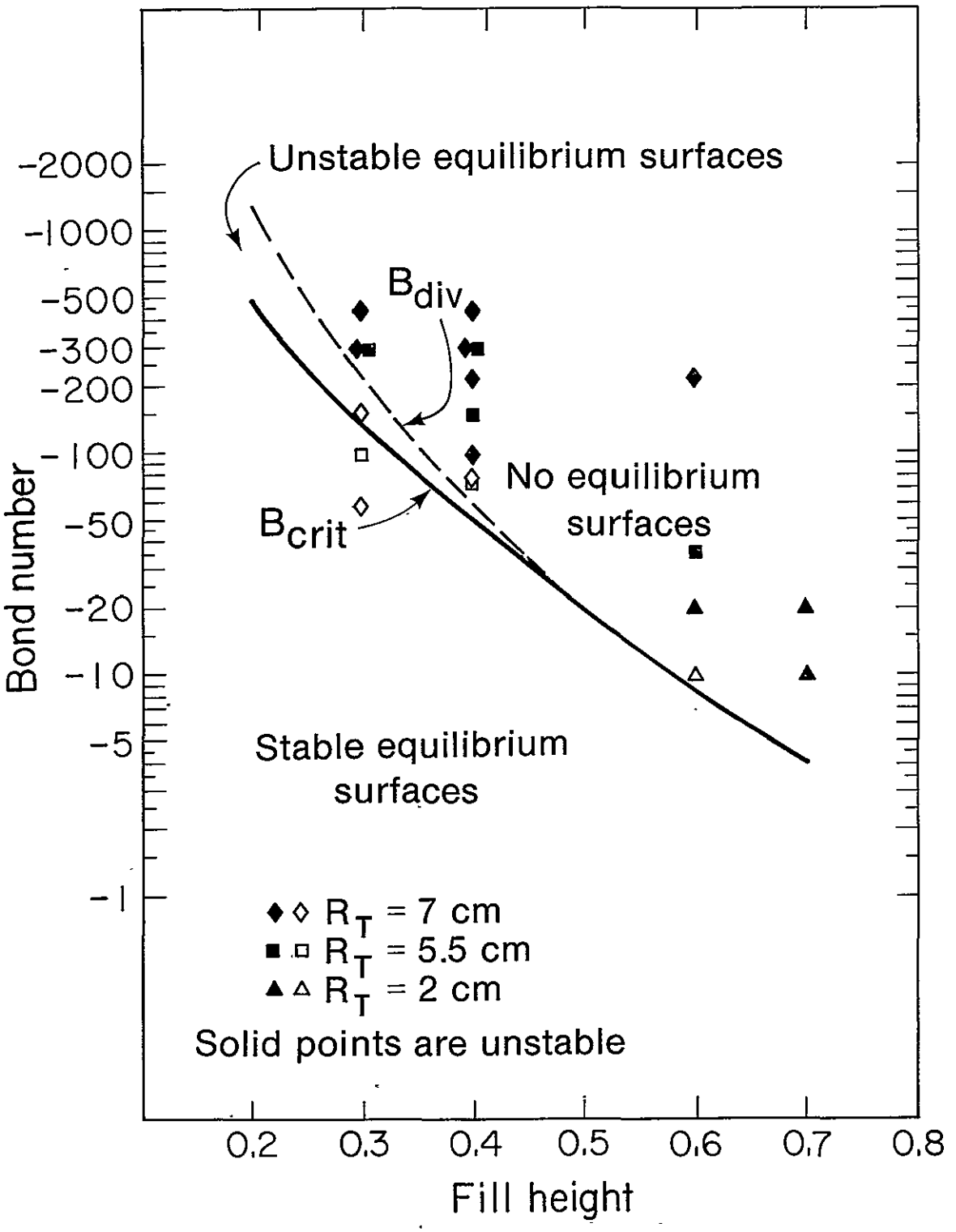


Figure 5. $B_{crit}$ and $B_{div}$ as functions of fill height compared with experimental points.

approximately 2.5 sec of free fall followed by approximately 2.5 sec of negative low-g fall. During the first 2.5 sec the liquid surface adjusts from one g to zero g. During the next 2.5 sec instabilities may be observed if they grow sufficiently rapidly. Solid data points correspond to experimental parameter values for which the surface was observed to be unstable. Open data points correspond to parameter values for which the surface did not develop a noticeable instability within the 2.5-sec time interval. The experimental data and the numerically calculated curves agree quite well. All the experiments in which the surface was observed to be unstable have Bond numbers $B < B_{crit} < 0$.

$B_{div}$ is an approximation to $B_{eq}$. The accuracy of this approximation can be investigated by considering the cases $h_v = 0.60$ and $0.70$. For $h_v = 0.60$ CAPIL diverges for some Bond number in the range $(-8.42, -8.43)$ and $B_{eq} = -8.4411$. The relative error in this case is less than 0.003. For $h = 0.70$ CAPIL diverges for some Bond number in the range $(-3.98, -3.99)$ and $B_{eq} = -4.0020$. The relative error in this latter case is less than 0.005.

From this we infer that the correct value of $B_{eq}$ for $h_v = 0.50$ is slightly less than the value found here for the 21 point surfaces, and that there is a small range of Bond numbers between $B_{crit}$ and $B_{eq}$ for this value of $h_v$. This is supported by a calculation of the frequencies of individual normal modes, which is discussed in the next two sections. Based on an approximate calculation of the frequencies, the R0$\theta$1 mode becomes marginally stable at $B = -20.243$, while all the other modes approach instability as $B$ approaches $-20.276$.

## 11. Frequencies of the Normal Modes of a Liquid in a Vertical Right Circular Cylinder with a Concave Spheroidal Bottom

The frequencies of the small-amplitude periodic sloshing modes of a liquid in a vertical right circular cylinder with a concave spheroidal bottom were calculated by the program SLOSH for contact angle $\gamma = 0°$ . The axial ratio of the spheroidal bottom is $b/a = 0.724$ . The equilibrium free surfaces were approximated by 21 points of the meridian, as described in Section 10. These 21 points were the endpoints and midpoints of 10 intervals on the meridian. The velocity potential $\phi$ for perturbations to these surfaces was represented by its value at the 10 midpoints of these intervals, by its value at 10 points on the meridian on the cylinder wall, and at 10 points on the meridian on the bottom. We shall refer to this as the 10-point approximation to $\phi$ . Surfaces corresponding to numerous values of $h_v$ and B were used.

A few surfaces approximated by 41 points on the meridian were used to check the accuracy of the frequencies calculated using the 21 point surfaces. For these cases $\phi$ was represented by its value at 20 points each on the meridians on the free surface, the cylinder wall, and the bottom. We shall refer to this as the 20-point approximation to $\phi$ .

The squares of frequencies for various normal modes and for various values of $h_v$ and B calculated by SLOSH using the 10-point approximation are shown in Tables A 1 through A 11. Typically the values of $\omega^2$ in these tables have a relative error of 1-2% for values of $\omega^2$ that are not too small and for Bond numbers that are not

too near $B_{div}$ . This will be discussed in more detail in Section 12.

These squares of frequencies are plotted as functions of B in Figures 6-12 for $h_v = 0.20, 0.30, \ldots 0.70$ . Note that in Figures 10-12 ( $h_v = 0.50 - 0.70$ ) a different scale for $\omega^2$ is used for each mode that is plotted. The purpose is to show that all these modes have a similar dependence of $\omega^2$ on B . However, in Figures 6-9 ( $h_v = 0.20 - 0.40$ ) all the RO modes ( RO$\theta$1, RO$\theta$2, RO$\theta$3, ... ) that are plotted in a given figure use the same scale for $\omega^2$ . This is to show for each value of B which mode is most negative.

We shall first describe the general features of these figures, and then consider numerical details for particular cases and discuss the accuracy of the calculations.

Figure 6 shows graphs of $\omega^2(B)$ for the modes RO$\theta$1, RO$\theta$2, RO$\theta$3, RO$\theta$4, RO$\theta$6, and R1$\theta$0 for $h_v = 0.20$ . The mode R1$\theta$0 is plotted with a scale 1000 times that of the other modes. (An accuracy check shows the values for the R1$\theta$0 mode are about 10% too large. However, we include it in Figure 6 for a rough comparison with the RO modes.) Note that the Bond numbers for which the various RO modes become marginally stable [for which $\omega^2(B) = 0$] lie in a small range.

Figure 7 shows this more clearly. The order in which the modes become unstable is as one would expect: First RO$\theta$1 , then RO$\theta$2 , RO$\theta$3 , RO$\theta$4 , and RO$\theta$6 . (RO$\theta$5 was not calculated for $h_v = 0.20$ .) Note also that because the higher $\theta$ modes have steeper slopes ($d\omega^2/dB$ ), each mode, in turn, becomes the dominant unstable mode (most negative value of $\omega^2$ ) for a short range of Bond numbers.

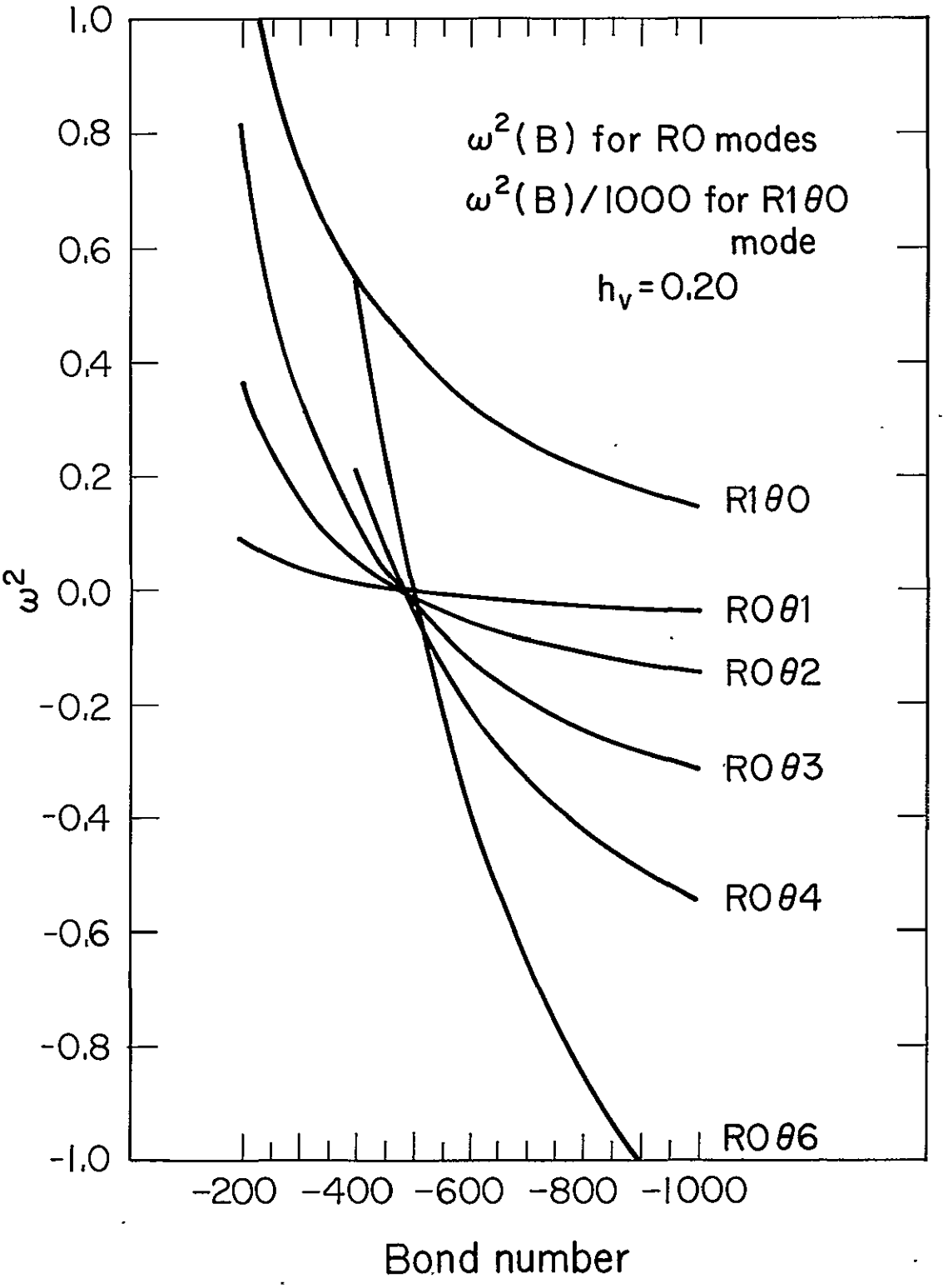


Figure 6. $\omega^2(B)$ of various modes for $h_v = 0.20$ . XBL781-95

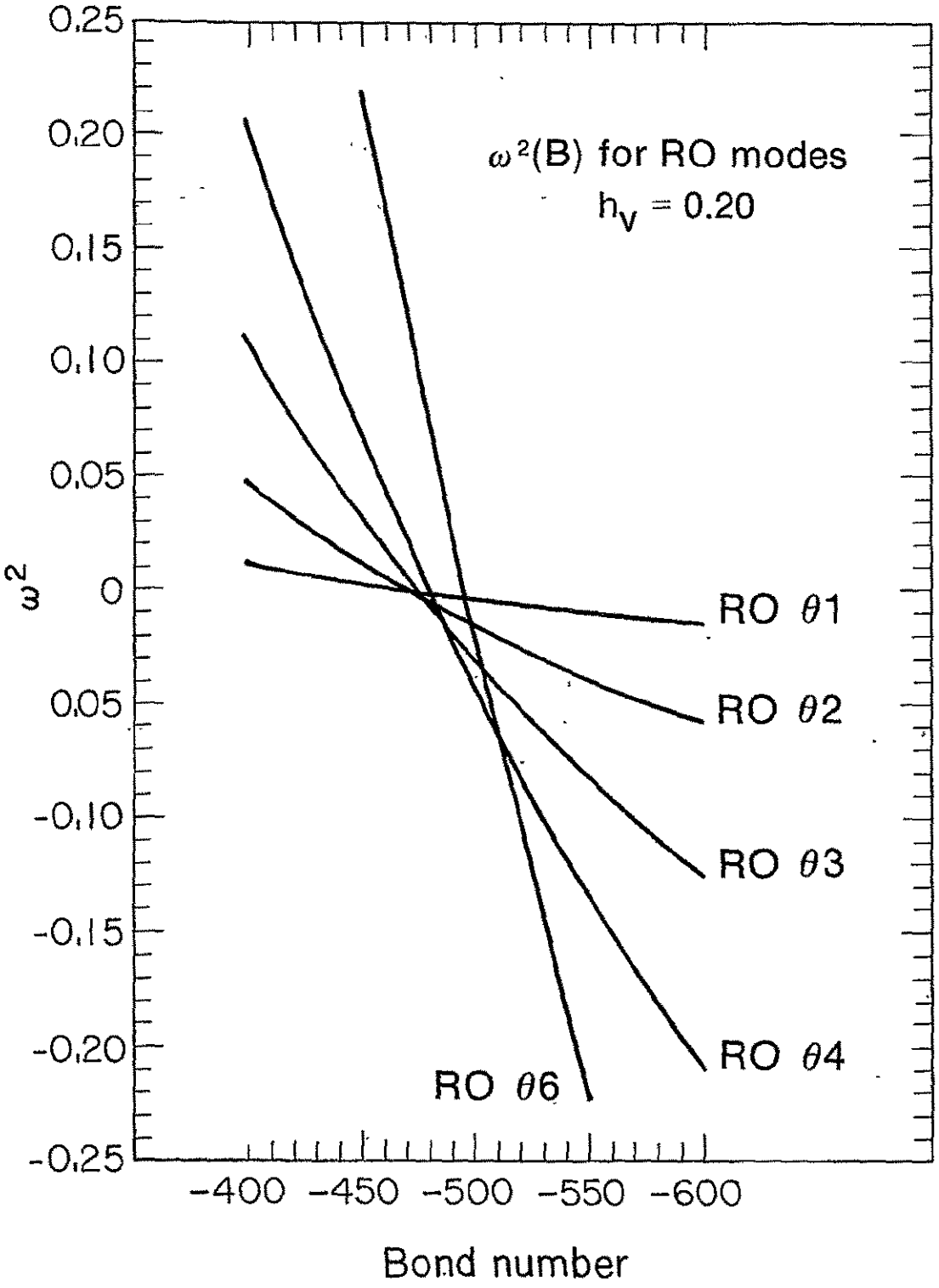


Figure 7. $\omega^2(B)$ of RO modes for $h_v = 0.20$ . XBL781-101

This same pattern for the R0 modes is shown in Figure 8 for $h_v = 0.30$ . A new feature appears in this figure. It is that $\omega^2$ for the R1θ0 mode passes through a point of inflection and begins to curve downward. The rate at which it approaches zero, the magnitude of $d\omega^2/d(B)$ , increases as B approaches $B_{div}$ . The functions $\omega^2(B)$ for the other R1 modes, R1θ1 to R1θ6 , have similar shapes and differ from that of R1θ0 by only a few percent, as shown in Table A 3. The functions $\omega^2(B)$ for the modes R2θ0 to R2θ6 have shapes similar to those for the R1 modes but magnitudes about five times larger. All the R1 and R2 modes curve downward as B approaches $B_{div}$

Figure 9 shows that for $h_v = 0.40$ $\omega^2$ becomes negative between $B_{crit}$ and $B_{conv}$ only for four modes: R0θ1 , R0θ2 , R0θ3 , and R0θ4 . Furthermore, only the first three modes become dominant instabilities in this range. The rate at which the R1θ0 mode approaches zero, $|d\omega^2/dB|$ , becomes very great as B approaches $B_{div}$ . Note also that $\omega^2(B)$ for each of the R0 modes passes through an inflection point and curves downward as B approaches $B_{div}$ .

Figures 10, 11, and 12 are for the cases $h_v = 0.50$ , 0.60 , and 0.70 , respectively. In each case the functions $\omega^2(B)$ for the various modes have similar shapes. They all curve downward for B near $B_{crit}$ , and the rate at which they approach zero becomes very great as B approaches $B_{crit}$ . All modes apparently go to zero at or near $B_{crit}$ . This behavior of $\omega^2(B)$ is consistent with the nonexistence of an equilibrium free surface nearby the critical one for $h_v \geqslant h_v^*$ and $B < B_{crit} < 0$ . It is in sharp contrast to the behavior seen in

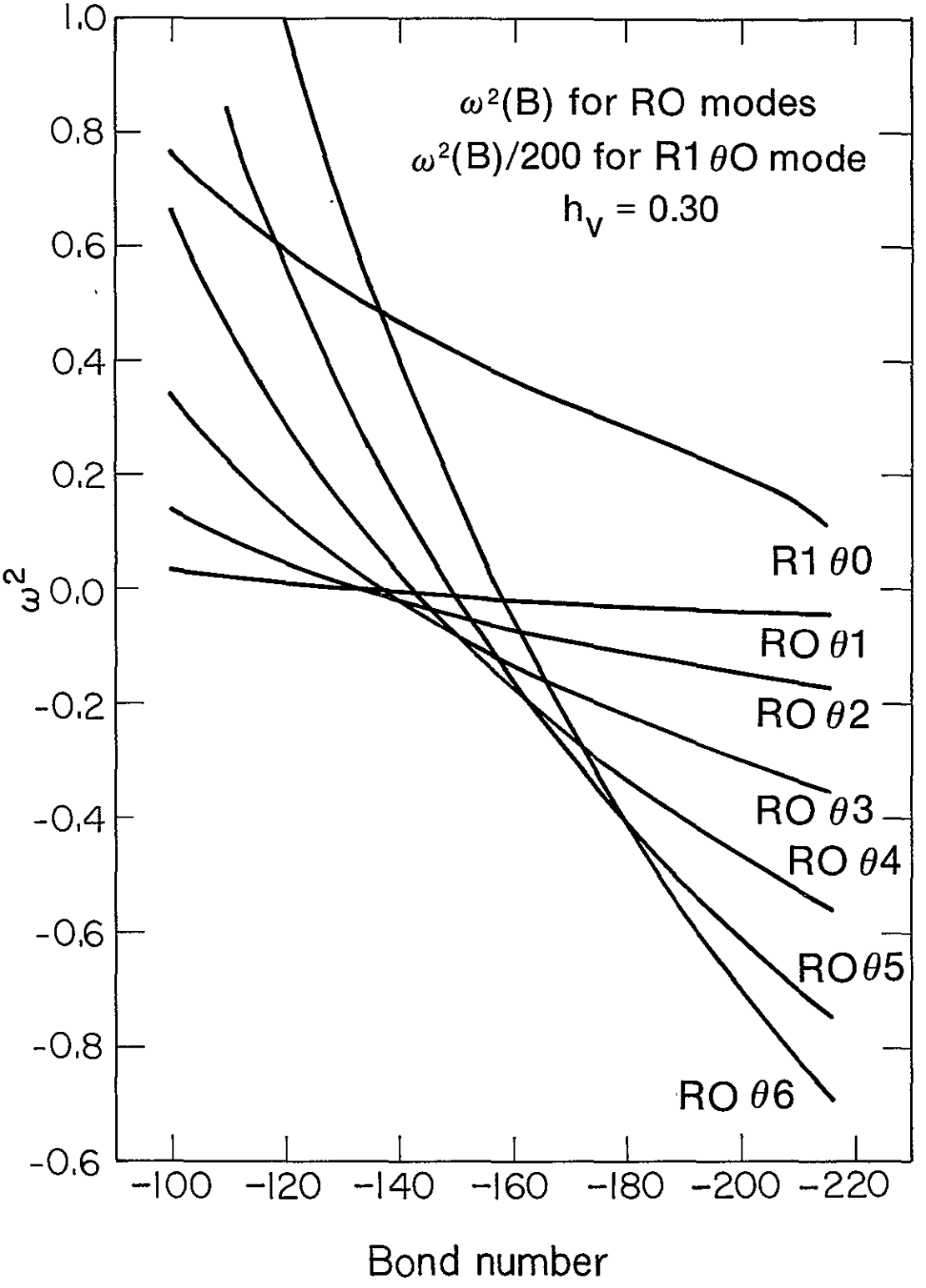


Figure 8. $\omega^2(B)$ of various modes for $h_v = 0.30$ . XBL781-96

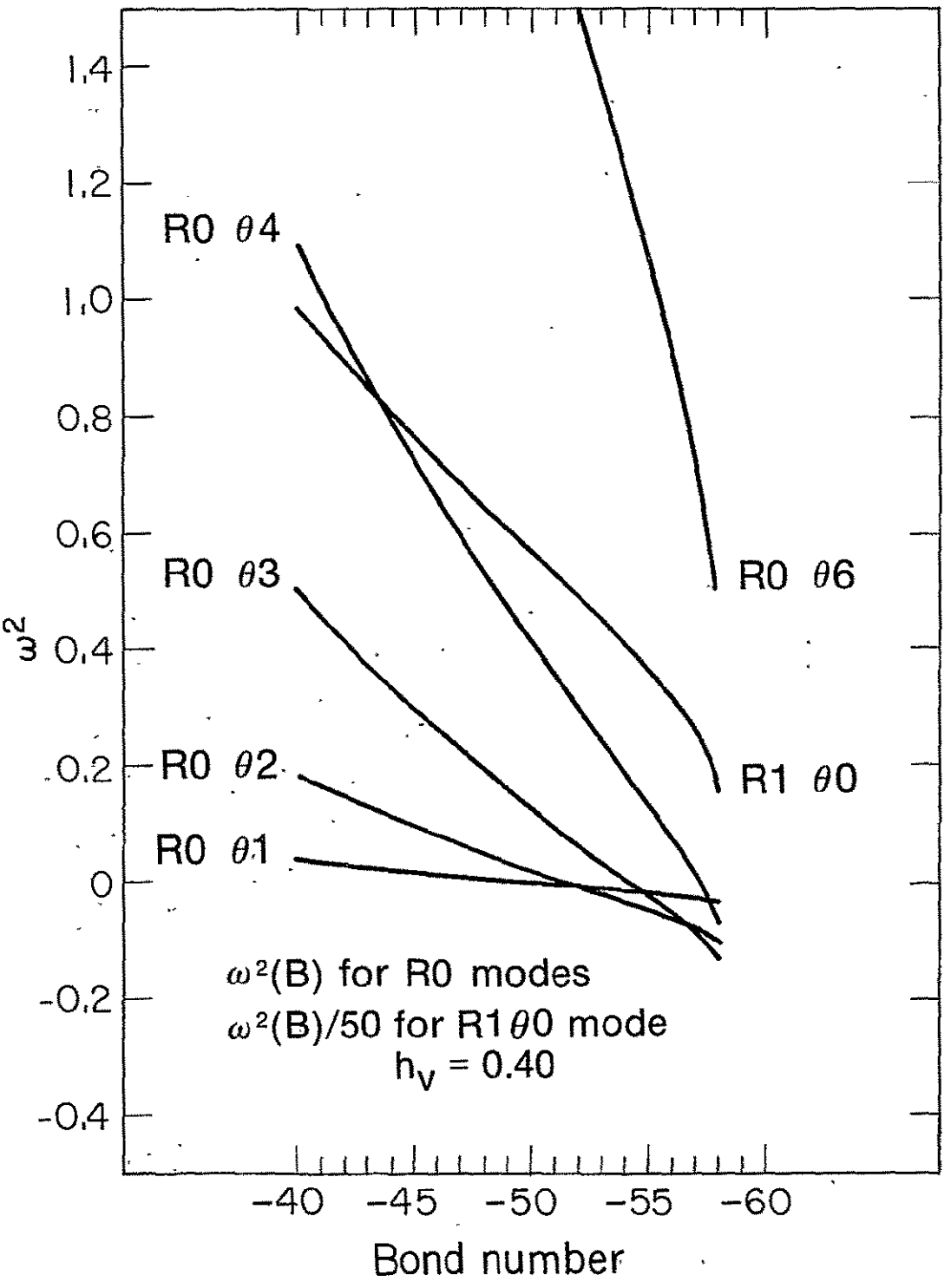


Figure 9. $\omega^2(B)$ of various modes for $h_v = 0.40$. XBL781-100

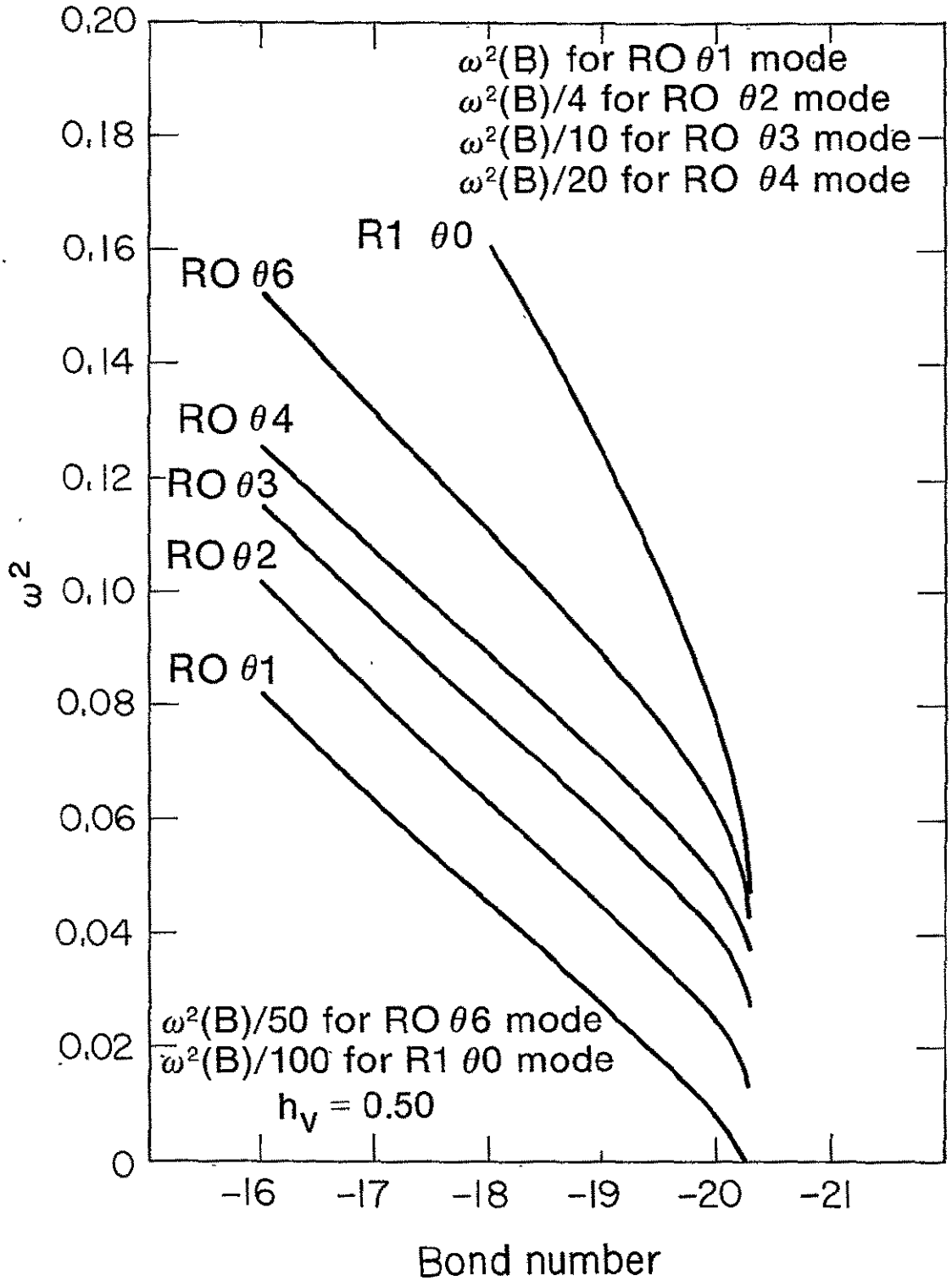


Figure 10. $\omega^2$(B) of various modes for $h_v$ = 0.50 . XBL 781-98

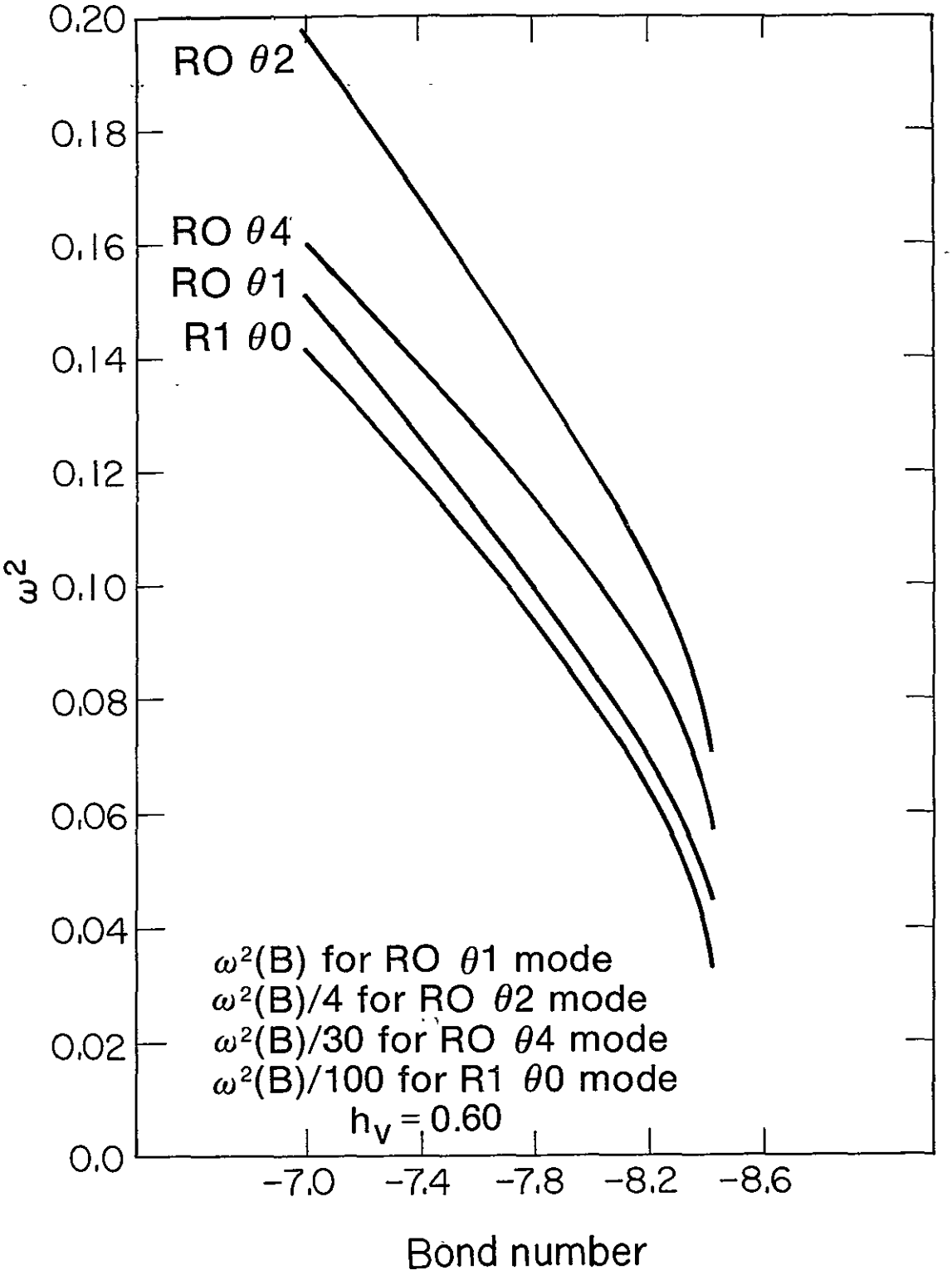


Figure 11. $\omega^2(B)$ of various modes for $h_v = 0.60$ . XBL781-97

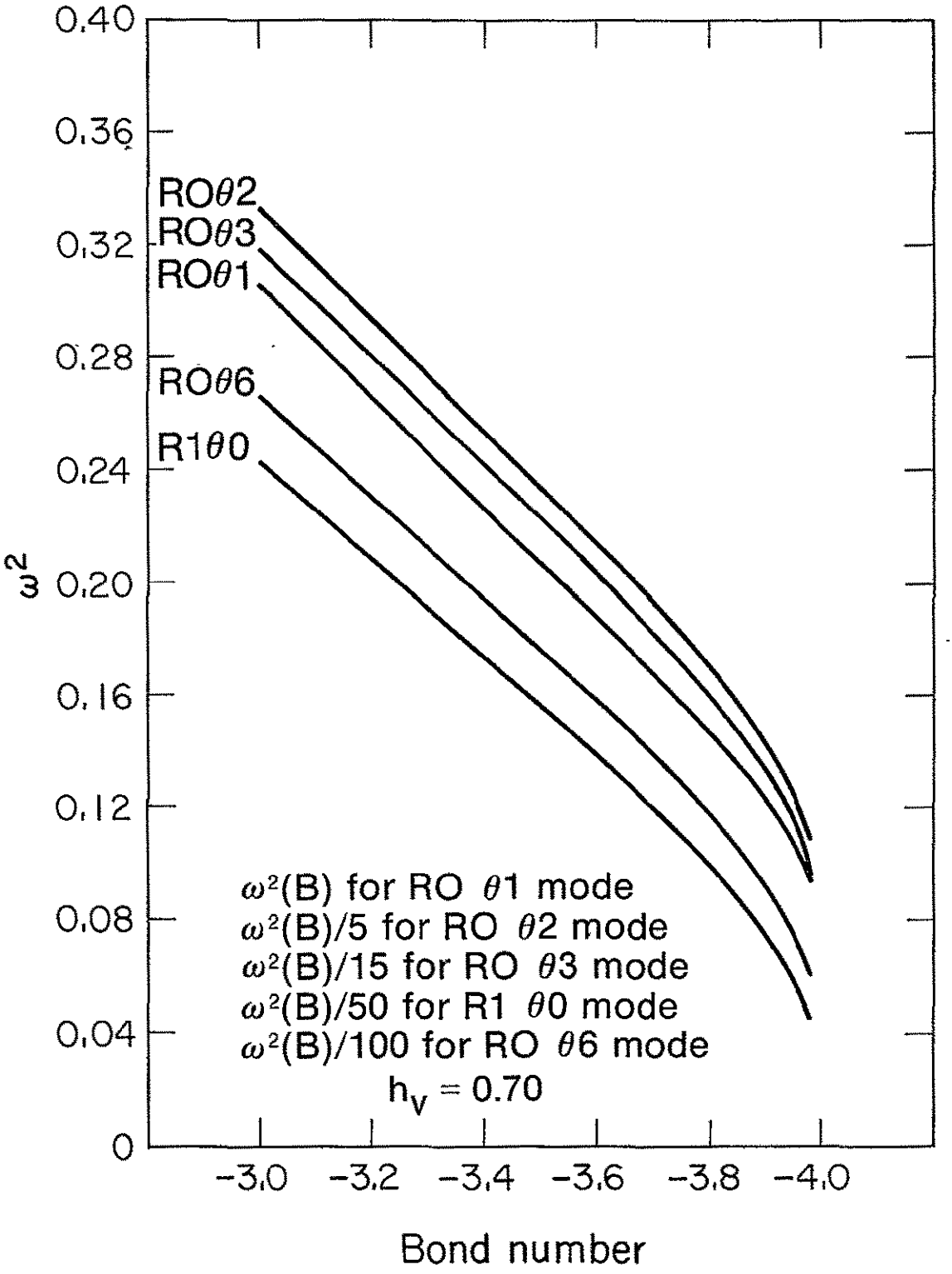


Figure 12. $\omega^2(B)$ of various modes for $h_v = 0.70$ . XBL 781-99

the cases $h_v = 0.20\text{-}0.40$ , in which only a few RO modes were unstable for a range of Bond numbers beyond $B_{crit}$ .

For the case $h_v = 0.50$ the RO01 mode becomes marginally stable at a slightly higher Bond number than the other modes. In the 10-point approximation it becomes marginally stable at $B = -20.243$ , while all the other modes approach instability as B approaches $-20.276$ . It appears that for this case there exists a very small range of Bond numbers between $B_{crit}$ and $B_{eq}$ .

12. Frequencies of the Normal Modes Continued -- Accuracy

The bulk of our data are values of $\omega^2$ calculated by the 10-point approximation, Tables A 1 - A 11. Throughout this section we shall investigate the accuracy of these data. The few values of $\omega^2$ calculated by the 20-point approximation are used solely to estimate the accuracy of these data and how they can be improved. We shall refer to these values as $\omega_{10}^2$ and $\omega_{20}^2$, respectively.

We are most interested in the accuracy of $\omega_{10}^2$ for the growing RO modes. These negative values of $\omega^2$ are small numbers, so a small (absolute) error in them can be significant. We shall show that the error in $\omega_{10}^2(B)$ is approximately $-(d\omega^2/dB)\Delta B^*$, where $\Delta B^*$ is a function of $h_v$ but not of the mode number, that is,

$$\omega^2(B) \approx \omega_{10}^2(B) + (d\omega^2/dB)\Delta B^* , \tag{12.1}$$

or, equivalently,

$$\omega^2(B-\Delta B^*) \approx \omega_{10}^2(B) . \tag{12.2}$$

Thus, a value of $\omega_{10}^2(B)$ from Tables A 1, A 2, or A 4 actually corresponds to the Bond number $B-\Delta B^*$.

Five comparisons of calculated quantities support this description of the approximate dependence of the error in $\omega_{10}^2$ on the parameters $h_v$, B, and mode number. The first comparison is between the values of $B_{crit}$ calculated by the 10-point approximation, which we shall denote by $B_{crit,10}$, and those calculated to four decimal places from a static analysis [1]. $\Delta B^*$ is defined as the difference in these values.

$$\Delta B^* = B_{crit,10} - B_{crit} .$$

These quantities are shown in Table 7. $\Delta B^*$ is approximately 1 - 2% of $B_{crit}$.

Table 7. $B_{crit}$, $B_{crit,10}$, and $\Delta B^*$ for three fill heights

| $h_v$ | $-B_{crit}$ | $-B_{crit,10}$ | $\Delta B^*$ |
|---|---|---|---|
| 0.20 | 480.43 | 468.2 | 12.2 |
| 0.30 | 132.96 | 130.73 | 2.23 |
| 0.40 | 49.91 | 49.35 | 0.56 |

The second comparison is between the values of $\omega^2(B_{crit})$ for the R0θ1 mode calculated by the 10-point and 20-point approximations. Since the correct value of $\omega^2$ is zero in this case, these values are errors. They show that the error in the calculated values of $\omega^2$ depends as $1/N^2$ on the number of points used to approximate $\phi$. These values are shown in Table 8. Note that $\omega_{20}^2$ is approximately 1/4 of $\omega_{10}^2$.

Table 8. $\omega_{10}^2$ and $\omega_{20}^2$ at $B_{crit}$ for the R0θ1 mode.

| $h_v$ | $-\omega_{10}^2$ | $-\omega_{20}^2$ |
|---|---|---|
| 0.20 | 0.00180 | 0.00045 |
| 0.30 | 0.00183 | 0.00046 |
| 0.40 | 0.00209 | 0.00053 |

The third comparison is between $\omega_{10}^2$ and $\omega_{20}^2$ for various RO modes, fill heights, and Bond numbers. Define $\Delta\omega^2$ as

$$\Delta\omega^2 = \omega_{20}^2 - \omega_{10}^2$$

Since the error in $\omega_{20}^2$ is approximately 1/4 of the error in $\omega_{10}^2$, it follows that $\Delta\omega^2$ is approximately -3/4 of the error in $\omega_{10}^2$. The values of $\Delta\omega^2$ are shown in Table 9. They vary greatly with mode number.

Table 9. $\Delta\omega^2$ for various RO modes, fill heights, and Bond numbers.

| $h_v$ | -B | RO$\theta$1 | RO$\theta$2 | RO$\theta$3 |
|---|---|---|---|---|
| 0.30 | 130. | 0.00141 | 0.0055 | 0.0120 |
| | 132.96 | 0.00137 | | |
| | 140. | 0.00127 | 0.0050 | 0.0108 |
| 0.40 | 45. | 0.00193 | 0.0070 | |
| | 49.91 | 0.00156 | | |
| | 50. | | 0.0059 | |

Define $\Delta B$ as

$$\Delta B = \Delta\omega^2 (dB/d\omega^2)$$

The values of $d\omega^2/dB$ can be calculated approximately by central differences of the data in Tables A 2 and A 4. The resulting values of $\Delta B$ are shown in Table 10. Note that for a given fill height, while $\Delta\omega^2$ varies greatly with mode number, $\Delta B$ does not. Our fourth comparison is between the values of $\Delta B$ and $\Delta B^*$. Table 10 shows that the values of $\Delta B$ are approximately 3/4 of the corresponding values

of $\Delta B^*$ . Since $\Delta\omega^2$ is approximately -3/4 of the error in $\omega_{10}^2$ , this implies that the error in $\omega_{10}^2$ is approximately $-(d\omega^2/dB)\Delta B^*$ for some range of Bond numbers containing $B_{crit}$ .

Table 10. $\Delta B$ for various RO modes, fill heights, and Bond numbers.

| $h_v$ | -B | RO$\theta$1 | RO$\theta$2 | RO$\theta$3 |
|---|---|---|---|---|
| 0.30 | 130. | 1.68 | 1.65 | 1.59 |
| | 132.96 | 1.71 | | |
| | 140. | 1.74 | 1.71 | 1.66 |
| 0.40 | 45. | 0.47 | 0.43 | |
| | 49.91 | 0.44 | | |
| | 50. | | 0.42 | |

For a given fill heights, let $B_{\theta n}$ denote the Bond number for which the RO$\theta$n mode becomes neutrally stable, that is, for which $\omega^2(B_{\theta n}) = 0$ . Table 11 shows the values of the Bond numbers for the neutral stability of various modes as calculated by the 10-point approximation to $\phi$ , which we shall denote by $B_{\theta n,10}$ . As B increases the various modes become unstable in order of increasing $\theta$ mode number, so $B_{\theta 1}$ is $B_{crit}$ . We have already compared the accurate values of $B_{crit}$ with the corresponding values of $B_{crit,10}$ , that is, with $B_{\theta 1,10}$ .

Table 11. $-B_{\theta n,10}$ for various modes and fill heights.

| $h_v$ | RO$\theta$1 | RO$\theta$2 | RO$\theta$3 | RO$\theta$4 | RO$\theta$5 | RO$\theta$6 |
|---|---|---|---|---|---|---|
| 0.20 | 468.25 | 471.42 | 475.42 | 480.89 | | 495.85 |
| 0.30 | 130.73 | 133.22 | 137.11 | 142.49 | 149.28 | 157.60 |
| 0.40 | 49.35 | 51.28 | 54.19 | 57.19 | | |

Our last comparison is between the values of $B_{\theta n,10}$ and $B_{\theta n,20}$. Define $\Delta B_{\theta n}$ as

$$\Delta B_{\theta n} = B_{\theta n,10} - B_{\theta n,20} .$$

Table 12 shows values of $\Delta B_{\theta n}$ for various modes and fill heights. It shows that the values of $\Delta B_{\theta n}$ are approximately 3/4 of the corresponding values of $\Delta B^*$. For a given fill height $\Delta B_{\theta n}$ is approximately the same for each mode. This implies that the error in $\omega_{10}^2$ is approximately $-(d\omega^2/dB)\Delta B^*$ for some range of Bond numbers containing these $B_{\theta n}$.

Table 12. $\Delta B_{\theta n}$ for various modes and fill heights.

| $h_v$ | RO$\theta$1 | RO$\theta$2 | RO$\theta$3 |
|---|---|---|---|
| 0.30 | 1.68 | 1.69 | 1.59 |
| 0.40 | 0.42 | 0.42 | |

When the values of $B_{\theta n}$ given in Table 11 are adjusted by adding $\Delta B^*$, the values shown in Table 13 are obtained.

Table 13: Adjusted values of $-B_{\theta n}$ for various modes and fill heights.

| $h_v$ | R0θ1 | R0θ2 | R0θ3 | R0θ4 | R0θ5 | R0θ6 |
|---|---|---|---|---|---|---|
| 0.20 | 480.43 | 483.6 | 487.6 | 493.1 | | 508.0 |
| 0.30 | 132.96 | 135.5 | 139.3 | 144.7 | 151.5 | 159.8 |
| 0.40 | 49.91 | 51.8 | 54.8 | 57.8 | | |

We consider finally the R1 modes. Table 14 shows the relative difference in $\omega^2$ calculated with the 10-point and 20-point approximations, that is, $(\omega_{20}^2 - \omega_{10}^2)/\omega_{10}^2$. The value of $\omega^2$ differed by 10% for the R1θ1 mode with $h_v = 0.20$. It differed by 2.6 - 2.7% for the R1θ1 and R1θ2 modes with $h_v = 0.40$ for Bond number 55, which is near $B_{div}$. The value of $\omega^2$ differed by only 1 - 2% for all the R1 modes with $h_v = 0.30$ or 0.40 and Bond numbers not near $B_{div}$.

Table 14. Range of $\Delta\omega^2/\omega^2$ for various modes and fill heights.

| $h_v$ | range of -B | R1θ1 | R1θ2 | R1θ3 |
|---|---|---|---|---|
| 0.20 | 450.-500. | 0.100 | | |
| 0.30 | 130.-140. | 0.015-0.016 | 0.015-0.016 | 0.015-0.016 |
| 0.40 | 45.- 50. | 0.015-0.019 | 0.014-0.019 | |
| 0.40 | 55. | 0.026 | 0.027 | |

13. Growth Rates and Accuracy for Fill Height = 0.30

Figure 8 and Table A 2 show $\omega^2(B)$ of the various RO modes for $h_v = 0.30$ . They show which is the maximally unstable mode for each value of B . The information for the maximally unstable mode is displayed in Table 15. The values of B listed in this table have been adjusted by $\Delta B^*$ .

For example, the RO$\theta$1 mode is the maximally unstable one for $-134.04 < B < -132.96$ , the RO$\theta$2 mode for $-140.27 < B < -134.04$ , etc. The value of $(d\omega^2/dB)\Delta B^*$ is an estimate of the accuracy of $\omega^2$ before adjustment by $\Delta B^*$ . We feel the error remaining in $\omega^2$ after this adjustment is less than $(d\omega^2/dB)\Delta B^*$ . In particular, we feel the errors remaining in $\omega^2$ for the RO$\theta$1 , RO$\theta$2 , and RO$\theta$3 modes are 1/10 to 1/4 of $(d\omega^2/dB)\Delta B^*$ .

Table 15. $\omega^2(B)$ of the maximally unstable mode for $h_v = 0.30$.

| -B | $\omega^2$ | maximally unstable | $(d\omega^2/dB)\Delta B^*$ |
|---|---|---|---|
| 132.96 | 0.0 | | |
| | | RO$\theta$1 | 0.0017 |
| 134.04 | 0.0025 | | |
| | | RO$\theta$2 | 0.007 |
| 140.27 | 0.0218 | | |
| | | RO$\theta$3 | 0.014 |
| 149.99 | 0.0808 | | |
| | | RO$\theta$4 | 0.021 |
| 163.48 | 0.204 | | |
| | | RO$\theta$5 | 0.028 |
| 179.76 | 0.407 | | |
| | | RO$\theta$6 | 0.032 |
| 202.23 | 0.701 | | |

The dimensionless growth rate $\Gamma$ of the maximally unstable mode is shown in Table 16. The corresponding growth period in seconds is

$$\Gamma^{-1}(\bar{t}/t) = \Gamma^{-1}[\rho a^3/\sigma(1+|B|)]^{\frac{1}{2}} \quad .$$

This is calculated for a cylinder of radius 7 cm for the three liquids ethanol, freon, and FC78. The values of $\rho/\sigma$ used for these were 0.03538, 0.08489, and 0.131 $sec^2/cm^3$, respectively. Ethanol has the fastest growth rates and FC78 has the slowest. $B_{crit}$ is -132.96 for this case. At Bond number $B = -150$ the growth periods range from 1.0 to 1.9 sec. At $B = -202$, which is 50% beyond $B_{crit}$, they range from 0.29 to 0.56 sec. It is not likely that growth would be observed in these cases in an experiment with a negative-B phase of only 2.5 sec, since only 2-8 growth periods would elapse.

Table 16. Maximal growth rates and growth periods for $h_v = 0.30$.

| dimensionless values | | growth period (sec) | | |
|---|---|---|---|---|
| -B | $\Gamma$ | ethanol | freon | FC78 |
| 132.96 | 0.0 | $\infty$ | $\infty$ | $\infty$ |
| 134.04 | 0.050 | 5.9 | 9.2 | 11.4 |
| 140.27 | 0.148 | 1.99 | 3.1 | 3.8 |
| 149.99 | 0.284 | 1.00 | 1.54 | 1.92 |
| 163.48 | 0.451 | 0.60 | 0.93 | 1.16 |
| 179.76 | 0.638 | 0.41 | 0.63 | 0.78 |
| 202.23 | 0.837 | 0.29 | 0.45 | 0.56 |

The errors in $\omega^2$ for the smaller values of $\omega^2$ (the R0$\theta$1, R0$\theta$2, and R0$\theta$3 modes) have a greater percentage reduction from the $\Delta B^*$ adjustment than those for larger values of $\omega^2$. However, these

errors were initially larger fractions of their values of $\omega^2$ than those for the larger values of $\omega^2$ . As a result of these two effects, the errors in $\omega^2$ remaining after this adjustment probably lie in the range 5 - 20%, the larger values of $\omega^2$ being more accurate. The corresponding errors in the growth rate probably lie in the range 2 - 10% . However, these are only the computational errors in $\Gamma$ ; they represent the accuracy with which the growth rates were calculated from the assumed model of the liquid motion. The accuracy with which they describe experimentally observed growth rates depends also on the accuracy of that model. In this model the fluid motion was assumed to be nonviscous and irrotational, and the contact angle was assumed to be time independent. These assumptions could be tested by computing the fluid motion with a complete hydrodynamics code that includes all the relevant effects.

## 14. Summary

In this paper we calculate the small-amplitude periodic sloshing modes of a liquid in a vertical right circular cylinder with a concave spheroidal bottom, for the case in which there is not sufficient liquid to cover the bottom entirely. Numerical results are obtained for a container currently used for the storage of liquid fuels in the Centaur space vehicles, for which the axial ratio of the bottom is $b/a = 0.724$ .

We follow the derivation in [2] for obtaining the equations of motion for the case studied here, but we use a different technique for obtaining the numerical solution. The liquid is subject to surface and gravitational forces. The equilibrium surface is the solution of the time-independent Bernoulli equation subject to a contact-angle condition.

It is assumed for the dynamical equations that the fluid flow is irrotational and incompressible. The fluid velocity is the gradient of a potential function that satisfies Laplace's equation. The velocity potential and its gradient on the free surface are related by the linearized time-dependent Bernoulli equation and the contact-angle condition. The sloshing motion is analyzed in terms of normal modes. The discrete form of these equations yields a generalized eigenvalue problem for $\omega^2$ , the square of the normal-mode frequency. This problem was solved numerically using the IMSL routine EIGZF.

The accuracy of this numerical procedure was tested by calculating the eigenvalues and eigenvectors for the small-amplitude periodic sloshing modes of a liquid contained between two concentric vertical

circular cylinders for contact angle $\gamma = 90°$ and comparing with the known analytic solution for this case. The numerical values of $\omega^2$ were correct typically to about 1 or 2%, a satisfactory accuracy for our purposes.

Equilibrium surfaces of a liquid in a vertical circular cylinder with a concave spheroidal bottom were calculated for contact angle $\gamma = 0°$, axial ratio of the spheroidal bottom $b/a = 0.724$, fill heights $h_v$ ranging from 0.20 to 0.70, and many values of the Bond number. These equilibrium surfaces are members of a family with parameters $B$ and $h_v$. $B_{crit}$ was defined above as the critical value of the Bond number for the stability of surfaces of this family for a given fill height. $B_{eq}$ was defined as the critical value of the Bond number for the nonexistence of equilibrium surfaces of this family. Stable equilibrium surfaces exist for $B_{crit} \leq B$, unstable equilibrium surfaces exist for $B_{eq} \leq B < B_{crit} < 0$ if $B_{eq} \neq B_{crit}$, and no equilibrium surfaces exist for $B < B_{eq}$.

For all the values of the fill height that were studied, stable equilibrium surfaces were found for a range of Bond numbers, $B_{crit} \leq B \leq 0$. To the accuracy of these calculations, we found the same value for $B_{crit}$ as was found in the static analysis of the same problem [1].

For fill heights ranging from 0.20 to 0.45, we found unstable equilibrium surfaces for a range of Bond numbers $B_{conv} \leq B < B_{crit}$, but no equilibrium surfaces of this family were found for $B \leq B_{div} < B_{conv}$. ($B_{conv}$ and $B_{div}$ are approximations to $B_{eq}$.)

For $h_v = 0.50$ unstable equilibrium surfaces were found for a very small range of Bond numbers. For $h_v = 0.60$ and $0.70$ no equilibrium surfaces of this family were found for $B < B_{crit}$. To the accuracy of these calculations, these results are consistent with [1], which found that $B_{eq} = B_{crit}$ for $h_v \geqslant h_v^* = 0.503$, but that $B_{eq} < B_{crit}$ for $h_v < h_v^*$.

The qualitative nature of the stability of the individual normal modes differs for the two cases $h_v < h_v^*$ and $h_v \geqslant h_v^*$. For fill heights $h_v = 0.20$, $0.30$, and $0.40$, the normal modes $R0\theta1$, $R0\theta2$, $R0\theta3$, ... become marginally stable at a sequence of Bond numbers ... $B_{\theta3} < B_{\theta2} < B_{\theta1} = B_{crit} < 0$. Each $R0$ mode is the fastest growing mode for a small range of Bond numbers. For fill heights $h_v = 0.60$ and $0.70$ all the modes that were studied approach instability as the Bond number approaches $B_{crit}$. For each mode the function $\omega^2(B)$ curves toward the $\omega^2 = 0$ axis, approaching zero with increasing rapidity as $B$ approaches $B_{crit}$. For $h_v = 0.50$, which is near the critical fill height $h_v^*$, the $R0\theta1$ mode becomes marginally stable at a slightly higher Bond number than the other modes. The instability of all modes for $h_v \geqslant h_v^*$ and $B < B_{crit}$ is consistent with the nonexistence of equilibrium surfaces nearby the critical one for this range of parameters.

Most of the calculations of $\omega^2$ were made by approximating the velocity potential on a meridian along the free surface by its value at 10 points. It was possible to correct partially these calculated values of $\omega^2$ by applying an adjustment based on a study of the errors.

Growth rates of the maximally unstable mode were calculated for the case $h_v = 0.30$ using the adjusted values of $\omega^2$. Each of the modes RO$\theta$1, RO$\theta$2, ... RO$\theta$6, in succession, was the maximally unstable one for a small range of Bond numbers. The corresponding growth periods in seconds were calculated for a cylinder of radius 7 cm for the three liquids ethanol, freon, and FC78. Ethanol has the fastest growth rates and FC78 has the slowest. $B_{crit}$ is -132.96 for this case. At Bond number $B = -150$ the growth periods range from 1.0 to 1.9 sec. At $B = -202$, which is 50% beyond $B_{crit}$, they range from 0.29 to 0.56 sec. It is not likely that growth would be observed in these cases in an experiment with a negative-B phase of only 2.5 sec, since only 2 to 8 growth periods would elapse.

ACKNOWLEDGMENTS

We would like to thank Eugene P. Symons for stimulating our interest in this problem and for sharing experimental data related to it. We would also like to thank Said Doss for developing and programming the Laplace solver that was used in the program SLOSH and Ru-Mei Kung for adapting the program CAPIL for use on the LBL computer system.

This work was supported in part by the National Aeronautics and Space Administration and by the Department of Energy.

REFERENCES

1. P. Concus and I. Karasalo, "A Numerical Study of Capillary Stability in a Circular Cylindrical Container with a Concave Spheroidal Bottom," Lawrence Berkeley Laboratory Report LBL-6144, (1977).

2. P. Concus, G.E. Crane, H.M. Satterlee, "Small Amplitude Lateral Sloshing in Spheroidal Containers under Low Gravitational Conditions," NASA CR-72500 Lewis Research Center, Cleveland, Ohio (1969).

3. P. Concus and V. Pereyra, "CAPIL: A Package for Meniscus Computations," Lawrence Berkeley Laboratory Report (to be published).

4. M. Lentini and V. Pereyra, "An Adaptive Finite Difference Solver for Nonlinear Two-point Boundary Problems with Mild Boundary Layers," SIAM J. Numer. Anal. 14, 91 (1977).

5. S. Doss, "Numerical Solution of the Rotationally Separable Laplace Equation by an Integral Equation Method," Lawrence Berkeley Laboratory Report (to be published).

6. E.P. Symons (private communication).

## LIST OF SYMBOLS

| | |
|---|---|
| $a$ | Radius of cylindrical container and horizontal semiaxis of spheroidal bottom. |
| $A$ | Diagonal matrix in the discretized time-dependent Bernoulli equation. |
| $b$ | Vertical semiaxis of spheroidal bottom. |
| $B$ | Bond number = $\kappa a^2$ . |
| $B_{crit}$ | Critical Bond number for stability of equilibrium surfaces. |
| $B_{eq}$ | Critical Bond number for the nonexistence of equilibrium surfaces of the family considered in this report. |
| $B_{conv}$, $B_{div}$ | Approximations to $B_{eq}$ |
| $B_{\theta m}$ | Critical Bond number for stability of the $R0\theta m$ mode. |
| $c,d$ | Constants in a linear combination of Bessel functions. |
| $C$ | Matrix in the discrete solution of the Laplace equation. |

| | |
|---|---|
| $D$, $E$, $F$ | Matrices. |
| $\mathcal{D}$ | A rectangular domain. |
| $e_j$ | Vector with a one in the $j^{th}$ position and zeros elsewhere. |
| $g$ | Acceleration due to gravity, considered positive when directed vertically downward. |
| $h_v$ | Dimensionless fill height. |
| $h_v^*$ | Critical $h_v$ for existence of unstable equilibrium surfaces of the family considered in this report. These exist for $h_v < h_v^*$ and $B_{eq} \leq B < B_{crit}$. |
| $\bar{H}$ | Mean curvature at a point on the free surface, considered negative when the surface is concave upward. |
| $H$ | Scaled mean curvature = $\bar{H}a$. |
| $H_0$ | A constant = $(p_g - p_0)a/2\sigma$, interpreted as the extrapolated value of $H$ at the height $z = 0$. |
| $\tilde{H}(s,\theta,t)$ | Displacement $\eta$ of the free surface. |
| $H(s)$ | A factor in the normal mode expression of the displacement of the free surface. |
| $J_m$ | Bessel function of the first kind of order $m$. |

| | |
|---|---|
| $k$ | The argument of the Bessel function is $kr$ . |
| K, L | Terms representing the contact-angle conditions. |
| m | Number of angular nodes in the normal mode. |
| M | The meridians of the cylinder wall and spheroidal bottom in the cross-sectional plane are divided into M intervals. |
| n | Each of the meridians of the free surface, cylinder walls, and flat bottom in the cross-sectional plane of two concentric cylinders is divided into n intervals. |
| subscript n | Outward normal derivative. |
| N | The meridian of the free surface in the cross-sectional plane is divided into N intervals. |
| $P_g$ | Gas pressure. |
| $P_0$ | Liquid static pressure at the height $z = 0$ . |
| $P_j$ | The integral of $Q(s)\ R(s)$ over the $j^{th}$ interval. |
| Q(s), Q(r) | A functional of the free surface appearing in the linearized Bernoulli equation. |
| $\bar{r}$ | Radial coordinate. |
| r | Scaled radial coordinate = $\bar{r}/a$ . |
| subscript r | d/dr . |

| | |
|---|---|
| $r_0$, $r_1$ | Radii of two concentric right circular cylinders. |
| R(s) | Radius of the equilibrium free surface as a function of the arc length along the meridian. |
| RO, R1, R2, ... | Normal modes with 0, 1, 2, .., radial nodes in $\phi$ . |
| s | Arc length along the meridians of the free surface, cylinder wall, and spheroidal bottom in the cross-sectional plane: $0 \leqslant s \leqslant S$ on the free surface. |
| subscript s | d/ds . |
| s, $\theta$, $\eta$ | Surface polar normal coordinates. |
| $s_1$, $s_2$, ... $s_N$ | Midpoints of the N intervals on the meridian of the free surface in the cross-sectional plane. |
| $\bar{t}$ | Time coordinate. |
| t | Scaled time coordinate = $\bar{t}[(1+\lvert B\rvert)\sigma/\rho a^3]^{\frac{1}{2}}$ |
| subscript t | d/dt . |
| $t_1$, $t_2$, ... $t_{N+1}$ | Endpoints of the N intervals on the meridian of the free surface in the cross-sectional plane. |
| T | Tridiagonal matrix in the discretized time-dependent Bernoulli equation. |

| | |
|---|---|
| $U(z)$ | A factor of the velocity potential in the liquid contained between two concentric cylinders. |
| $v$ | Fluid velocity. |
| $V$ | Volume of the liquid in the cylinder. |
| $W$ | Matrix in the discrete solution of the Laplace equation. |
| $X(r)$ | A factor of the velocity potential in the liquid contained between two concentric cylinders. |
| $Y_m$ | Bessel function of the second kind of order $m$ . |
| $\bar{z}$ | Vertical coordinate. |
| $z$ | Scaled vertical coordinate = $\bar{z}/a$ . |
| $z_0$ | Height of liquid contained between two concentric cylinders. |
| $Z(s)$ | Height of the equilibrium surface as a function of the radius. |
| $Z_B(r)$ | Height of the spheroidal bottom as a function of the radius. |
| $\gamma$ | Contact angle. |
| $\Gamma$ | Dimensionless growth rate of maximally growing mode. |
| $\Delta B$ | $= \Delta\omega^2/(d\omega^2/dB)$ . |

| | |
|---|---|
| $\Delta B^*$ | $= B_{crit,10} - B_{crit}$ , where $B_{crit,10}$ is the value of $B_{crit}$ calculated by the 10-point approximation. |
| $\Delta B_{\theta n}$ | $= B_{\theta n,10} - B_{\theta n,20}$ . |
| $\Delta\omega^2$ | $= \omega_{20}^2 - \omega_{10}^2$ , where $\omega_{20}^2$ and $\omega_{10}^2$ are the values of $\omega^2$ calculated by the 20- and 10-point approximations, respectively. |
| $\eta$ | Displacement normal to the equilibrium surface. |
| $\theta$ | Angle around the cylinder axis. |
| $\theta 0$, $\theta 1$, $\theta 2$, ... | Normal modes with 0, 1, 2, ... angular nodes. |
| $\kappa$ | Capillary constant = $\rho g/\sigma$ . |
| $\rho$ | Difference in densities between the liquid and gas phases. |
| $\sigma$ | Gas-liquid surface tension. |
| $\tilde{\phi}(r,z,\theta,t)$ | Potential function for the fluid velocity. |
| $\phi(r,z)$ | A factor in the normal mode expression of velocity potential. |
| $\Phi_1$ | Vector of values of $\phi$ at N points on the meridian on the free surface. |

$\Phi_2$ — Vector of values of $\phi$ at M points on the meridians on the cylinder wall and bottom.

$\Phi$ — Vector = $(\Phi_1, \Phi_2)$

$\chi$ — Angle in the cross-sectional plane between the horizontal and the tangent to the meridian on the bottom.

$\psi$ — Angle in the cross-sectional plane between the horizontal and the tangent to the meridian on the free surface.

$\omega$ — Frequency of the normal mode.

Table A 1. $\omega^2(B)$ for various $\theta$ modes; fill height = 0.20; radial mode = RO.

| -Bond | θ1 | θ2 | θ3 | θ4 | θ6 |
|---|---|---|---|---|---|
| 200. | 0.0910 | 0.363 | 0.817 | 1.46 | 3.30 |
| 400. | 0.0116 | 0.0473 | 0.111 | 0.208 | 0.535 |
| 450. | 0.0027 | 0.0121 | 0.032 | 0.069 | 0.226 |
| 500. | -0.0044 | -0.0161 | -0.031 | -0.043 | -0.020 |
| 550. | -0.0101 | -0.0392 | -0.083 | -0.134 | -0.223 |
| 600. | -0.0151 | -0.0585 | -0.126 | -0.210 | -0.392 |
| 700. | -0.0227 | -0.0889 | -0.194 | -0.330 | -0.657 |
| 800. | -0.0285 | -0.112 | -0.245 | -0.420 | -0.856 |
| 900. | -0.0330 | -0.130 | -0.285 | -0.491 | -1.01 |
| 1000. | -0.0366 | -0.144 | -0.317 | -0.547 | -1.14 |

Table A 2. $\omega^2(B)$ for various θ modes; fill height = 0.30; radial mode = R0.

| -Bond | θ1 | θ2 | θ3 | θ4 | θ5 | θ6 |
|---|---|---|---|---|---|---|
| 50. | 0.170 | 0.686 | 1.57 | 2.86 | 4.60 | 6.84 |
| 100. | 0.0328 | 0.139 | 0.339 | 0.666 | 1.16 | 1.86 |
| 110. | 0.0202 | 0.0883 | 0.226 | 0.464 | 0.841 | 1.40 |
| 120. | 0.0096 | 0.0460 | 0.131 | 0.295 | 0.576 | 1.01 |
| 130. | 0.0006 | 0.0100 | 0.050 | 0.151 | 0.351 | 0.688 |
| 140. | -0.0072 | -0.0210 | -0.020 | 0.027 | 0.157 | 0.407 |
| 150. | -0.0140 | -0.0481 | -0.081 | -0.081 | -0.012 | 0.163 |
| 160. | -0.0200 | -0.0720 | -0.135 | -0.176 | -0.160 | -0.051 |
| 180. | -0.0302 | -0.113 | -0.225 | -0.336 | -0.410 | -0.411 |
| 200. | -0.0389 | -0.147 | -0.301 | -0.468 | -0.612 | -0.701 |
| 210. | -0.0431 | -0.163 | -0.336 | -0.527 | -0.701 | -0.826 |
| 216. | -0.0462 | -0.175 | -0.358 | -0.562 | -0.750 | -0.892 |

Table A 3. $\omega^2(B)$ for various $\theta$ modes; fill height = 0.30; radial mode = R1.

| -Bond | θ0 | θ2 | θ4 | θ6 |
|---|---|---|---|---|
| 50. | 350. | 352. | 359. | 370. |
| 100. | 153. | 154. | 158. | 163. |
| 110. | 135. | 136. | 139. | 144. |
| 120. | 119. | 120. | 123. | 127. |
| 130. | 105. | 106. | 109. | 113. |
| 140. | 93.5 | 94.4 | 96.8 | 101. |
| 150. | 82.9 | 83.7 | 86.1 | 89.8 |
| 160. | 73.3 | 74.1 | 76.3 | 79.8 |
| 180. | 56.1 | 56.9 | 58.9 | 62.1 |
| 200. | 39.6 | 40.3 | 42.2 | 45.1 |
| 210. | 30.1 | 30.7 | 32.5 | 35.2 |
| 216. | 21.1 | 21.7 | 23.4 | 25.8 |

Table A 4. $\omega^2(B)$ for various θ modes; fill height = 0.40; radial mode = R0.

| -Bond | θ1 | θ2 | θ3 | θ4 | θ6 |
|---|---|---|---|---|---|
| 20. | 0.225 | 0.936 | 2.24 | 4.28 | 11.3 |
| 40. | 0.0384 | 0.182 | 0.503 | 1.10 | 3.52 |
| 45. | 0.0161 | 0.0920 | 0.298 | 0.724 | 2.59 |
| 50. | -0.0024 | 0.0172 | 0.127 | 0.411 | 1.81 |
| 55. | -0.0193 | -0.0498 | -0.025 | 0.133 | 1.09 |
| 56. | -0.0229 | -0.0635 | -0.055 | 0.077 | 0.938 |
| 57. | -0.0268 | -0.0784 | -0.088 | 0.017 | 0.768 |
| 58. | -0.0329 | -0.100 | -0.134 | -0.069 | 0.497 |

Table A 5. $\omega^2(B)$ for various θ modes; fill height = 0.40; radial mode = R1.

| -Bond | θ0 | θ2 | θ4 | θ6 |
|---|---|---|---|---|
| 20. | 132. | 135. | 144. | 158. |
| 40. | 49.2 | 50.8 | 55.4 | 62.8 |
| 45. | 38.2 | 39.7 | 43.8 | 50.2 |
| 50. | 28.3 | 29.6 | 33.2 | 38.9 |
| 55. | 18.1 | 19.3 | 22.3 | 27.0 |
| 56. | 15.8 | 16.8 | 19.7 | 24.2 |
| 57. | 13.0 | 14.0 | 16.7 | 20.7 |
| 58. | 8.07 | 8.89 | 11.1 | 14.3 |

Table A 6. $\omega^2(B)$ for various $\theta$ modes; fill height = 0.50; radial mode = RO.

| -Bond | θ1 | θ2 | θ3 | θ4 | θ6 |
|---|---|---|---|---|---|
| 8. | 0.359 | 1.56 | 3.93 | 7.88 | 22.1 |
| 16. | 0.0821 | 0.407 | 1.15 | 2.51 | 7.62 |
| 18. | 0.0455 | 0.254 | 0.782 | 1.78 | 5.53 |
| 19. | 0.0281 | 0.181 | 0.604 | 1.42 | 4.46 |
| 20. | 0.0082 | 0.0993 | 0.398 | 0.989 | 3.09 |
| 20.1 | 0.0055 | 0.0882 | 0.369 | 0.926 | 2.88 |
| 20.2 | 0.0021 | 0.0743 | 0.333 | 0.845 | 2.61 |
| 20.25 | -0.0003 | 0.0645 | 0.306 | 0.785 | 2.40 |
| 20.2759 | -0.0027 | 0.0549 | 0.280 | 0.722 | 2.18 |

Table A 7. $\omega^2(B)$ for various θ modes; fill height = 0.50; radial mode = R1.

| -Bond | θ0 | θ2 | θ4 | θ6 |
|---|---|---|---|---|
| 8. | 71.1 | 75.8 | 89.6 | 113. |
| 16. | 23.3 | 25.8 | 32.7 | 44.6 |
| 18. | 16.1 | 18.1 | 24.0 | 34.1 |
| 19. | 12.4 | 14.2 | 19.4 | 28.4 |
| 20. | 7.75 | 9.24 | 13.4 | 20.9 |
| 20.1 | 7.06 | 8.49 | 12.5 | 19.7 |
| 20.2 | 6.17 | 7.53 | 11.3 | 18.0 |
| 20.25 | 5.52 | 6.80 | 10.4 | 16.8 |
| 20.2759 | 4.85 | 6.06 | 9.41 | 15.5 |

Table A 8. $\omega^2(B)$ for various $\theta$ modes; fill height = 0.60; radial mode = RO.

| -Bond | θ1 | θ2 | θ3 | θ4 | θ6 |
|---|---|---|---|---|---|
| 3.5 | 0.531 | 2.47 | 6.62 | 13.8 | 39.0 |
| 7.0 | 0.152 | 0.790 | 2.26 | 4.81 | 13.4 |
| 8.0 | 0.0849 | 0.487 | 1.44 | 3.06 | 8.16 |
| 8.2 | 0.0697 | 0.415 | 1.24 | 2.61 | 6.81 |
| 8.4 | 0.0483 | 0.308 | 0.917 | 1.88 | 4.59 |
| 8.41 | 0.0466 | 0.299 | 0.889 | 1.81 | 4.40 |
| 8.42 | 0.0443 | 0.286 | 0.847 | 1.72 | 4.11 |

Table A 9. $\omega^2(B)$ for various θ modes; fill height = 0.60; radial mode = R1.

| -Bond | θ0 | θ2 | θ4 | θ6 |
|---|---|---|---|---|
| 3.5 | 44.3 | 51.5 | 73.7 | 117. |
| 7.0 | 14.2 | 17.8 | 28.9 | 51.3 |
| 8.0 | 7.98 | 10.7 | 19.0 | 35.8 |
| 8.2 | 6.39 | 8.82 | 16.2 | 31.0 |
| 8.4 | 3.83 | 5.70 | 11.3 | 22.4 |
| 8.41 | 3.61 | 5.43 | 10.8 | 21.6 |
| 8.42 | 3.30 | 5.04 | 10.2 | 20.6 |

Table A 10. $\omega^2(B)$ for various θ modes; fill height = 0.70; radial mode = RO.

| -Bond | θ1 | θ2 | θ3 | θ4 | θ6 |
|---|---|---|---|---|---|
| 1.5 | 0.771 | 3.94 | 11.1 | 23.5 | 65.1 |
| 3.0 | 0.306 | 1.67 | 4.79 | 9.99 | 26.6 |
| 3.2 | 0.266 | 1.47 | 4.20 | 8.72 | 23.0 |
| 3.4 | 0.227 | 1.27 | 3.63 | 7.49 | 19.5 |
| 3.6 | 0.188 | 1.07 | 3.06 | 6.22 | 15.9 |
| 3.8 | 0.148 | 0.855 | 2.40 | 4.78 | 11.8 |
| 3.9 | 0.124 | 0.719 | 1.98 | 3.86 | 9.26 |
| 3.94 | 0.111 | 0.647 | 1.75 | 3.36 | 7.93 |
| 3.98 | 0.0945 | 0.543 | 1.42 | 2.65 | 6.07 |

Table A 11. $\omega^2(B)$ for various $\theta$ modes; fill height = 0.70; radial mode = R1.

| -Bond | θ0 | θ2 | θ4 | θ6 |
|---|---|---|---|---|
| 1.5 | 30.7 | 41.5 | 78.5 | 162. |
| 3.0 | 12.2 | 18.1 | 38.6 | 85.7 |
| 3.2 | 10.4 | 15.8 | 34.5 | 77.6 |
| 3.4 | 8.67 | 13.6 | 30.5 | 69.2 |
| 3.6 | 6.91 | 11.2 | 26.2 | 59.8 |
| 3.8 | 4.96 | 8.59 | 21.1 | 48.3 |
| 3.9 | 3.75 | 6.89 | 17.7 | 40.7 |
| 3.94 | 3.14 | 6.02 | 15.9 | 36.6 |
| 3.98 | 2.30 | 4.79 | 13.3 | 30.9 |

| 1. Report No. NASA CR-135346 | 2 Government Accession No. | 3. Recipient's Catalog No |
|---|---|---|
| 4 Title and Subtitle MATHEMATICAL AND COMPUTATIONAL STUDIES OF THE STABILITY OF AXISYMMETRIC ANNULAR CAPILLARY FREE SURFACES | | 5 Report Date November 1977<br>6 Performing Organization Code |
| 7. Author(s) Norman Albright, Paul Concus, and Ilkka Karasalo | | 8. Performing Organization Report No. UCID-3983<br>10 Work Unit No |
| 9. Performing Organization Name and Address Lawrence Berkeley Laboratory University of California Berkeley, California 94720 | | 11. Contract or Grant No DOE W-7405-ENG-48; NASA 67705-C |
| 12. Sponsoring Agency Name and Address U. S. Department of Energy and National Aeronautics and Space Administration Washington, D.C. | | 13. Type of Report and Period Covered Contractor Report<br>14 Sponsoring Agency Code Report no. DOE/NASA/7405-78/2 |

15. Supplementary Notes Final Report. Project Manager, Eugene P. Symons, NASA Lewis Research Center, Cleveland, Ohio. Principal Investigator, Paul Concus, Lawrence Berkeley Laboratory, University of California, Berkeley, California.

16. Abstract

The stability of axisymmetric, annular capillary free surfaces is studied mathematically and computationally. Of principal interest is the stability of a perfectly wetting liquid in an inverted, vertical, right circular-cylindrical container having a concave spheroidal bottom. The mathematical conditions that the contained liquid be in stable static equilibrium are derived, including those for the limiting case of zero contact angle. Based on these results, a computational investigation is carried out for a particular container that is used for the storage of liquid fuels in NASA Centaur space vehicles, for which the axial ratio of the container bottom is 0.724. It is found that for perfectly wetting liquids the qualitative nature of the onset of instability changes at a critical liquid volume, which for the Centaur fuel tank corresponds to a mean fill level of approximately 0.503 times the tank's radius. We calculate small-amplitude periodic sloshing modes for this tank; oscillation frequencies or growth rates are given for several Bond numbers and liquid volumes, for normal modes having up to six angular nodes. The results are found to be in close accord with those of the static analysis and to agree well with experiments.

| 17. Key Words (Suggested by Author(s)) | 18. Distribution Statement |
|---|---|
| Liquid-vapor interfaces; Interface stability; Static stability; Dynamic stability; Liquid sloshing; Propellant tanks; Centaur launch vehicle; Weightlessness; Reduced gravity; Numerical analysis; Differential equations; Eigenvalues; Eigenvectors. | Unclassified - unlimited<br>STAR Category 34<br>DOE Category UC-32 |

| 19. Security Classif. (of this report) | 20. Security Classif. (of this page) | 21 No. of Pages | 22 Price* |
|---|---|---|---|
| Unclassified | Unclassified | 189 | A09 |

* For sale by the National Technical Information Service Springfield Virginia 22161

*USGPO: 1978 — 757-139/1202 Region 5-11